FACOLTÀ DI INGEGNERIA

Corso di Laurea in Ingegneria delle Telecomunicazioni

Tesi di Laurea

Wake Fields in Particle Accelerators with Finite Thickness and Conductivity

Relatore:

Prof. Stefania Petracca

Correlatore:

Dott. Arturo Stabile

Candidata:

Truocchio Antonella

Matr. 196/588

Anno accademico 2010/2011

Index

Introduction

Wake fields describe the interaction between a particle beam and the surrounding pipe wall. For perfectly conducting pipes and ultra-relativistic motion ($v = c$) wake fields are negligible. In the realistic case of walls of finite conductivity, and/or relatively low values of the relativistic factor γ, wake fields might be quite relevant. In addition, for low revolution frequencies, the finite thickness of the pipe wall should be properly taken into account [5]. Much has been written on the subject of wake fields, since the early work of N. Piwinski [6], who first studied the case of a homogeneous conducting pipe much thicker than the electromagnetic penetration depth. L. Palumbo and V. G. Vaccaro extended Piwinski's results for this latter case, by computing higher order wake field multipoles [7]. A. W. Chao [4] first gave a formula which fully exploits the dependence of the wake field on the pipe wall thickness, but his analysis was restricted to the monopole term. More recently, Ohmi and Zimmerman presented a thorough analysis of the sub-relativistic effect [20]. Finally, Y. Yokoya and K. Shobuda studied the finite conductivity and thickness pipe wall problem, in the frame of a transmission line analogy, in the limit where the electromagnetic skin depth is much smaller than the smallest pipe transverse dimension [8]. In this communication we compute the fields of a beam in a pipe with walls of finite conductivity and thickness, for a circular pipe. We solve the problem by computing the Fourier transform of the wake potential Green's function produced by a point particle running at constant velocity $\beta c\hat{u}_z$, at a distance r_0 off-axis of a circular cylindrical pipe with radius b, conductivity σ and thickness Δ. The solution found is exact but complicated, so that one has to resort to suitable limiting forms appropriate, in particular, to LHC and DAΦNE.

The content of this Thesis is organized into four chapter. In Chapter 1 there is an introduction to the different accelerators built so far, to their main elements and to their uses into several fields of research.

In Chapter 2 it is introduced the electromagnetism to study the particles motion into the vacuum chamber, the wake field described into the cavity as well as the wake function and the coupling impedances.

In Chapter 3 it is presented a thorough analysis and a full solution in the frequency domain for the wake fields of a bunched beam in a circular pipe with walls of finite thickness and conductivity.

The space time wake field multipoles for a multi-bunch beam in a circular ring are computed in analytic form displaying the wake field dependence on wall conductivity and thickness. Suitable asymptotic forms, applicable to typical rings, such as LHC and DAΦNE, are introduced.

Chapter 4 contains a review of the Literature existing on the subject.

Chapter 1

Introduction to accelerators

Accelerators are devices that control and manipulate the motion of charged subatomic particles (protons, electrons, neutrons) impressing high kinetic energies by the action of electromagnetic or electrostatic fields. The accelerated particles are sent against an appropriate “target” to investigate further the structure of matter and its constituents. Atoms are not elementary particles but composite entities with a complex internal structure. The basic idea is simple. Particles are grouped into two classes. The first contains heavy particles, called hadrons, such as neutrons and protons. The other one contains leptons, such as electrons and other light particles which interact weakly. In most experiments there are collisions of hadrons to high energy. This type of investigation was initially conducted using “natural” fast particles, as well as those emitted by radioactive substances or those making up the cosmic radiation. Subsequently, the construction of accelerators brought enormous advantages with respect to “natural” source both for the beam intensity and for the production of a multitude of new short-lived particles. The principle of phase stability is much important for the efficient working of accelerators and for the acceleration of particles to relativistic velocities. According to the principle one has stability when the particles are in the acceleration gap in synchronism with the accelerating electric field. [1]

Depending on the acceleration device and the particle trajectory one has several type of accelerators:

- Electrostatic accelerators
- Linear accelerators
- Circular accelerators

1.1 Electrostatic accelerators

Particles are accelerated by an electric field along a straight line through the difference of potential between two electrodes. They consist of an acceleration tube, to whose extremity there are the particle source and the target, and of a high voltage generator. These accelerators allow to accelerate electrons and protons beams to high energies and they are useful for the study of nuclear reactions to low energies, to inject fast particles in high energies accelerators and to produce beams of neutrons and penetrating X-rays. [1]

To the class of electrostatic accelerators belongs to:

- Cockcroft and Walton Accelerator
- Van de Graaff Accelerator
- Tandem Accelerator

Cockcroft and Walton Accelerator **Fig. 1.1 a)**

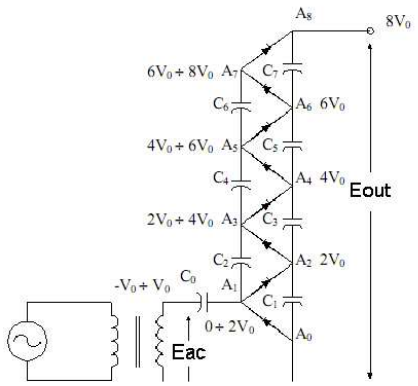

Fig. 1.1 a) Its main characteristic is the high voltage generator based on a voltage multiplying circuit which consists of two columns of capacitors in series connected to several diodes in series. A column is connected to the secondary of a transformer and the second one has an extremity to earth and another one is brought to an high direct voltage. The maximum energy reached is 2 MeV.

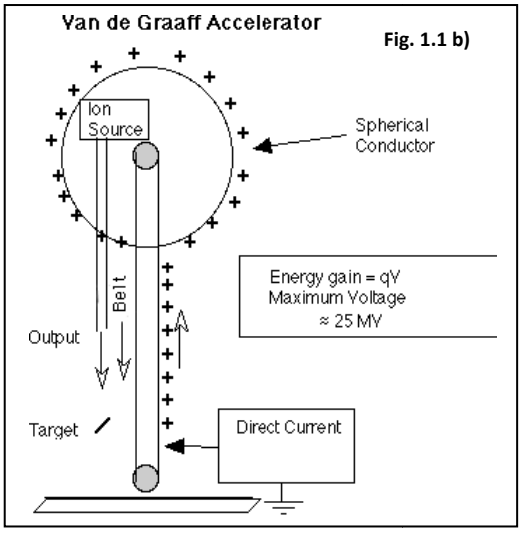

Fig. 1.1 b) The accelerating voltage is produced by the transport and the storage of electric charges on a metallic sphere supported by an insulating column. Electric charges are on the base of an insulating moving belt that transports the charges on the other side of the belt to charge the sphere, while the belt becomes neuter again. These kind of accelerators are used to accelerate ions or electrons used for the study of nuclear reactions or to produce X-rays of high intensity for medical or industrial purposes.

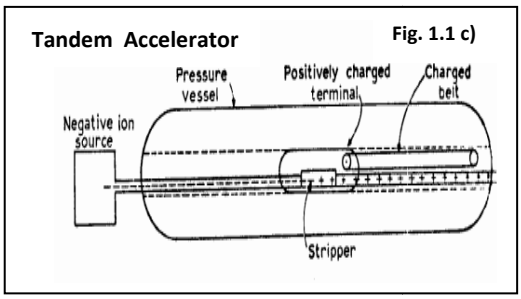

Fig. 1.1 c) It's a type of Van de Graaff accelerator with two phases. In the first one, protons are changed in H^- ions so they are accelerated by the electric field that exists between the source to earth and the high voltage electrode. Ions H^- are changed in ions H^+ which are accelerated towards the target to earth in the second phase.

1.2 Linear accelerators

The particles are accelerated along straight trajectories by a longitudinal electric field generated by electrodes in succession. [1]

To the class of linear accelerators belongs to:

- Linear Accelerator of Electrons
- Linear Accelerator of Protons

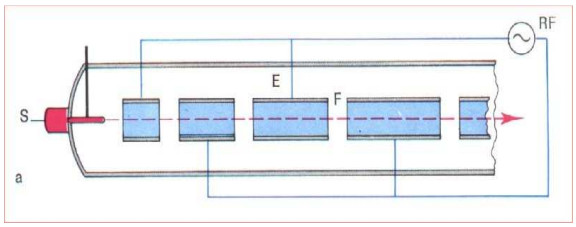

Linear Accelerator of Electrons **Fig. 1.2 a)**

Fig. 1.2 a) Each section is composed of a wave guide, in the shape of cylindrical conductor, fed by a radio-frequency generator. Inside there are several conducting drift tubes through which the beam moves. Electrons, injected by an electrostatic accelerator at the speed of light, travel in phase with electromagnetic wave in the same direction, and they are always accelerated by the electric field. Under these assumptions the principle of phase stability is enforced.

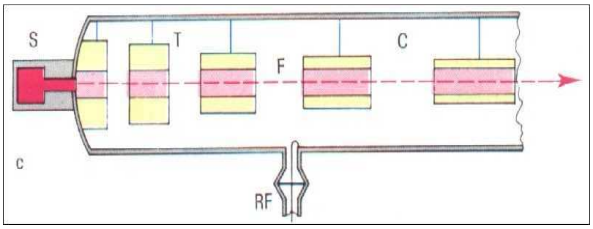

Linear Accelerator of Protons **Fig. 1.2 b)**

Fig. 1.2 b) It's composed of a resonant cavity excited by a radio-frequency oscillator. The synchronism between the electric field and the particle, occurs by introducing in the cavity several cylinders that have increasing length and decreasing diameter. In this way, the protons are always in synchronism with the electric field so one has always acceleration. These machines are used to inject particles in the proto-synchrotrons.

1.3 Circular accelerators

The charged particles describe curved trajectories by the presence of a magnetic field. [1]

There are different types of circular accelerators:

- Cyclotrons
- Synchro-cyclotrons
- Betatrons
- Synchrotrons

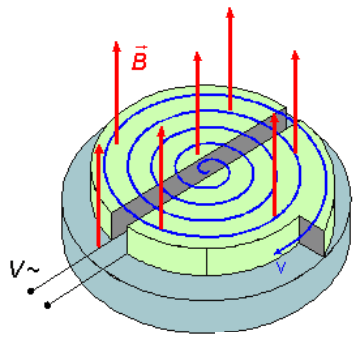

Cyclotron Fig. 1.3 a)

Fig. 1.3 a) It's composed of a circular cavity where there are two copper electrodes, in the shape of *D,* that are connected to the voltage radio-frequency generator. Ions describe spiral trajectories and, going out from the first electrode, they suffer the action of the electric field, which accelerate them towards the second electrode. After going along a semicircle they appear and they are accelerated by the electric field. Energies reached: 20-25 MeV.

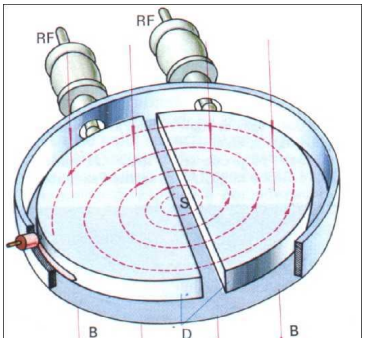

Synchro-cyclotron Fig. 1.3 b)

Fig. 1.3 b) This type of accelerator is used to accelerate protons in the energy relativistic region: in a range of energy until *200 MeV* for nuclear studies and until *700 MeV* for the production of mesons and their interactions. The rotation frequency depends on the energy. According to the principle of phase stability, the phase synchronism occurs by decreasing the frequency of oscillator.

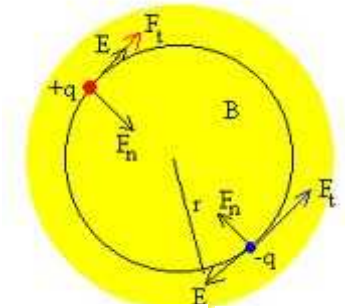

Betatron **Fig. 1.3 c)**

Fig. 1.3 c) It's an accelerator of electrons that acts as a transformer: the primary is composed of an envelopment and the secondary is composed of a beam of electrons. Electrons are supported on a circular orbit by the magnetic field and they are accelerated by the induced electric field. The beam is deviated from the orbit and it's directed towards a target. Energies reached: 350 MeV.

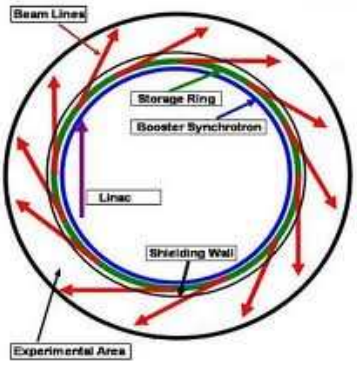

Synchrotron **Fig. 1.3 d)**

Fig. 1.3 d) It's an accelerator of electrons (electro-synchrotron) or protons (proto-synchrotron) based on the principle of phase stability. Particles are supported on a circular orbit in synchronism with the accelerating electric field. They have annular magnet frequency modulation of electric field and periodic modulation of magnetic field. Energies reached: 1 TeV.

1.5 Large Hadron Collider

Energies reached by accelerators continue to grow further. Just think to LHC, which has recently reached 7 TeV. It is the largest and the most powerful accelerator ever produced. It is built within a 27 Km long underground tunnel located on the border between France and Switzerland at 100 meters of depth.

The most important components are the superconducting magnets that produce a magnetic field of about 7 Tesla. The machine accelerates two beams of particles moving in the opposite directions and colliding at four points along the orbit. [1]

Here there are the four most important experiments of particle physics:

- ATLAS (A Toroidal LHC ApparatuS)
- CMS (Compact Muon Solenoid)
- LHCb (LHC to study the physics of Bosons)
- ALICE (A Large Ion Collider Experiment).

These devices consist of several detectors that use different technologies and work around the points where the beams collide.

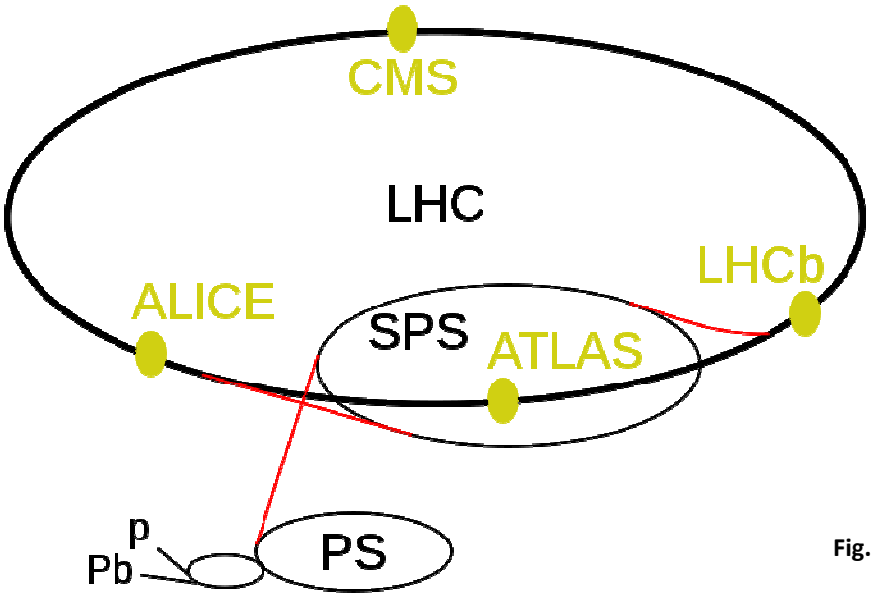

Fig. 1.5

Fig. 1.5 The LHC experiments and the pre-accelerators. The path of the protons (and ions) begins at linear accelerators (marked p and Pb, respectively). They continue their way in the booster (the small unmarked circle), in the Proton Synchrotron (PS), in the Super Proton Synchrotron (SPS) and finally they get into the 27 km long LHC tunnel. In the LHC there are four large experiments marked with yellow dots and text.

1.6 Structure of accelerators

Characteristic elements of an accelerator are:

- the source of charged particles
- the accelerating cavity surrounding the vacuum chamber in which the particles are released and accelerated
- the generator of electric field
- the focusing and the bending devices to maintain and concentrate the particles in a homogeneous beam of well-defined energy and trajectory
- the nuclear target, inside or outside the acceleration chamber, subjected to the bombardment of the accelerated particles
- various devices of measurement and control. [1]

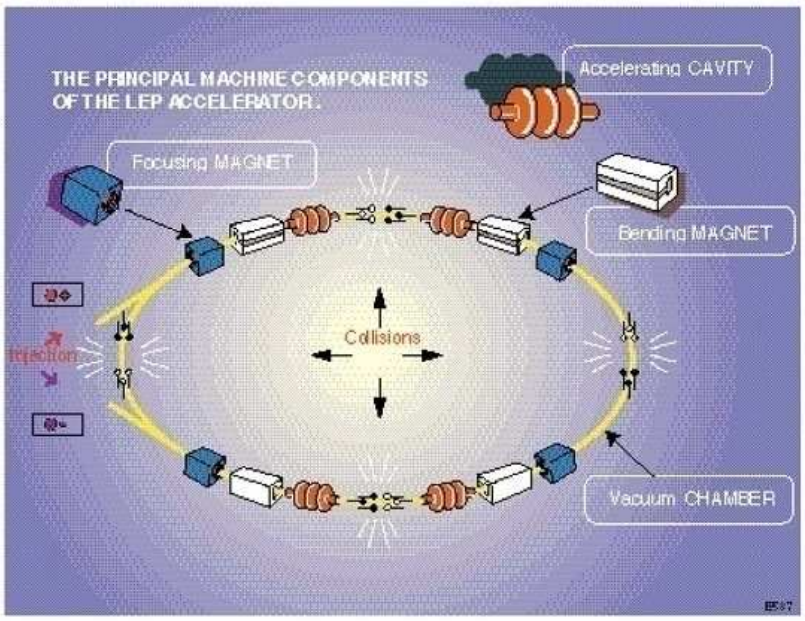

Fig. 1.6

Fig. 1.6 The principal machine components of the LEP Accelerators.

The charged particles move in the vacuum chamber that usually consists of a metallic pipe but also of insulating materials such as ceramics. [2] The inner surface of the chamber is often covered by a thin layer of metal in order to prevent any distortions of the motion of the beam by electric charges accumulating on the insulating wall. The interaction between a particle beam and the surrounding pipe wall is described by *wake fields*. In many accelerators, in particular those operating with light particles such as electrons and positrons, the particles are grouped into one or more *bunches*. Generally the electromagnetic fields, generated by the beam, contain a longitudinal component directed along the average particle motion, that may change the effective amplitude and phase of the applied accelerating field and thereby the rate of acceleration, as well as the energy distribution in the bunch and its effective length; and transverse field components (horizontal and vertical or radial and azimuthal) which may increase the cross section of a bunch, change its closed orbit, its frequency of oscillation around it and shorten its life time. The normalized integral over the electromagnetic force due to fields excited by a point charge or delta function distribution is called *wake function*. On the other hand, the integrated effect over a finite distribution of charged particles is described by the *wake potential*. The Fourier transforms of the wake functions are the so called *coupling impedances.* From this definition it follows that they are integrated quantities which can be used only under the assumption that the average beam motion remains undisturbed. They are, therefore, a property of the surrounding structure only, and do not depend on beam parameters except on its velocity v, which is assumed ultra-relativistic in case of high-energy accelerators. The coupling impedance, such as the wake function, can be divided into two components, longitudinal and transverse, according to the direction of the forces which are involved. The impedance is in general a complex function where the real part, i.e. resistive, describes the energy loss while the imaginary part, i.e. reactive, shifts the frequency of the beam oscillation. If the frequency shift of any two low order oscillation modes leads to their degeneracy, a *mode-coupling instability* may occur. The instability can be multi-bunch, which depends on narrow resonances at frequency below or near the cut-off of the beam, or single-bunch, which depends on the short range wake fields. [2]

1.7 Uses of accelerators

Use of accelerators has expanded beyond the traditional field of research in particle physics, with the development of specialized accelerators used for: [3]

- nuclear physics research including a broad spectrum of studies emphasizing energy precision, beam intensity, beam species and polarized beams
- synchrotron radiation sources for a wide variety of applications of ultraviolet and x-ray beams in material science
- medical applications in the therapy of tumors with penetrating X-rays
- nuclear chemistry research through the polymerization by irradiation with electrons and X-rays, production of radioactive elements and radioactive isotopic tracers
- radiobiology applications through the study of radiation effects on organic cells
- industrial techniques such as the radiography of metals, study of their properties and the sterilization of food packaging

Chapter 2

Electromagnetism in accelerators

2.1 Wake field

A charged particle beam interacts electromagnetically with its vacuum chamber surroundings in an accelerator. The beam is assumed to move with the speed of light. The wake field is that seen by a test charge that follows the beam at a fixed relative distance. The case of a relativistic beam does not generate wake fields in a perfectly conducting smooth pipe but if the vacuum chamber is not a smooth pipe or if it is smooth but not perfectly conducting, a beam will generate behind it an electromagnetic wake. [4]

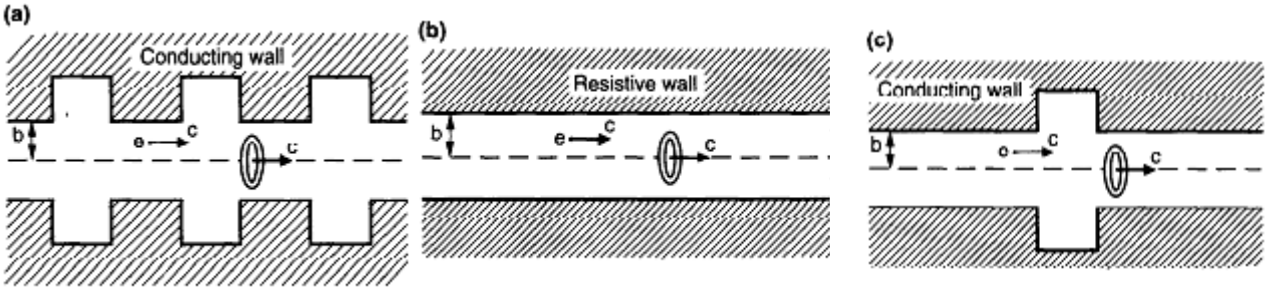

Fig. 2.1 Examples of vacuum chamber pipe that generates wake fields. **(a)** Case of periodic structure. **(b)** Case of resistive wall. **(c)** Case of single structure.

It is assumed that the pipe wall has infinite thickness and that the beam moves with the speed of light with a charge and current distribution given by:

$$\rho_m = \frac{I_m}{\pi a^{m+1}(1+\delta_{m0})}\delta(s-ct)\delta(r-a)cosm\vartheta \qquad (2.1)$$

$$\vec{J}_m = c\rho_m\hat{s} \qquad (2.2)$$

The charge is distributed as an infinitesimally thin ring with radius a and with a $cosm\vartheta$ angular dependence, where the quantity I_m is the mth moment of the beam and $\delta_{m0} = \begin{cases} 1 & m=0 \\ 0 & m=1 \end{cases}$

The Maxwell's equations (See Appendix A) in cylindrical coordinates are :

$$\frac{1}{r}\frac{\partial(rE_r)}{\partial r} + \frac{1}{r}\frac{\partial E_\vartheta}{\partial \vartheta} + \frac{\partial E_s}{\partial s} = 4\pi\rho$$

$$\left(\frac{1}{r}\frac{\partial B_s}{\partial \vartheta} - \frac{\partial B_\vartheta}{\partial s}\right) - \frac{1}{c}\frac{\partial E_r}{\partial t} = \frac{4\pi}{c}J_r$$

$$\frac{\partial B_r}{\partial s} - \frac{\partial B_s}{\partial r} - \frac{1}{c}\frac{\partial E_\vartheta}{\partial t} = \frac{4\pi}{c}J_\vartheta$$

$$\frac{1}{r}\left(\frac{\partial(rB_\vartheta)}{\partial r} - \frac{\partial B_r}{\partial \vartheta}\right) - \frac{1}{c}\frac{\partial E_s}{\partial t} = \frac{4\pi}{c}J_s \qquad (2.3)$$

$$\left(\frac{1}{r}\frac{\partial E_s}{\partial \vartheta} - \frac{\partial E_\vartheta}{\partial s}\right) + \frac{1}{c}\frac{\partial B_r}{\partial t} = 0$$

$$\frac{\partial E_r}{\partial s} - \frac{\partial E_s}{\partial r} + \frac{1}{c}\frac{\partial B_\vartheta}{\partial t} = 0$$

$$\frac{1}{r}\left(\frac{\partial(rE_\vartheta)}{\partial r} - \frac{\partial E_r}{\partial \vartheta}\right) + \frac{1}{c}\frac{\partial B_s}{\partial t} = 0$$

$$\frac{1}{r}\frac{\partial(rB_r)}{\partial r} + \frac{1}{r}\frac{\partial B_\vartheta}{\partial \vartheta} + \frac{\partial B_s}{\partial s} = 0$$

where:

ρ e $J_s \propto cosm\vartheta$

$E_r, B_\vartheta, E_s \propto cosm\vartheta$

$E_\vartheta, B_r, B_s \propto senm\vartheta$

We can write the field components in terms of Fourier transformations:

$$(E_r, B_\vartheta, E_s) = cosm\vartheta \int_{-\infty}^{\infty} \frac{1}{2\pi} e^{jkz}\left(\tilde{E}_r, \tilde{B}_\vartheta, \tilde{E}_s\right)dk \tag{2.4}$$

$$(E_\vartheta, B_r, B_s) = senm\vartheta \int_{-\infty}^{\infty} \frac{1}{2\pi} e^{jkz}\left(\tilde{E}_\vartheta, \tilde{B}_r, \tilde{B}_s\right)dk \tag{2.5}$$

where $\tilde{E}_r, \tilde{B}_\vartheta, \tilde{E}_s$ are complex quantities and are functions of k and r. The solution must satisfy the condition that no wake field is produced ahead of the beam, i.e. in the region $z > 0$, and that is possible because the field components do not have singularities in the upper complex k-plane.

Case $m = 0$

Setting the condition $m = 0$ in equations (2.4),(2.5), equations (2.3) become: [4]

$$\tilde{E}_s = A \qquad r < b$$

$$\tilde{E}_r = \tilde{B}_\vartheta = \begin{cases} -jkA\dfrac{r}{2} & r < a \\ -jkA\dfrac{r}{2} + \dfrac{2q}{r} & b < r < a \end{cases} \tag{2.6}$$

For a perfectly conducting wall , $\tilde{E}_s = 0$ for $r = b, A = 0$.

For a resistive wall, A is obtained from the boundary conditions at $r = b$ and calculating the field inside the metal wall, $r > b$. Metal is a material that obeys the conditions:

$$\rho = 0 \quad , \quad \vec{J} = \sigma \vec{E} \tag{2.7}$$

Substituting equations (2.4),(2.5) in (2.3) and applying the conditions (2.7) follows:

$$\frac{1}{r}\frac{\partial}{\partial r}\left(r\frac{\partial \tilde{E}_s}{\partial r}\right) + \lambda^2 \tilde{E}_s = 0$$

$$\tilde{E}_r = \frac{jk}{\lambda^2}\frac{\partial \tilde{E}_s}{\partial r} \tag{2.8}$$

$$\tilde{B}_\vartheta = \left(1 + \frac{\lambda^2}{k^2}\right)\tilde{E}_r$$

where: $\lambda = \sqrt{\frac{2\pi\sigma|k|}{c}}\,[\mathrm{j} + \mathrm{sgn(k)}]$.

Under the approximation $|\lambda| \gg \frac{1}{b}$ if $|z| \ll \frac{b}{\chi}$, where $\chi = \frac{c}{4\pi\sigma b}$, one obtains:

$$\tilde{E}_s = Ae^{j\lambda(r-b)}$$

$$\tilde{E}_r = -\frac{k}{\lambda}Ae^{j\lambda(r-b)} \tag{2.9}$$

$$\tilde{B}_\vartheta = -\frac{k}{\lambda}\left(1 + \frac{\lambda^2}{k^2}\right)Ae^{j\lambda(r-b)}$$

The coefficient A is determined by the continuity of $\tilde{B}_\vartheta$ at $r = b$, yielding the result:

$$A \approx \frac{2\mathrm{q/b}}{\frac{\mathrm{jkb}}{2} - \frac{\lambda}{\mathrm{k}}}$$

Performing the inverse Fourier transform of $\tilde{E}_r, \tilde{B}_\vartheta, \tilde{E}_s$ for the region $r < b$ and for $z < 0$, i.e. behind the beam, one obtains the following fields:

$$E_s = \frac{q}{2\pi b}\sqrt{\frac{c}{\sigma}}\frac{1}{|z|^{3/2}}$$

$$B_\vartheta = E_r = -\frac{3}{4}\frac{q}{2\pi b}\sqrt{\frac{c}{\sigma}}\frac{1}{|z|^{5/2}} \qquad (2.10)$$

For $z > 0$, i.e. ahead of the beam, the fields vanishes due to causality. From equations (2.10) shows that the longitudinal field component decreases as $|z|^{-3/2}$ and is independent of r and ϑ and the transverse field components decrease as $|z|^{-5/2}$ and are proportional to r.

Under the assumptions $\left|\frac{\lambda}{k}\right| \gg |kb|$ if $|z| \gg \chi^{1/3}b$, i.e. in the region $\frac{b}{\chi} \gg |z| \gg \chi^{1/3}b$, the quantity A becomes:

$$A \approx -\frac{2\mathrm{qk}}{\mathrm{b}\lambda}$$

The problem that arises in this case is that the test charge trailing the beam at a distance $|z|$ is accelerated if it has the same sign as q. If this were true for $z \to 0$, one would expect the point charge to gain energy as it travels down the resistive pipe. To prevent this phenomenon occurs we have to compute the field at very short distances behind the beam. In this case we consider the complete expression of the coefficient A.

The results in the pipe region are:

$$E_s = -\frac{16q}{b^2}\left(\frac{1}{3}e^u cos\sqrt{3}u - \frac{\sqrt{2}}{\pi}\int_0^\infty \frac{x^2 e^{ux^2}}{x^6+8}dx\right)$$

$$B_\vartheta = E_r = \frac{8qr}{(2\chi)^{1/3}b^3}\left(\frac{1}{3}e^u cos\sqrt{3}u - \frac{1}{\sqrt{3}}e^u sen\sqrt{3}u\frac{\sqrt{2}}{\pi}\int_0^\infty \frac{x^4 e^{ux^2}}{x^6+8}dx\right) \qquad (2.11)$$

where $u = \frac{z}{(2\chi)^{1/3}b} < 0$.

Case $m \geq 1$

Setting the condition $m \geq 1$ in equations (2.4),(2.5), equations (2.3), in the region $r < b$, become: [4]

$$\frac{\partial \tilde{E}_s}{\partial r} = -\frac{m}{r}\tilde{B}_s$$

$$\frac{\partial \tilde{B}_s}{\partial r} = -\frac{m}{r}\tilde{E}_s$$

$$\frac{1}{r}\frac{\partial}{\partial r}(r\tilde{E}_r) - \frac{m}{r}\tilde{B}_r = \frac{4I_m}{a^{m+1}}\delta(r-a) - J\left(k + \frac{m^2}{kr^2}\right) = \tilde{E}_s \qquad (2.12)$$

$$\frac{1}{r}\frac{\partial}{\partial r}(r\tilde{B}_r) - \frac{m}{r}\tilde{E}_r = -J\left(k + \frac{m^2}{kr^2}\right) = \tilde{B}_s$$

$$\tilde{B}_\vartheta = \tilde{E}_r - j\frac{m}{kr}\tilde{B}_s$$

$$\tilde{E}_\vartheta = -\tilde{B}_r + j\frac{m}{kr}\tilde{E}_s$$

From the first pair of these equations one obtains the longitudinal components of the field:

$$\tilde{E}_s = Ar^m$$

$$\tilde{B}_s = -Ar^m \qquad (2.13)$$

From the second pair one obtains the radial components of the field:

$$\tilde{E}_r = \begin{cases} -\frac{jkA}{2(m+1)} r^{m+1} + \frac{1}{2}\left(-\frac{jmA}{k} + B - \frac{4I_m}{a^{2m}}\right) r^{m-1} & r < a \\ \frac{2I_m}{r^{m+1}} - \frac{jkA}{2(m+1)} r^{m+1} + \frac{1}{2}\left(-\frac{jmA}{k} + B\right) r^{m-1} & a < r < b \end{cases}$$

$$\tilde{B}_r = \begin{cases} \frac{jkA}{2(m+1)} r^{m+1} + \frac{1}{2}\left(\frac{jmA}{k} + B - \frac{4I_m}{a^{2m}}\right) r^{m-1} & r < a \\ -\frac{2I_m}{r^{m+1}} + \frac{jkA}{2(m+1)} r^{m+1} + \frac{1}{2}\left(\frac{jmA}{k} + B\right) r^{m-1} & a < r < b \end{cases} \quad (2.14)$$

Finally, from the third pair the azimuthal components:

$$\tilde{E}_\vartheta = \begin{cases} -\frac{jkA}{2(m+1)} r^{m+1} + \frac{1}{2}\left(\frac{jmA}{k} - B + \frac{4I_m}{a^{2m}}\right) r^{m-1} & r < a \\ \frac{2I_m}{r^{m+1}} - \frac{jkA}{2(m+1)} r^{m+1} + \frac{1}{2}\left(\frac{jmA}{k} - B\right) r^{m-1} & a < r < b \end{cases}$$

$$\tilde{B}_\vartheta = \begin{cases} -\frac{jkA}{2(m+1)} r^{m+1} + \frac{1}{2}\left(\frac{jmA}{k} + B - \frac{4I_m}{a^{2m}}\right) r^{m-1} & r < a \\ \frac{2I_m}{r^{m+1}} - \frac{jkA}{2(m+1)} r^{m+1} + \frac{1}{2}\left(\frac{jmA}{k} + B\right) r^{m-1} & a < r < b \end{cases} \quad (2.15)$$

For a perfectly conducting wall: $A = 0$ because $\tilde{E}_s = 0 \ for \ r = b$

$$B = \frac{4I_m}{b^{2m}} \text{ because } \tilde{E}_\vartheta = 0 \ for \ r = b$$

For a resistive wall, the coefficients are obtained by replacing equations (2.7) in the system (2.3):

$$\frac{1}{r}\frac{\partial}{\partial r}\left(r\frac{\partial \tilde{E}_s}{\partial r}\right) + \left(\lambda^2 - \frac{m^2}{r^2}\right)\tilde{E}_s = 0$$

$$\frac{1}{r}\frac{\partial}{\partial r}\left(r\frac{\partial \tilde{B}_s}{\partial r}\right) + \left(\lambda^2 - \frac{m^2}{r^2}\right)\tilde{B}_s = 0$$

$$\tilde{E}_r = \frac{c}{4\pi\sigma}\left(\frac{m}{r}\tilde{B}_s + \frac{\partial \tilde{E}_s}{\partial r}\right) \quad (2.16)$$

$$\tilde{E}_\vartheta = -\frac{c}{4\pi\sigma}\left(\frac{m}{r}\tilde{E}_s + \frac{\partial \tilde{B}_s}{\partial r}\right)$$

$$\tilde{B}_r = \frac{c}{4\pi\sigma}\frac{\partial \tilde{B}_s}{\partial r} + \left(\frac{c}{4\pi\sigma} + \frac{j}{k}\right)\frac{m}{r}\tilde{E}_s$$

$$\tilde{B}_\vartheta = \frac{c}{4\pi\sigma}\frac{m}{r}\tilde{B}_s + \left(\frac{c}{4\pi\sigma} + \frac{j}{k}\right)\frac{\partial \tilde{E}_s}{\partial r}$$

Assuming $|z| \ll \frac{b}{\chi}$, the solutions of equations are:

$$\tilde{E}_s = -\tilde{B}_s = Ab^m e^{j\lambda(r-b)}$$

$$\tilde{E}_r = \tilde{E}_\vartheta = -\frac{k}{\lambda}Ab^m e^{j\lambda(r-b)} \qquad (2.17)$$

$$\tilde{B}_\vartheta = -\left(\frac{k}{\lambda} + \frac{\lambda}{k}\right)Ab^m e^{j\lambda(r-b)}$$

$$\tilde{B}_r = \left(\frac{k}{\lambda} + \frac{jm}{kb}\right)Ab^m e^{j\lambda(r-b)}$$

And the coefficients A and B are:

$$A = \frac{4I_m}{b^{2m+1}\left(\frac{jkb}{m+1} - \frac{\lambda}{k} - \frac{jm}{kb}\right)} \quad , \quad B = -\frac{\lambda}{k}bA$$

If one supposes $|z| \gg b\chi^{1/3}$, the constants A and B become:

$$A = -\frac{4I_m k}{b^{2m+1}\lambda} \quad , \quad B = \frac{4I_m}{b^{2m}}\left[1 + j\frac{k^2 b}{(m+1)\lambda} - \frac{jm}{b\lambda}\right]$$

Performing the inverse Fourier transform of $\tilde{E}_r, \tilde{E}_\vartheta, \tilde{E}_s$ and of $\tilde{B}_r, \tilde{B}_\vartheta, \tilde{B}_s$ for the region $r < b$ and for $z < 0$, i.e. behind the beam, one obtains the following fields:

$$E_s = \frac{I_m}{\pi b^{2m+1}}\sqrt{\frac{c}{\sigma}}r^m cosm\vartheta \frac{1}{|z|^{3/2}}$$

$$E_r = -\frac{3I_m}{4\pi b^{2m+1}}\sqrt{\frac{c}{\sigma}}\frac{1}{m+1}r^{m-1}cosm\vartheta(r^2+b^2)\frac{1}{|z|^{5/2}} \qquad (2.18)$$

$$E_\vartheta = -\frac{3I_m}{4\pi b^{2m+1}}\sqrt{\frac{c}{\sigma}}\frac{1}{m+1}r^{m-1}senm\vartheta(r^2-b^2)\frac{1}{|z|^{5/2}}$$

$$B_s = -\frac{I_m}{\pi b^{2m+1}}\sqrt{\frac{c}{\sigma}}r^m senm\vartheta \frac{1}{|z|^{3/2}}$$

$$B_r = -E_\vartheta - \frac{2I_m}{\pi b^{2m+1}}\sqrt{\frac{c}{\sigma}}mr^{m-1}senm\vartheta \frac{1}{|z|^{1/2}}$$

$$B_\vartheta = E_r - \frac{2I_m}{\pi b^{2m+1}}\sqrt{\frac{c}{\sigma}}mr^{m-1}cosm\vartheta \frac{1}{|z|^{1/2}}$$

Similar to the case $m = 0$, for $z > 0$ the fields vanishes due to causality. From equations (2.18) shows that the longitudinal component of electric field decreases as $|z|^{-3/2}$ and the transverse field components of electric field decrease as $|z|^{-5/2}$.

Unlike the case $m = 0$ the longitudinal component of magnetic field decreases as $|z|^{-3/2}$ and the transverse field components of magnetic field decrease as $|z|^{-1/2}$.

If $|z| \ll b\,\chi^{1/3}$ the constant A is:

$$A \approx -j\frac{4I_m(m+1)}{kb^{2m+2}}$$

2.2 Wake function

Wake functions can be defined in principle for particle velocities $v < c$ in the case of closed cavities or more general geometries. For high-energy accelerators it is sufficient to compute the wake function in the limit $v \to c$.

One assumes that the walls are perfectly conducting and that the considered structures are straight. In order to determine the motion of charged particles it is sufficient to study only their integrated interaction with the electromagnetic fields. The wake functions are defined as integrals over the normalized forces due to the electromagnetic fields excited in a structure by a point charge q and evaluated at a distance s behind it. According to the direction of the integrated forces we distinguish between *longitudinal and transverse wake functions*. One assumes that the charge moves unperturbed along a straight trajectory with ultra-relativistic constant velocity ($v \approx c$). A direct consequence of this is the vanishing of the wake function everywhere ahead of the exciting charge. This is often referred to as *causality*, but it expresses the fact that the fields, which propagate at most with velocity of light, cannot get ahead of particles when they move with the same speed. In reality, since particles must always be slower than light velocity, the fields can get far ahead in sufficiently long time, without violating any causality principle. These fields are weakened by wall dissipation and by reflections from obstacles in the beam pipe, so they can be neglected in most cases. Another important property is the *Fundamental Theorem of beam loading* that shows that the center of a bunch sees only the effect of half the charges. Finally one can say that the first maximum of the wake function is the largest extreme, so it is not possible to accelerate a second particle on the same trajectory to more than twice the energy of the first one before it has lost all its energy. The calculation of wake functions is possible through analytic methods for simplified geometries but also through numerical methods which work both in the time and frequency domain. In the time domain the solution of Maxwell's equations leads to find fields excited by distributions of finite length, i.e. bunches of particles. In this case the wake function cannot be compute exactly but one can have only an approximation by calculating the wake potential of a very short bunch. In the frequency domain the wake functions can be approximated by computing a large number of resonances of a structure. [2]

2.2.1 Longitudinal wake function

The *longitudinal wake function* [2] is obtained by integrating over the longitudinal component of the electric field E_z normalized by a test charge q which moves along a trajectory parallel to the axis of the structure:

$$G_{\parallel}(\boldsymbol{r}_b, \boldsymbol{r}_e, s) = -\frac{1}{q}\int_{-\infty}^{\infty} dz E_z\left(\boldsymbol{r}_b, \boldsymbol{r}_e, z, t = \frac{z+s}{c}\right) \qquad (2.19)$$

where $\boldsymbol{r}_b$ is the transverse offset of the test charge, $\boldsymbol{r}_e$ is the transverse offset of the exciting charge and s is the distance at which the test charge travels behind the exciting charge. One can express the longitudinal wake function as an expansion in azimuthal modes. For structures with axial symmetry it is most appropriate to use cylindrical coordinates r, ϑ, s :

$$G_{\parallel}(r_b, r_e, \vartheta_b, \vartheta_e, s) = \sum_{m=0}^{\infty} \varepsilon_{mo} r_b^m r_e^m cosm(\vartheta_e - \vartheta_b) G_{\parallel}{}^m(s) \qquad (2.20)$$

where: $\varepsilon_{mo} = \begin{cases} 1 & per\ m = 0 \\ 2 & per\ m \neq 0 \end{cases}$

r_b, ϑ_b are the radial and azimuthal offset of the test charge

r_e, ϑ_e are the radial and azimuthal offset of the exciting charge

The test charge follows the same trajectory of the exciting one, in fact $r_b = r_e$ and $\vartheta_b = \vartheta_e$. Furthermore the functions $G_{\parallel}{}^m(s)$ express the dependence on the longitudinal distance s between the two charges. The numerical calculation of the longitudinal wake functions is speeded by a technique of integration, different from that along the axis, which limits the integration interval to the finite length of the gap cavity at the radius of the beam pipe. [2]

2.2.2 Transverse wake function

The *transverse wake function* is the integral over the transverse electromagnetic forces along a straight path at a distance s behind an exciting point charge, travelling with ultra-relativistic velocity, and divided by the value of the charge: [2]

$$\boldsymbol{G}_{\perp} = \frac{1}{q}\int_{-\infty}^{\infty} dz\ (\boldsymbol{E} + \boldsymbol{v} \times \boldsymbol{B})_{\perp} \tag{2.21}$$

This definition can be used for structures without any symmetry, but in general, since the transverse wake function is a vector with a component along the horizontal direction and with a component along the vertical direction, for symmetric structures the horizontal wake function is calculated for a purely horizontal offset and the vertical wake for a purely vertical offset. Therefore, since the more common structures used in accelerators have one or more symmetry planes one can see that the wake function is proportional to the displacement of the trajectory. For this reason it is important to re-define the transverse wake function as the integral over the force normalized by the dipole moment of the charge $q\xi$: [2]

$$\boldsymbol{G}_{\perp}{}' = \frac{1}{q\xi}\int_{-\infty}^{\infty} dz\ (\boldsymbol{E} + \boldsymbol{v} \times \boldsymbol{B})_{\perp} \tag{2.22}$$

The equation (2.22) represents the dipole transverse wake function independent on the location of the integration path. For structures with axial symmetry it is useful to use the cylindrical coordinates r, ϑ ,s:

$$\boldsymbol{G}'_{\perp}(r,\vartheta,s) = \sum_{m=1}^{\infty} {r_b}^{m-1}{r_e}^{m}\left[\hat{r}\ cosm\vartheta - \hat{\vartheta}\ senm\vartheta\right] G_{\perp}^{m}(s) \tag{2.23}$$

2.3 Wake potential

The *wake potential* is defined as the integral over the electromagnetic forces exerted by wake fields at the position of a test charge following on the same trajectory. The exciting charge is now a bunch of particles of finite length and whose distance to the test charge $s = v\,\tau$, is measured from the bunch centre. The wake functions are, therefore, the wake potentials of a delta function distribution and can be considered Green's functions for the wake potentials of a finite distribution in the structure considered. [2]

2.3.1 Longitudinal wake potential

The *longitudinal wake potential* for a bunch of arbitrary shape can be found from the convolution of the longitudinal wake function with the normalized line density $\lambda(\tau)$: [2]

$$W_{\parallel}(\tau) = \int_{-\infty}^{\tau} dt\; G_{\parallel}(\tau - t)\lambda(t) = \int_{0}^{\infty} dt G_{\parallel}(t)\lambda(\tau - t) \qquad (2.24)$$

One can use particular methods to determine longitudinal wake potentials numerically. One of these is to decompose an arbitrary distribution into an infinite series of orthogonal polynomials whose coefficients are obtained using the orthogonality of the expansion functions. The wake potentials of the higher order polynomials can be computed directly or derived by numerical differentiation of the wake potential of the corresponding basis functions. These wake potentials are stored in appropriate tables to speed up simulation of particle motion. This method has a problem due to the limited accuracy which leads to a subsequent truncation of the expansion at a relatively low order. This type of limitation is removed by using simpler but not orthogonal expansion functions, such as rectangular or triangular bases. For example, the expansion in rectangular bases yields a rough approximation of the distribution with discontinuous steps, while an expansion in triangular bases yields a piecewise linear approximation of the distribution. [2]

2.3.2 Transverse wake potential

Similar to the longitudinal case, when one assumes a constant displacement of the bunch from the axis, the *transverse wake potential* is: [2]

$$W_{\perp}(\tau) = \int_{-\infty}^{\tau} dt\; G_{\perp}(\tau - t)\lambda(t) = \int_{0}^{\infty} dt\; G'_{\perp}(t)\lambda(\tau - t) \qquad (2.25)$$

If the bunch has several displacements $\xi(\tau)$, the function $\lambda(\tau)$ is replaced by $\xi(\tau)\lambda(\tau)$ and the result is divided by the average displacement $\bar{\xi}$:

$$W_{\perp}(\tau) = \frac{1}{\bar{\xi}} \int_{0}^{\infty} dt\;\; G'_{\perp}(t)\; \lambda(\tau - t)\;\; \xi(\tau - t) \qquad (2.26)$$

2.4 Coupling impedance

The concept of impedance, useful for solving problems in the frequency domain, comes from the application of Ohm's law:

$$V = R \cdot I$$

where V is the voltage drop across a resistance R traversed by a current I which can be Direct (DC) or Alternating (AC). In this case the resistance R is replaced by a complex impedance $Z = R + jX$, where the real part R is the resistance and the imaginary part X is the reactance.

In particle accelerators the current consists of a beam of charged particles moving in high vacuum. The electromagnetic fields, excited by the moving charges, induce currents and voltages in the surrounding vacuum chamber walls. The relationship between the currents and voltages is related to the concept of *coupling impedance* [2].

The impedance can be calculated analytically only for few and idealized structures or numerically for more complicated geometries, expanding the solutions into infinite series and computing the expansion coefficients. According to the direction of the electromagnetic fields the impedance is divided into two components: longitudinal and transverse. The latter is divided in turn into other two components: horizontal or radial and vertical or azimuthal [2]. For structures with axial symmetry it is sufficient to compute only the single transverse impedance since the horizontal and vertical components have equal values but opposite signs.

2.4.1 Longitudinal coupling impedance

For a beam moving with constant velocity v at an offset $\boldsymbol{r}_b$ from the z-axis, the *longitudinal coupling impedance* is the integral over the only electric force which acts on the beam along the direction of beam motion: [2]

$$Z_{\parallel}(\boldsymbol{r}_b, \omega) = -\frac{1}{\tilde{I}} \int_{-\infty}^{\infty} dz\, \tilde{E}_z\,(\boldsymbol{r}_b, z) e^{jkz} \tag{2.27}$$

For an ultra-relativistic beam the *longitudinal coupling impedance* is the Fourier transform of the longitudinal wake function: [2]

$$Z_{\parallel}(\omega) = \int_{-\infty}^{\infty} d\tau\, G_{\parallel}(\tau)\, e^{-j\omega\tau} \tag{2.28}$$

with the inverse transformation:

$$G_{\parallel}(\tau) = \int_{-\infty}^{\infty} \frac{d\omega}{2\pi} Z_{\parallel}(\omega) e^{j\omega\tau} \tag{2.29}$$

Since the wake function is a purely real function, the real and imaginary parts can be written as cosine and sine transforms:

$$ReZ_{\parallel}(\omega) = \int_{-\infty}^{\infty} d\tau\ G_{\parallel}(\tau)\cos(\omega\tau)$$

$$ImZ_{\parallel}(\omega) = -\int_{-\infty}^{\infty} d\tau\ G_{\parallel}(\tau)\,\mathrm{sen}(\omega\tau) \qquad (2.30)$$

From equations (2.30) it follows that the real part is symmetric, while the imaginary one is anti-symmetric.

2.4.2 Transverse coupling impedance

In the case of *transverse coupling impedance* both electric and magnetic field components act on the beam through the Lorentz force:

$$\boldsymbol{F}_{\perp} = q[\boldsymbol{E}_{\perp} + (\boldsymbol{v}\times\boldsymbol{B})_{\perp}] \qquad (2.31)$$

The integral over this force is normalized by the transverse moments of charge $q\boldsymbol{r}_b$: [2]

$$\boldsymbol{Z}_{\perp}(\boldsymbol{r}_b,\omega) = \frac{j}{q\boldsymbol{r}_b}\int_{-\infty}^{\infty} dz\ \left[\widetilde{\boldsymbol{E}}(\boldsymbol{r}_b,z) + \boldsymbol{v}\times\widetilde{\boldsymbol{B}}(\boldsymbol{r}_b,z)\right]_{\perp} e^{j\omega z/v} \qquad (2.32)$$

In general, the transverse impedance has two spatial components, horizontal or radial directed along x-axis and vertical or azimuthal along y - axis : [2]

$$Z_x(\omega) = \frac{j}{x_b\tilde{I}}\int_{-\infty}^{\infty} dz\ \left[\tilde{E}_x(z) - v_z\,\tilde{B}_y(z)\right]_{|x=x_b,y=0}\ e^{jkz} \qquad (2.33)$$

$$Z_y(\omega) = \frac{j}{y_b\tilde{I}}\int_{-\infty}^{\infty} dz\ \left[\tilde{E}_y(z) + v_z\,\tilde{B}_x(z)\right]_{|x=0,y=y_b}\ e^{jkz} \qquad (2.34)$$

2.4.3 General properties

Coupling impedances have some important properties that are useful to simplify impedance calculations and to verify their correctness. The first is the symmetry of the real and imaginary parts of the impedances with respect to frequency: [2]

$$Z_{\parallel}(-\omega) = {Z_{\parallel}}^{*}(\omega) \tag{2.35}$$

$$Z_{\perp}(-\omega) = -{Z_{\perp}}^{*}(\omega) \tag{2.36}$$

This implies that the real part of the longitudinal impedance and the imaginary one of the transverse impedance are even functions of frequency. On the other hand the imaginary part of the longitudinal impedance and the real one of the transverse impedance are odd functions of frequency. A second property concerns the causality, i.e. the impedances must not have singularities in the upper complex plane of frequency. It follows from Cauchy Theorem that the real and imaginary parts of the impedances must be related by the Hilbert transforms: [2]

$$\begin{aligned}
Re\, Z_{\parallel}(\omega) &= \frac{1}{\pi}\, PV \int_{-\infty}^{\infty} d\omega' \frac{Im\, Z_{\parallel}(\omega')}{\omega' - \omega} \\
Im\, Z_{\parallel}(\omega) &= -\frac{1}{\pi}\, PV \int_{-\infty}^{\infty} d\omega' \frac{Re\, Z_{\parallel}(\omega')}{\omega' - \omega} \\
Re\, Z_{\perp}(\omega) &= \frac{1}{\pi}\, PV \int_{-\infty}^{\infty} d\omega' \frac{Im\, Z_{\perp}(\omega')}{\omega' - \omega} \\
Im\, Z_{\perp}(\omega) &= -\frac{1}{\pi}\, PV \int_{-\infty}^{\infty} d\omega' \frac{Re\, Z_{\perp}(\omega')}{\omega' - \omega}
\end{aligned} \tag{2.37}$$

2.4.4 The Panofsky – Wenzel Theorem

There exist relations between the transverse derivative of the longitudinal wake function and the longitudinal derivative of the transverse wake function. Similar relations are valid also for the impedances. The only condition necessary is that the transverse components of the particle velocity can be neglected and its longitudinal component is constant [2]. The trajectory of the exciting point charge is assumed parallel to the z- axis. One considers the following Maxwell's equation:

$$\nabla \times \boldsymbol{E} = -\frac{\partial \boldsymbol{B}}{\partial t} \tag{2.38}$$

which yields the magnetic induction $\boldsymbol{B}$:

$$\boldsymbol{B} = -\int_{t_1}^{t} dt\ \nabla \times \boldsymbol{E} \tag{2.39}$$

The Lorentz force, acting on the trailing particle, can be written as:

$$\boldsymbol{F} = q\left[\boldsymbol{E} - \boldsymbol{v} \times \int_{t_1}^{t} dt'\ \nabla \times \boldsymbol{E}\right] \tag{2.40}$$

Assuming the particle velocity constant the equation (2.40) becomes:

$$\boldsymbol{F} = q\left[\boldsymbol{E} - \int_{t_1}^{t} \nabla\,(\boldsymbol{v} \cdot \boldsymbol{E}) - \boldsymbol{v}\,(\nabla \cdot \boldsymbol{E}) dt'\right] \tag{2.41}$$

One separates the longitudinal and transverse components:

$$F_{\parallel} = q\,E_z \qquad , \qquad \boldsymbol{F}_{\perp} = q\left[\boldsymbol{E}_{\perp} - v\int_{t_1}^{t} dt'\left(\nabla_{\perp} E_z - \frac{\partial \boldsymbol{E}_{\perp}}{\partial z}\right)\right] \tag{2.42}$$

Using the definitions of the longitudinal and the transverse wake functions one obtains:

$$G_{\parallel}(\boldsymbol{r}_q, \boldsymbol{r}_e, s) = -\frac{1}{q}\int_{-\infty}^{\infty} dt' E_{z|(r_q, r_e, z=vt'-s, t')} \tag{2.43}$$

$$\boldsymbol{G}_{\perp}(\boldsymbol{r}_q, \boldsymbol{r}_{\perp}, s) = \frac{v}{q}\int_{-\infty}^{\infty} dt \left[\boldsymbol{E}_{\perp} - v\int_{t_1}^{t} dt' \left(\nabla_{\perp} E_z - \frac{\partial \boldsymbol{E}_{\perp}}{\partial z}\right)\right]_{|(r_q, r_e, z=vt'-s, t')} \tag{2.44}$$

The desired relation is: [2]

$$\frac{\partial \boldsymbol{G}_{\perp}}{\partial s}|(\boldsymbol{r}_q, \boldsymbol{r}_e, s) = \nabla_{\perp} G_{\parallel}(\boldsymbol{r}_q, \boldsymbol{r}_e, s) \tag{2.45}$$

One obtains a similar relation also for the impedances: [2]

$$\boldsymbol{Z}_{\perp}(\omega, \boldsymbol{r}_e) = \frac{v}{\omega}\, \nabla_{\perp} Z_{\parallel}(\omega, \boldsymbol{r}_e) \tag{2.46}$$

2.5 Loss Factors

As the beam traverses an impedance, it loses a certain amount of energy which is referred to as the *Parasitic Loss.* Physically this is because particles exert forces on each other and the energy gain of one particle necessarily means energy loss of an equal amount by another particle. The calculation of energy loss of bunched beams, passing through vacuum chambers of high energy particle accelerators, can be simplify by the use of *Loss Factor.* The energy lost by the beam has to restored so as not to cause overheating of sensitive elements of chamber which could be deformed or even destroyed by too high temperatures. The concept of a loss factor has been generalized to include the change of energy loss with displacement of the beam trajectory, supposed usually parallel to the axis. One can divide the *longitudinal loss factor* from the *transverse loss factor* which is often called *kick factor*. [2]

2.5.1 Longitudinal Loss Factor

The quantity of energy, which is changed into a structure, is the product of its charge q and the induced voltage $V_{ind} = -Z_{\|} I_b = -Z_{\|} \frac{q\omega_0}{2\pi}$. The total energy change is proportional to the square of the charge and can be written as:

$$\Delta\epsilon = -k_{\|} q^2 \tag{2.47}$$

where the proportionality factor $k_{\|}$ is called *longitudinal Loss Factor.* In the frequency domain it is given by the infinite sums: [2]

$$k_{\|} = \frac{\omega_0}{2\pi} \sum_{p=-\infty}^{\infty} Z_{\|}\,(p\omega_0) h(p\omega_0) \tag{2.48}$$

where $h(\omega) = \tilde{\lambda}(\omega)\tilde{\lambda}^*(\omega)$ is the power density of the particle distribution. Since the infinite sums are often difficult to evaluate one tends to replace them by integrals limited to positive frequencies. Therefore, since the loss factor depends not only on the structure but also on the bunch shape, it can be expressed by the integral in terms of rms length σ: [2]

$$k_{\|}(\sigma) = \frac{1}{2\pi} \int_{-\infty}^{\infty} d\omega\; Z_{\|}(\omega) h(\omega, \sigma) \tag{2.49}$$

Since the power density is also an even function of frequency, while the imaginary part of an impedance is odd, their product does not contribute to the integral which extends over both frequencies. Hence it is sufficient to integrate only over the even real part of the impedance along the positive frequencies and double the result to obtain: [2]

$$k_{\|}(\sigma) = \frac{1}{\pi} \int_{0}^{\infty} d\omega\;\; Re\big[Z_{\|}(\omega)\big]\, h(\omega, \sigma) \tag{2.50}$$

In the time domain the loss factor is obtained by integrating the product of the longitudinal wake potential and the line density of the particle distribution:

$$k_{\parallel}(\sigma) = \int_{-\infty}^{\infty} d\tau \; W_{\parallel}(\tau)\lambda(\tau) \tag{2.51}$$

Since this integral is difficult to evaluate, one often prefers an alternate method which consists to express the longitudinal wake potential as a convolution with the longitudinal wake function:

$$k_{\parallel}(\sigma) = \int_{0}^{\infty} dt \; G_{\parallel}(t)S(t) \tag{2.52}$$

where:

$$S(t) = \int_{-\infty}^{\infty} d\tau \; \lambda(\tau)\lambda(\tau - t) \tag{2.53}$$

is the auto - correlation function of the line density.

2.5.2 Transverse Loss Factor

The *transverse Loss Factor,* in the frequency domain, is: [2]

$$k_{\perp}(\sigma) = \frac{1}{2\pi} \int_{-\infty}^{\infty} d\omega \; Z_{\perp}(\omega)h(\omega,\sigma) = \frac{1}{\pi} \int_{0}^{\infty} d\omega \; Im[Z_{\perp}(\omega)] \; h(\omega,\sigma) \tag{2.54}$$

Its definition is similar to the longitudinal case. Hence in the time domain one obtains:

$$k_{\perp}(\sigma) = \int_{-\infty}^{\infty} d\tau \; W_{\perp}(\tau)\lambda(\tau) = \int_{0}^{\infty} dt \; G_{\perp}(t)S(t) \tag{2.55}$$

2.6 Beam Instabilities

The parasitic loss is the main responsible for the various collective beam instabilities. The instability mechanisms are illustrated using a model in which the beam is represented as one or two macro-particles. In one-particle model, the bunch is a single rigid point charge N_e which consists of N particles of charge e, whose only motion allowed is its center of charge motion. In a two-particle model, the bunch is represented as two rigid point charges $N_e/2$, one leading and another trailing at a distance $|z|$ behind, whose center of charge is free to move. These charges interact with the accelerator environment and with each other through the wake fields. There exist three types of instabilities corresponding, respectively, to the components of the wake field for $m = 0, m = 1, m = 2$: [4]

- $m = 0$, causes a parasitic energy loss and an energy spread across the length of the bunch
- $m = 1$, causes a dipole mode instability called *beam breakup effect*
- $m = 2$, causes a beam breakup in the quadrupole mode

The $m = 0$ wake field, excited by the beam, produces a longitudinal force on particles in the beam which is a retarding voltage causing energy changes of individual particles. In a one-particle model the parasitic loss per particle is: [4]

$$\Delta E = -\frac{1}{2} N_e^2 G_{0\parallel}(z = 0^-) \tag{2.56}$$

where $G_{0\parallel}$ is the longitudinal wake function for $m = 0$.
In two-particle model the parasitic loss per particle in the leading particle is half of that for one-particle model. The trailing particle, due to the wake field left behind by the leading particle, loses an energy of:

$$\Delta E = -\frac{1}{2} N_e^2 G_{0\parallel}(z) \tag{2.57}$$

The energy spread is:

$$\frac{\Delta E}{E} \approx \frac{\frac{1}{2}N_e^2 G_{0\parallel}}{GL_0} \approx \frac{\frac{1}{2}N_e^2}{Gb^2} \tag{2.58}$$

where G is the acceleration gradient, $G_{0\parallel} \approx \frac{L_0}{b^2}$ is the longitudinal wake function for $m = 0$ and b is the vacuum chamber radius characterizing the size of the accelerating cavities. Generally, particles ahead of the bunch lose energy due to the wake field, while particles in the back of the bunch can gain or lose energy, depending on the length of the bunch.

The $m = 1$ wake produces a transverse wake force connected with the transverse wake potential, $W_{1\perp}(z)$. It has also a dipole longitudinal wake force connected with the longitudinal wake potential, $W_{1\parallel}(z)$, that affects the beam energy spread. For this wake the one-particle model is not very useful so one prefers to use a two-particle model with a leading particle, unperturbed by its own transverse wake field, with displacement y_1 and a trailing particle, which is a distance |z| behind and has a displacement y_2. This implies that a particle in the trailing macro-particle sees, in addition to a transverse wake potential $-\frac{1}{2}N_e^2 W_{1\perp}(z)$, a longitudinal wake potential. So one has: [4]

$$\Delta E = -\frac{1}{2}N_e^2 W_1(z)\mathrm{y}_1\mathrm{y}_2 \tag{2.59}$$

The equation (2.59) represents the energy spread in the beam that depends on both the longitudinal and transverse positions of the particle, in contrast with the $m = 0$ wake force, where the energy spread depends only on the longitudinal position of the particle. The $m = 2$ wake causes a quadrupole beam breakup instability that becomes significant when the transverse beam size is comparable to the pipe radius. What happens then is that the quadrupole wake field, generated by the bunch head, perturbs the focusing force on the bunch tail, leading to an instability if the beam is sufficiently intense. [4]

Chapter 3

Wake fields of Bunched Beams in Rings with Resistive Walls of Finite Thickness

The electromagnetic interaction between a particle beam and the surrounding pipe wall in an accelerator is described by wake fields. For perfectly conducting pipes and ultra-relativistic particles ($v = c$), wake fields are negligible while, they become relevant in the realistic case of walls of finite conductivity, acting back on the beam, perturbing its motion and leading to collective instability and eventual beam loss. For low revolution frequencies, the finite wall thickness must be taken into account in describing electromagnetic penetration into the pipe wall [5]. The first to study the wake field was N. Piwinski [6], who studied the case of a metal-coated ceramic vacuum chamber under the assumption of a skin depth much thinner than the thickness of the conductive coating. N. Piwinski [6] also computed the fields for the monopole term for a bunched beam with Gaussian distribution in the longitudinal direction. L. Palumbo and V. G. Vaccaro [7] then extended Piwinski's results by computing higher order wake field multipoles. A. W. Chao [4] first gave a formula which fully exploits the dependence of the wake field on the pipe wall thickness by limiting the analysis to the monopole term under suitable conditions. Finally, Y. Yokoya and K. Shobuda [8] studied the finite conductivity and thickness of the pipe wall, in the frame of a transmission line analogy, which can be applied to beam pipes with general transverse geometry and multi-layered walls, in the limit where the skin depth is much smaller than the pipe transverse dimension.

In this chapter the authors, L. Cappetta and I. M. Pinto [11] ,solve the problem in full generality.

In Section 3.1 it is given the general solution of the problem by computing the Fourier transform of the wake potential Green's function produced by a point particle running at constant velocity $\beta c\hat{u}_z$, at a distance r_0 off-axis of a circular cylindrical pipe with radius b, wall conductivity σ and thickness Δ. The solution found is exact but complicated, so that in most cases of practical interest one may resort to suitable limit forms.

Section 3.2 contains the appropriate boundary conditions.

In Section 3.3 the spectral features of a bunched beam in a closed-ring machine are introduced.

In Sections 3.4, 3.5 several asymptotic approximations for different prototype ring machines, such as LHC and DAΦNE, are introduced.

In Section 3.6 the authors switch back to the space-time domain, and evaluate the wake potential multipoles for a multi-bunched beam in a circular accelerator.

Finally in Section 3.7 it is treated the effects of finite wall conductivity and thickness on Tune Shift.

3.1 Wake field

In this section it is computed the Fourier transform of the wake potential Green's function produced by a point charge q_0 running at a constant velocity $\beta c\hat{u}_z$, at an azimuthal coordinate ϑ_0 and a distance r_0 off-axis of a circular cylindrical pipe with inner radius b, conductivity σ and finite thickness Δ [11]. L. Cappetta and I. M. Pinto compute the Green's function (See Appendix C) and the corresponding boundary conditions (See Appendix B) for the following regions:

- Within the hollow pipe ($r_0 \leq r \leq b, r \leq r_0$)
- Inside the vacuum chamber ($b \leq r \leq b + \Delta$)
- Outside the beam ($r > b + \Delta$)

The charge density of a bunched beam running parallel to the pipe axis can be written as the product of a transverse and longitudinal density:

$$\rho(r,\vartheta,\xi) = \rho_t(r,\vartheta) f(\xi) \tag{3.1}$$

where r and ϑ are the radial and azimuthal coordinates, and ξ depends on the time variable t and on the longitudinal coordinate z through the relation $\xi = z - \beta ct$. The associated scalar potential Φ depends in turn on z and t only through ξ, and the wave equation for Φ is:

$$\nabla_t^2 \Phi + \frac{1}{\gamma^2}\frac{\partial^2 \Phi}{\partial \xi^2} = -\frac{\rho(r,\vartheta,\xi)}{\varepsilon_0} \tag{3.2}$$

where $\gamma = (1-\beta^2)^{-1/2}$.

Given the point source:

$$\delta(r,\vartheta,\xi|r_0,\vartheta_0,\xi_0) = \frac{\delta(r-r_0)}{r_0}\delta(\vartheta-\vartheta_0)\delta(\xi-\xi_0) \tag{3.3}$$

in view of the obvious representation:

$$\rho(r,\vartheta,\xi) = \int_0^{2\pi} r_o d\vartheta_0 \int_0^b dr_0 \int_{-\infty}^{+\infty} d\xi_0 \, \rho_t(r_0,\vartheta_0)\, f(\xi_0)\, \delta(r,\vartheta,\xi|r_0,\vartheta_0,\xi_0) \tag{3.4}$$

and of the linearity of equation (3.2),

the general solution of equation (3.2) can be written as:

$$\Phi(r,\vartheta,\xi) = \int_0^{2\pi} r_o d\vartheta_0 \int_0^b dr_0 \int_{-\infty}^{+\infty} d\xi_0 \, \rho_t(r_0,\vartheta_0)\, f(\xi_0)\, G(r,\vartheta,\xi|r_0,\vartheta_0,\xi_0) \tag{3.5}$$

where the Green's function G is the solution of:

$$\nabla_t^2 G + \frac{1}{\gamma^2}\frac{\partial^2 G}{\partial \xi^2} = -\frac{\delta(r,\vartheta,\xi|r_0,\vartheta_0,\xi_0)}{\varepsilon_0} \tag{3.6}$$

The Green's function $G(\cdot)$ admits the following Fourier representation where $\phi = \vartheta - \vartheta_0$ and $s = \xi - \xi_0$:

$$G(s, r, r_0, \phi) = \sum_{m=-\infty}^{+\infty} G_m(s, r, r_0) e^{jm\phi} \tag{3.7}$$

where:

$$G_m(s, r, r_0) = \frac{1}{2\pi} \int_{-\infty}^{+\infty} \tilde{G}_m(k, r, r_0) e^{jks} dk \tag{3.8}$$

Using equations (3.7),(3.8) into (3.5) one obtains:

$$\Phi(r, \phi, s) = \frac{1}{2\pi} \sum_{m=-\infty}^{+\infty} e^{jm\phi} \left(\int_0^b r_0 \, dr_0 \; \rho_{t,m}(r_0) \right) \int_{-\infty}^{+\infty} \tilde{G}_m(k, r, r_0) \, F(k) e^{jks} dk \tag{3.9}$$

where:

$$\rho_{t,m}(r_0) = \frac{1}{2\pi} \int_0^{2\pi} \rho_t(r_0, \vartheta_0) e^{jm\vartheta_0} d\vartheta_0 \tag{3.10}$$

$$F(k) = \int_{-\infty}^{+\infty} f(s) e^{-jks} ds \tag{3.11}$$

are the m-th azimuthal harmonics of the transverse source density ρ_t, and the Fourier transform of the longitudinal source profile. [11]

Using equation (3.7) and substituting the following identities:

$$\delta(s) = \frac{1}{2\pi} \int_{-\infty}^{+\infty} e^{jks} dk \quad , \quad \delta(\phi) = \frac{1}{2\pi} \sum_{m=-\infty}^{+\infty} e^{jm\phi} \tag{3.12}$$

in equation (3.6) one obtains a differential equation for $\tilde{G}_m(k, r, r_0)$:

$$\frac{d^2 \tilde{G}_m}{dr^2} + \frac{1}{r} \frac{d\tilde{G}_m}{dr} - \left[\frac{m^2}{r^2} + \left(\frac{k}{\gamma} \right)^2 \right] \tilde{G}_m = -\frac{1}{2\pi\varepsilon_0} \frac{\delta(r - r_0)}{r_0} \tag{3.13}$$

whose solution is a superposition of modified Bessel functions I_m, K_m:

$$\tilde{G}_m(k,r,r_0) = \frac{q_0}{2\pi\varepsilon_0}\left\{\begin{pmatrix} K_m\left(\frac{kr}{\gamma}\right) & I_m\left(\frac{kr_0}{\gamma}\right) \\ K_m\left(\frac{kr_0}{\gamma}\right) & I_m\left(\frac{kr}{\gamma}\right) \end{pmatrix} + B_m I_m\left(\frac{kr}{\gamma}\right)\right\}, \quad r_0 \le r \le b, \;\; r \le r_0 \tag{3.14}$$

The constant B_m is determined by enforcing suitable boundary conditions at $r = b$.

For the special case of a perfectly conducting wall ($\sigma \to \infty$) one has: [11]

$$\tilde{G}_m^{\infty}(k,r,r_0) = \frac{q_0}{2\pi\varepsilon_0}\left\{\begin{pmatrix} K_m\left(\frac{kr}{\gamma}\right) & I_m\left(\frac{kr_0}{\gamma}\right) \\ K_m\left(\frac{kr_0}{\gamma}\right) & I_m\left(\frac{kr}{\gamma}\right) \end{pmatrix} - \frac{I_m\left(\frac{kr_0}{\gamma}\right)}{I_m\left(\frac{kb}{\gamma}\right)} K_m\left(\frac{kb}{\gamma}\right) I_m\left(\frac{kr}{\gamma}\right)\right\}, r_0 \le r \le b, r \le r_0 \tag{3.15}$$

where the constant B_m is determined from the boundary condition $\Phi(b,\phi,s) = 0$.

For a pipe with finite wall conductivity and thickness, in order to compute B_m, one has to write down the Green's function also in the regions $b \le r \le d$ and $r > d$, $d = b + \Delta$ being the external pipe radius.

In the finite thickness metal wall, $b \le r \le d$, the Green's function obeys the following equation:

$$\nabla_t^2 G^I + \frac{1}{\gamma^2}\frac{\partial^2 G^I}{\partial s^2} + \mu_0 \sigma \beta c \frac{\partial G^I}{\partial s} = 0 \tag{3.16}$$

where μ_0 is the vacuum magnetic permeability.

The general solution of equation (3.16) is:

$$G^I(s,r,r_0,\phi) = \frac{1}{2\pi}\sum_{m=-\infty}^{+\infty} e^{jm\phi}\int_{-\infty}^{+\infty} \tilde{G}_m^I(k,r,r_0)\, e^{jks} dk \tag{3.17}$$

Letting the solution (3.17) into (3.16) one obtains an homogeneous differential equation for $\tilde{G}_m^I$:

$$\frac{d^2\tilde{G}_m^I}{dr^2}+\frac{1}{r}\frac{d\tilde{G}_m^I}{dr}-\left(\frac{m^2}{r^2}+\bar{k}^2\right)\tilde{G}_m^I=0 \tag{3.18}$$

where:

$$\bar{k}=\sqrt{\left(\frac{k}{\gamma}\right)^2-j\sigma Z_0\beta k} \tag{3.19}$$

with $Z_0=\sqrt{\frac{\mu_0}{\varepsilon_0}}$ the vacuum characteristic impedance.

The solution of equation (3.18) is: [11]

$$\tilde{G}_m^I(k,r,r_0)=\frac{q_0}{2\pi\varepsilon_0}\left[C_mK_m(\bar{k}r)+D_mI_m(\bar{k}r)\right] \qquad b\le r\le d \tag{3.20}$$

where the constants C_m and D_m can be found by enforcing again suitable boundary conditions at $r=b$ and $r=d$.

In the external region, $r>d$, the Green's function is a solution of:

$$\nabla_t^2G^E+\frac{1}{\gamma^2}\frac{\partial^2G^E}{\partial s^2}=0 \tag{3.21}$$

whose solution is:

$$G^E(s,r,r_0,\phi)=\frac{1}{2\pi}\sum_{m=-\infty}^{+\infty}e^{jm\phi}\int_{-\infty}^{+\infty}\tilde{G}_m^E k,r,r_0)\,e^{jks}dk \tag{3.22}$$

Inserting equation (3.22) into (3.21) one has an homogeneous differential equation for $\tilde{G}_m^E$:

$$\frac{d^2\tilde{G}_m^E}{dr^2}+\frac{1}{r}\frac{d\tilde{G}_m^E}{dr}=0 \tag{3.23}$$

whose solution is: [11]

$$\tilde{G}_m^E(k,r,r_0) = \frac{1}{2\pi\varepsilon_0}[E_m K_m(kr)] \qquad r > d \tag{3.24}$$

where the constant E_m can be found by enforcing the boundary conditions at $r = d$.

3.2 Boundary conditions

The boundary conditions, which allow to determine the constants $\mathrm{B_m}$, $\mathrm{C_m}$, $\mathrm{D_m}$, $\mathrm{E_m}$, are obtained by enforcing the continuity of the tangential fields at $r = b$ and $r = d$. [11]

For $r \leq b$ and $r \geq d$ the vector potential in the Lorentz gauge is:

$$\boldsymbol{A} = \frac{\beta}{c} G \hat{u}_s \tag{3.25}$$

Therefore the fields in the region $r \leq b$ and $r \geq d$ are:

$$\boldsymbol{E} = -\nabla G - \frac{\partial \boldsymbol{A}}{\partial t} = -\nabla_t G - \left(\frac{\partial G}{\partial s} + \beta c \frac{\partial A_s}{\partial s}\right)\hat{u}_s = -\nabla_t G - \frac{1}{\gamma^2}\frac{\partial G}{\partial s}\hat{u}_s \tag{3.26}$$

$$\boldsymbol{H} = \frac{\beta}{Z_0}\nabla \times (G\hat{u}_s) \tag{3.27}$$

whence the tangential field components at $r = b$ are:

$$\begin{cases} \mathrm{E_s} = -\dfrac{1}{\gamma^2}\dfrac{\partial G}{\partial s} \\ \mathrm{H_\phi} = -\dfrac{1}{\mu_0}\dfrac{\partial A}{\partial r} = -\dfrac{\beta}{Z_0}\dfrac{\partial G}{\partial r} \end{cases} \tag{3.28}$$

Inserting equations (3.7),(3.8),(3.22),(3.24) into (3.28) one obtains the azimuthal harmonics of $\mathrm{E_s}$ and $\mathrm{H_\phi}$:

$$\begin{cases} \tilde{E}_{m,s}(k,r,r_0) = \dfrac{jk}{\gamma^2}\tilde{G}_m(k,r,r_0) \\ \tilde{H}_{m,\phi}(k,r,r_0) = -\dfrac{\beta}{Z_0}\dfrac{\partial \tilde{G}_m(k,r,r_0)}{\partial r} \end{cases} \quad r \le b \tag{3.29}$$

$$\begin{cases} \tilde{E}^E_{m,s}(k,r,r_0) = \dfrac{jk}{\gamma^2}\tilde{G}^E_m(k,r,r_0) \\ \tilde{H}^E_{m,\phi}(k,r,r_0) = -\dfrac{\beta}{Z_0}\dfrac{\partial \tilde{G}^E_m(k,r,r_0)}{\partial r} \end{cases} \quad r \ge d \tag{3.30}$$

Within the metal wall, $b \le r \le d$, the vector potential in the Lorentz gauge is: [7]

$$\boldsymbol{A} = A\hat{u}_s \qquad , \qquad \frac{\partial A}{\partial s} = -\mu_0\sigma G + \frac{\beta}{c}\frac{\partial G}{\partial s} \tag{3.31}$$

which translates in the k-domain as follows:

$$\tilde{A} = \left(\frac{\beta}{c} - \frac{\mu_0\sigma}{jk}\right)\tilde{G} \tag{3.32}$$

The fields in the region $b \le r \le d$ are thus:

$$\boldsymbol{E} = -\nabla G - \frac{\partial \boldsymbol{A}}{\partial t} = -\nabla_t G - \left(\frac{\partial G}{\partial s} + \beta c\frac{\partial A_s}{\partial s}\right)\hat{u}_s = -\nabla_t G - \left(\frac{1}{\gamma^2}\frac{\partial G}{\partial s} + \mu_0\sigma\beta c G\right)\hat{u}_s \tag{3.33}$$

$$\boldsymbol{H} = \nabla \times \left[\left(\frac{\beta}{Z_0}G - \sigma\int^S G(s',r,\vartheta)ds'\right)\hat{u}_s\right] \tag{3.34}$$

whence the tangential field components in the region $b \le r \le d$ are:

$$\begin{cases} \mathrm{E_s} = -\dfrac{1}{\gamma^2}\dfrac{\partial G}{\partial s} - \mu_0\sigma\beta c G \\ \mathrm{H_\phi} = -\dfrac{1}{\mu_0}\dfrac{\partial A}{\partial r} = -\dfrac{\beta}{Z_0}\dfrac{\partial G}{\partial r} + \sigma\displaystyle\int^S \frac{\partial G}{\partial r}(s',r,\vartheta)ds' \end{cases} \tag{3.35}$$

Inserting equations (3.17),(3.20) into (3.35) one gets the azimuthal field components in the wall:

$$\begin{cases} \tilde{E}^I_{m,s}(k,r,r_0) = \left(-\frac{jk}{\gamma^2} - \mu_0\sigma\beta c\right)\tilde{G}^I_m(k,r,r_0) = \frac{\bar{k}^2}{jk}\tilde{G}^I_m(k,r,r_0) \\ \tilde{H}^I_{m,\phi}(k,r,r_0) = \frac{Z_o\sigma - jk\beta}{jkZ_0}\frac{\partial\tilde{G}^I_m(k,r,r_0)}{\partial r} \end{cases} \qquad b \le r \le d \qquad (3.36)$$

Enforcing the continuity of the tangential field components at $r = b$ using equations (3.36),(3.29), and at $r = d$ using equations (3.36),(3.30), gives a linear system in the unknowns $\mathrm{B_m}$, $\mathrm{C_m}$, $\mathrm{D_m}$, $\mathrm{E_m}$ which yields the following solution for the Green's function in $r \le b$:

$$\tilde{G}_m(k,r,r_0) = \tilde{G}^{\infty}_m(k,r,r_0) + \frac{q_0}{2\pi\varepsilon_0}\left\{\frac{\gamma I_m\left(\frac{kr_0}{\gamma}\right)I_m\left(\frac{kr}{\gamma}\right)}{bkI_m\left(\frac{kb}{\gamma}\right)}\frac{N(k)}{D(k)}\right\} \qquad (3.37)$$

where:

$$N(k) = \bar{k}^2K'_m\left(\frac{kd}{\gamma}\right)\left[I_m(\bar{k}b)K_m(\bar{k}d) - I_m(\bar{k}d)K_m(\bar{k}b)\right] + \eta\frac{\bar{k}k}{\gamma}K_m\left(\frac{kd}{\gamma}\right)\left[K_m(\bar{k}b)I'_m(\bar{k}d) - I_m(\bar{k}b)K'_m(\bar{k}d)\right] \qquad (3.38)$$

$$D(k) = \bar{k}^2I'_m\left(\frac{kb}{\gamma}\right)K'_m\left(\frac{kd}{\gamma}\right)\left[I_m(\bar{k}b)K_m(\bar{k}d) - I_m(\bar{k}d)K_m(\bar{k}b)\right] + \eta\frac{\bar{k}k}{\gamma}I_m\left(\frac{kb}{\gamma}\right)K'_m\left(\frac{kd}{\gamma}\right)\left[K'_m(\bar{k}b)I_m(\bar{k}d) - I'_m(\bar{k}b)K_m(\bar{k}d)\right] + \eta\frac{\bar{k}k}{\gamma}K_m\left(\frac{kd}{\gamma}\right)I'_m\left(\frac{kb}{\gamma}\right)\left[K_m(\bar{k}b)I'_m(\bar{k}d) - I_m(\bar{k}b)K'_m(\bar{k}d)\right] + \eta^2\left(\frac{k}{\gamma}\right)^2I_m\left(\frac{kb}{\gamma}\right)K_m\left(\frac{kd}{\gamma}\right)\left[I'_m(\bar{k}b)K'_m(\bar{k}d) - I'_m(\bar{k}d)K'_m(\bar{k}b)\right] \qquad (3.39)$$

$$\eta = \frac{Z_o\sigma - jk\beta}{jk\beta} \qquad (3.40)$$

3.3 Bunched beams in a ring: Spectra

For storage rings and circular machines the beam is a periodic train of bunches, with spatial period $T_s = \frac{L_c}{N_b}$, where L_c is the ring circumference and N_b the total number of bunches.

The function $f(\cdot)$, into equation (3.1), is: [11]

$$f(s) = \sum_{n=-\infty}^{+\infty} f_n \, e^{j2\pi(N_b/L_c)ns} \tag{3.41}$$

where:

$$f_n = \frac{N_b}{L_c} \int_{[L_c/N_b]} f(s) e^{-j2\pi(N_b/L_c)ns} \, ds \approx \frac{N_b}{L_c} \mathcal{F}\left(2\pi \frac{N_b}{L_c} n\right) \tag{3.42}$$

where $\mathcal{F}$ is the Fourier transform of a single bunch with a length $\sigma_s \ll \frac{L_c}{N_b}$.

From equations (3.11),(3.41),(3.42) one obtains :

$$F(k) = \int_{-\infty}^{+\infty} f(s) e^{-jks} ds = 2\pi \left(\frac{N_b}{L_c}\right) \sum_{n=-\infty}^{+\infty} \mathcal{F}\left(2\pi \frac{N_b}{L_c} n\right) \delta\left(k - 2\pi \frac{N_b}{L_c} n\right) \tag{3.43}$$

Inserting equation (3.43) into (3.9) one has:

$$\Phi(r, \phi, s) = \sum_{m=-\infty}^{+\infty} e^{jm\phi} \left(\int_0^b r_0 dr_0 \, \rho_{t,m}(r_0) \right) \frac{N_b}{L_c} \sum_{n=-\infty}^{+\infty} \mathcal{F}\left(2\pi \frac{N_b}{L_c} n\right) \tilde{G}_m\left(2\pi \frac{N_b}{L_c} n, r, r_0\right) e^{j2\pi(N_b/L_c)ns} \tag{3.44}$$

The sums in equations (3.41),(3.43) and (3.44) can be truncated at $|n| \sim N_T$, where:

$$N_T \sim \frac{L_c}{2\pi N_b} \frac{\alpha}{\sigma_s} \tag{3.45}$$

, i.e. at the border of the single bunch spectrum $k_b \sim \frac{\alpha}{\sigma_s}$, where σ_s is the bunch length and α is a factor of order one.

Therefore the spectral argument k in functions $\tilde{G}_m(\cdot)$ and $\mathcal{F}(\cdot)$ in equation (3.44) takes only values that are integer multiples of the fundamental wave number:

$$k = \left(2\pi \frac{N_b}{L_c}\right) n \qquad \forall n = -N_T, \ldots., N_T \tag{3.46}$$

3.4 Asymptotic approximations

The solutions ever obtained are exact but of relatively little use in view of their rather complicated structure. For this reason, in most cases of practical interest, one may resort to suitable asymptotic limit forms since many problem specific parameters are either very large or very small.

In Section 3.4.1 the authors, L. Cappetta and I. M. Pinto, use an expansion valid for high values of conductivity, such that the parameters $\bar{k}b$ and $\bar{k}d$, in the spectral range of interest, are larger than unity. By exploiting the large argument forms of modified Bessel functions $I_m(\cdot)$, $K_m(\cdot)$ they give a simpler form of equation (3.37).

In Section 3.4.2 they focus on the parameters kb/γ and kd/γ. In the spectral range of interest, they turn out to be small and it is possibly to use the appropriate limiting forms of Bessel functions, so as to get a simple solution for the monopole term. For multipole terms a further limit is necessary.

Section 3.5 contains the applications of several asymptotic approximations to particular acceleration machines. For example, in Section 3.5.1 it is assumed $\left|\bar{k}d/\beta^2\gamma^2\right| < 1$, which applies to LHC and in Section 3.5.2 it is assumed $\left|\bar{k}d/\beta^2\gamma^2\right| > 1$, which applies to DAΦNE.

3.4.1 Large parameters

The following relations always hold in view of the assumed beam spectral features: [11]

$$|\bar{k}b| = \left|\sqrt{\left(\frac{k}{\gamma}\right)^2 - j\sigma\beta k Z_0}\right| b \sim \left|\sqrt{-j\sigma\beta k Z_0}\, b\right| \equiv \left|\frac{b}{\delta_{wall}}\right| \gg 1 \tag{3.47}$$

$$|\bar{k}d| = \left|\sqrt{\left(\frac{k}{\gamma}\right)^2 - j\sigma\beta k Z_0}\right| d \sim \left|\sqrt{-j\sigma\beta k Z_0}\, d\right| \equiv \left|\frac{d}{\delta_{wall}}\right| \gg 1 \qquad d \gtrsim b \tag{3.48}$$

where:

$$\delta_{wall} = (-j\sigma\beta k Z_0)^{-1/2} \tag{3.49}$$

is the complex electromagnetic skin depth.

Using the asymptotic large-argument forms for the modified Bessel functions with arguments $\bar{k}b$ and $\bar{k}d$:

$$I_m(z) \sim \frac{e^z}{\sqrt{2\pi z}} \quad , \quad K_m(z) \sim \sqrt{\frac{\pi}{2z}}\, e^{-z} \tag{3.50}$$

one gets a simpler form for both $N(k)$ and $D(k)$:

$$N(k) = -\bar{k}^2 K_m'\left(\frac{kd}{\gamma}\right) sinh\, \bar{k}\Delta + \eta \frac{\bar{k}k}{\gamma} K_m\left(\frac{kd}{\gamma}\right) cosh\, \bar{k}\Delta \tag{3.51}$$

$$\begin{aligned} D(k) = sinh\, \bar{k}\Delta \left[\left(\frac{k}{\gamma}\right)^2 \eta^2 I_m\left(\frac{kb}{\gamma}\right) K_m\left(\frac{kd}{\gamma}\right) - \bar{k}^2 I_m'\left(\frac{kb}{\gamma}\right) K_m'\left(\frac{kd}{\gamma}\right)\right] \\ + \eta \frac{\bar{k}k}{\gamma} \cosh \bar{k}\Delta \left[I_m'\left(\frac{kb}{\gamma}\right) K_m\left(\frac{kd}{\gamma}\right) - I_m\left(\frac{kb}{\gamma}\right) K_m'\left(\frac{kd}{\gamma}\right)\right] \end{aligned} \tag{3.52}$$

$$\eta \simeq -j\frac{Z_0\sigma}{k\beta} \tag{3.53}$$

The relative error stemming from use of equations (3.51),(3.52) into (3.37) is shown in **Fig. 3.1** as a function of kb, for the lowest order multipoles.
The absolute error within the spectral range of interest is $\sim 10^{-6} \div 10^{-7}$.

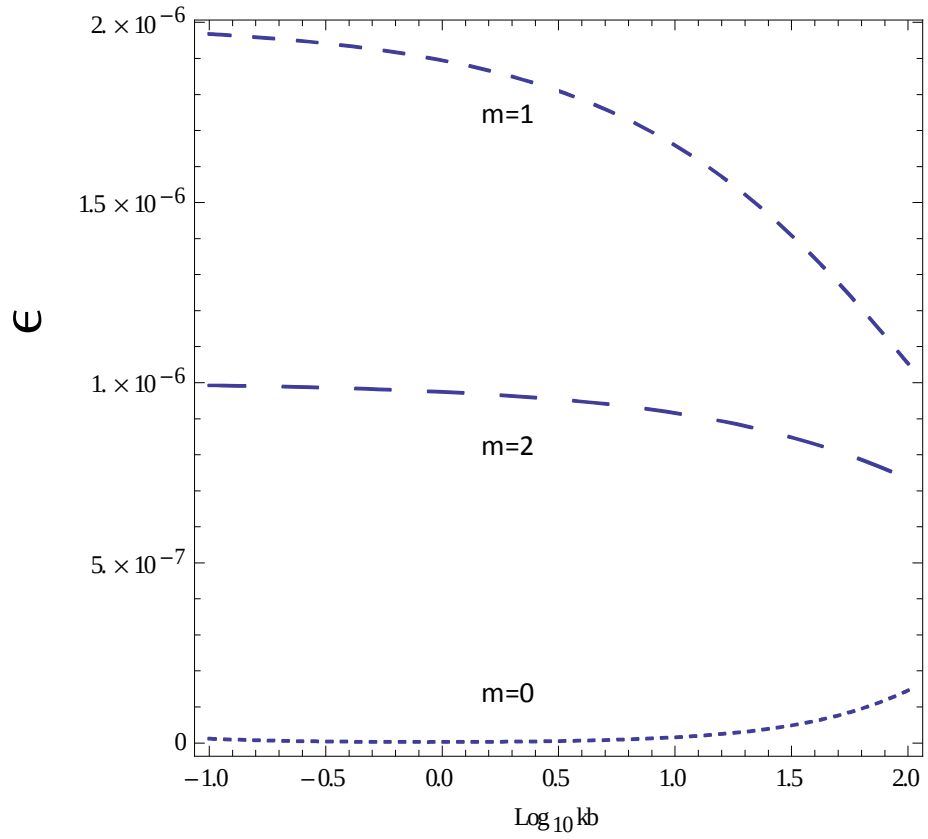

Fig. 3.1 Relative error $\epsilon = (2\pi\varepsilon_0/q)[\tilde{G}_m - \tilde{G}_m^{\infty}]$ versus kb after assuming $|\bar{k}b|$ >>1 and using equations (3.51),(3.52) in place of equation (3.37) for monopole, dipole and quadrupole terms (m=0,1,2).

3.4.2 Small parameters

In this case we assume the following relations: [11]

$$\frac{|k|b}{\gamma} \sim \frac{|k|d}{\gamma} \ll 1 \tag{3.54}$$

It is convenient to consider separately the monopole ($m = 0$) and multipole ($m \geq 1$) terms.

- Monopole term ($m = 0$)

The zero-th order modified Bessel functions approximation valid for small arguments ζ are: [12]

$$I_0(\zeta) \sim 1 \quad , \quad K_0(\zeta) = -\log(\zeta) \tag{3.55}$$

Using equations (3.51) and (3.52), the monopole term in equation (3.37) can be written as:

$$\tilde{G}_0(k, r, r_0) = \tilde{G}_0^{\infty}(k, r, r_0) + \frac{q_0}{2\pi\varepsilon_0}\frac{\gamma^2}{bk^2}\left[\frac{b}{2} + \eta\delta_{wall}\coth\left(\Delta/\delta_{wall}\right)\right]^{-1} \tag{3.56}$$

For a very thick pipe wall, $\left|\bar{\mathrm{k}}\Delta\right| \sim |\Delta/\delta_{wall}| \gg 1$, whence $|\coth\left(\Delta/\delta_{wall}\right)| \sim 1$, equation (3.56) becomes:

$$\tilde{G}_0(k, r, r_0) = \tilde{G}_0^{\infty}(k, r, r_0) + \frac{q_0}{2\pi\varepsilon_0}\frac{\gamma^2}{bk^2}\left(\frac{b}{2} + \eta\delta_{wall}\right)^{-1} \tag{3.57}$$

Assuming the further limit:

$$\left|\frac{2\eta\delta_{wall}}{b}\right| \gg 1 \tag{3.58}$$

the equation (3.58) becomes: [7]

$$\tilde{G}_0(k,r,r_0) = \tilde{G}_0^{\infty}(k,r,r_0) + \frac{q_0}{2\pi\varepsilon_0}(1+j)\frac{\beta\gamma^2}{b}\sqrt{\frac{\beta}{2\sigma Z_0 k}} \qquad (3.59)$$

For a finite thickness pipe wall, $|\Delta/\delta_{wall}| \geq 1$, equation (3.57) becomes:

$$\tilde{G}_0(k,r,r_0) = \tilde{G}_0^{\infty}(k,r,r_0) + \frac{q_0}{2\pi\varepsilon_0}(1+j)\frac{\beta\gamma^2}{b}\sqrt{\frac{\beta}{2\sigma Z_0 k}}\tanh(\Delta/\delta_{wall}) \qquad (3.60)$$

The relative error produced by using equation (3.60) in place of (3.37) is shown in **Fig. 3.2** as a function of kb.

- Multipole terms ($m \geq 1$)

The m-th order modified Bessel functions for small arguments ζ are: [12]

$$I_m(\zeta) \sim \left(\frac{\zeta}{2}\right)^m \frac{1}{m!} \quad , \quad K_m(\zeta) \sim \frac{(m-1)!}{\zeta}\left(\frac{\zeta}{2}\right)^{-m} \quad \forall m > 0 \qquad (3.61)$$

Hence, from equation (3.15):

$$\tilde{G}_m^{\infty}(r,r_0) \approx \tilde{G}_m^{\,free\ space}(r,r_0) - \frac{q_0}{2\pi\varepsilon_0}\frac{1}{2m}\left(\frac{rr_0}{b^2}\right)^m \qquad (3.62)$$

where:

$$\tilde{G}_m^{\,free\ space}(r,r_0) \approx \frac{q_0}{2\pi\varepsilon_0}\frac{1}{2m}\left(\frac{rr_0}{b^2}\right)^m \begin{cases} (r_0/r)^m & r_0 \leq r \leq b \\ (r/r_0)^m & r \leq r_0 \end{cases} \qquad (3.63)$$

Using equations (3.51) and (3.52), the multipole terms in equation (3.37) can be written as:

$$\tilde{G}_m(k,r,r_0) = \tilde{G}_m^{\infty}(k,r,r_0) + \frac{q_0}{2\pi\varepsilon_0}\frac{1}{m}\left(\frac{rr_0}{b^2}\right)^m \left[1 + \frac{k^2\eta b}{m\bar{k}\gamma^2}\tanh(\bar{k}\Delta)\frac{\frac{k^2\eta d}{m\bar{k}\gamma^2} + \coth(\bar{k}\Delta)}{\frac{k^2\eta d}{m\bar{k}\gamma^2} + \tanh(\bar{k}\Delta)}\right]^{-1} \tag{3.64}$$

Under the assumption of equations (3.49),(3.53) equation (3.64) can be equally written:

$$\tilde{G}_m(k,r,r_0) = \tilde{G}_m^{\infty}(k,r,r_0) + \frac{q_0}{2\pi\varepsilon_0}\frac{1}{m}\left(\frac{rr_0}{b^2}\right)^m \cdot$$

$$\cdot \left[1 + \frac{1}{m\beta^2\gamma^2}\frac{\mathrm{b}}{\delta_{\mathrm{wall}}}\tanh\left(\frac{\Delta}{\delta_{\mathrm{wall}}}\right)\frac{\left(\frac{1}{m\beta^2\gamma^2}\right)\left(\frac{\mathrm{d}}{\delta_{\mathrm{wall}}}\right) + \coth\left(\frac{\Delta}{\delta_{\mathrm{wall}}}\right)}{\left(\frac{1}{m\beta^2\gamma^2}\right)\left(\frac{\mathrm{d}}{\delta_{\mathrm{wall}}}\right) + \tanh\left(\frac{\Delta}{\delta_{\mathrm{wall}}}\right)}\right]^{-1} \tag{3.65}$$

The relative error produced by using equation (3.64) in place of (3.37) for $m = 0,1,2$ is shown in **Fig. 3.2**. As expected, the error increases with kb, but remains very small throughout the meaningful spectral range.

For a very thick pipe wall, $|\bar{\mathrm{k}}\Delta| \sim |\Delta/\delta_{wall}| \gg 1$, whence $sinh\,\bar{k}\Delta \sim \cosh\bar{k}\Delta$, equation (3.65) becomes: [11]

$$\tilde{G}_m(k,r,r_0) = \tilde{G}_m^{\infty}(k,r,r_0) + \frac{q_0}{2\pi\varepsilon_0}\frac{1}{m}\left(\frac{rr_0}{b^2}\right)^m \left(1 + \frac{1}{m\beta^2\gamma^2}\frac{\mathrm{b}}{\delta_{\mathrm{wall}}}\right)^{-1} \tag{3.66}$$

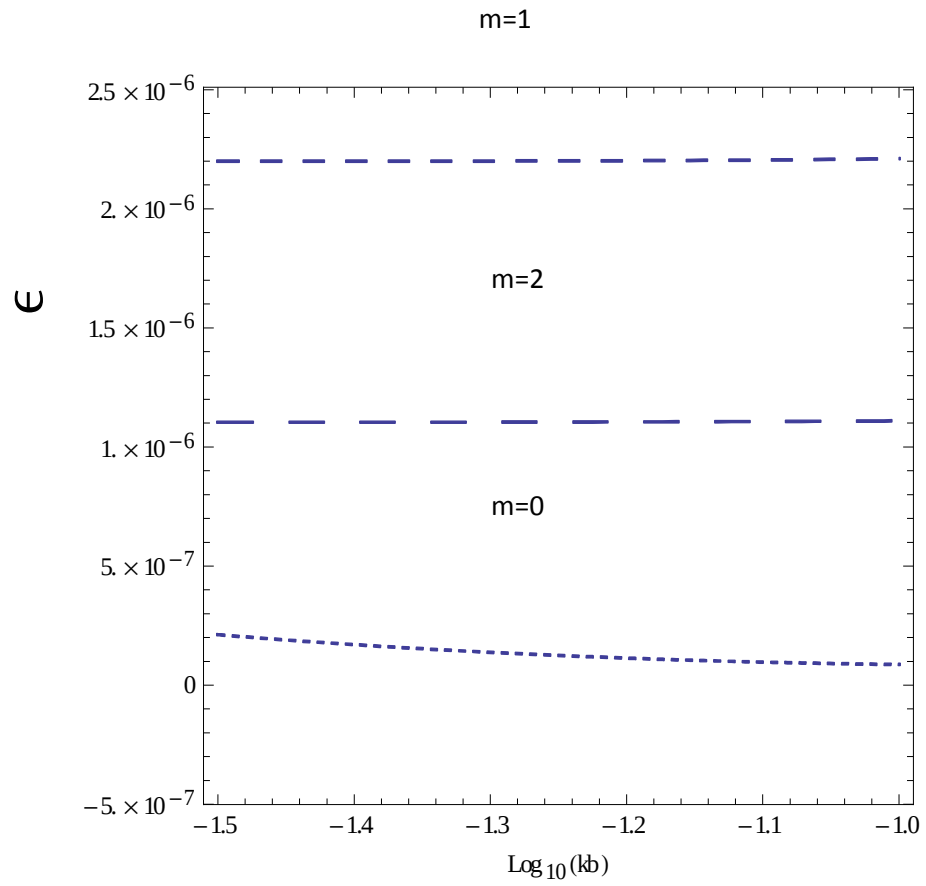

Fig. 3.2 Relative error $\epsilon = (2\pi\varepsilon_0/q)[\tilde{G}_m - \tilde{G}_m^{\infty}]$ versus kb after assuming kb<<1 and using equations (3.60),(3.64) in place of equation (3.37) for monopole, dipole and quadrupole terms (m=0,1,2).

3.5 Applications

3.5.1 LHC

LHC DESIGN PARAMETERS	
Nominal Circumference L_c	26658 m
Number of bunches N_b	2835
Bunch length σ_s	(7÷13) cm
Lorentz factor γ	500÷7000
Pipe diameter	3 cm
Wall thickness	50 μm (Cu) + 1 mm (SS)
Wall conductivity	$(5.7 \cdot 10^{7} \div 10^{10})\ \Omega^{-1}\mathrm{m}^{-1}$
Circulation frequency	11.2455 KHz

In the Large Hadron Collider (LHC) one has: [11]

$$\left|\frac{1}{\beta^2\gamma^2}\frac{b}{\delta_{\mathrm{wall}}}\right| \ll 1 \quad , \quad \left|\frac{1}{\beta^2\gamma^2}\frac{d}{\delta_{\mathrm{wall}}}\right| \ll 1 \tag{3.67}$$

Accordingly, if are valid the following relations:

$$\left|\tanh\left(\frac{\Delta}{\delta_{\mathrm{wall}}}\right)\right| \gg \left|\frac{1}{\beta^2\gamma^2}\frac{\mathrm{d}}{\delta_{\mathrm{wall}}}\right| \quad , \quad \left|\coth\left(\frac{\Delta}{\delta_{\mathrm{wall}}}\right)\right| \gg \left|\frac{1}{\beta^2\gamma^2}\frac{\mathrm{d}}{\delta_{\mathrm{wall}}}\right| \tag{3.68}$$

which occurs for not too small values of $|\Delta/\delta_{wall}|$, one has: [11]

$$\tilde{G}_m(k,r,r_0) = \tilde{G}_m^{\infty}(k,r,r_0) + \frac{q_0}{2\pi\varepsilon_0}\frac{1}{m}\left(\frac{rr_0}{b^2}\right)^m\left[1 - \frac{1}{m\beta^2\gamma^2}\frac{\mathrm{b}}{\delta_{\mathrm{wall}}}\coth\left(\frac{\Delta}{\delta_{\mathrm{wall}}}\right)\right] \qquad (3.69)$$

In the extreme limiting case $|\Delta/\delta_{wall}| \ll 1$,where:

$$\left|\tanh\left(\frac{\Delta}{\delta_{\mathrm{wall}}}\right)\right| \ll \left|\frac{1}{m\beta^2\gamma^2}\frac{\mathrm{d}}{\delta_{\mathrm{wall}}}\right| \quad , \quad \left|\coth\left(\frac{\Delta}{\delta_{\mathrm{wall}}}\right)\right| \gg \left|\frac{1}{m\beta^2\gamma^2}\frac{\mathrm{d}}{\delta_{\mathrm{wall}}}\right| \qquad (3.70)$$

one has: [11]

$$\tilde{G}_m(r,r_0) \approx \tilde{G}_m^{\,free\ space}(r,r_0) - \frac{q_0}{2\pi\varepsilon_0}\frac{1}{2m}\left(\frac{rr_0}{b^2}\right)^m\left[1 - 2\left(1+\frac{\mathrm{b}}{\mathrm{d}}\right)^{-1}\right] \qquad (3.71)$$

which reduces to the free-space term, if $\Delta \to 0$, i.e. $d \to b$, as expected.

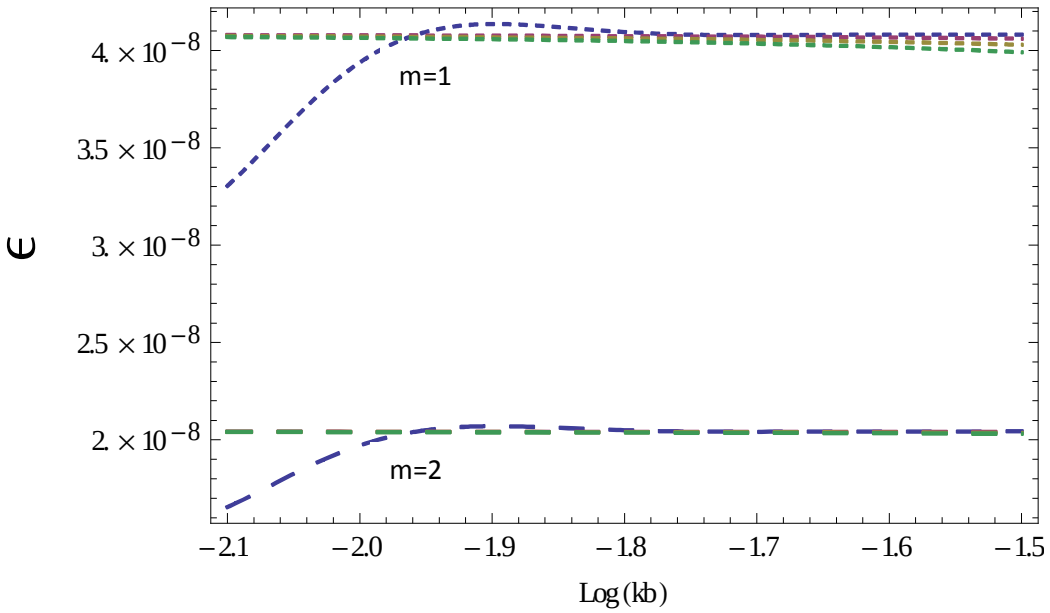

Fig. 3.3 Relative error $\epsilon = (2\pi\varepsilon_0/q)[\tilde{G}_m - \tilde{G}_m^{\infty}]$ produced by using equation (3.69) in place of equation (3.37) for dipole and quadrupole terms (m=1,2).

3.5.2 DAΦNE

DAΦNE DESIGN PARAMETERS	
Nominal Circumference L_c	97.69 m
Number of bunches N_b	120
Bunch length σ_s	2 cm
Lorentz factor γ	1000
Pipe diameter	10 cm
Wall thickness	2 mm (Al)
Wall conductivity	$3.4 \cdot 10^7\ \Omega^{-1}\mathrm{m}^{-1}$
Circulation frequency	368.26 MHz

In ultrashort bunch machines, including DAΦNE, one has: [11]

$$\left|\frac{1}{m\beta^2\gamma^2}\frac{b}{\delta_{\mathrm{wall}}}\right| \gg 1 \tag{3.72}$$

Accordingly, if are valid the following relations:

$$\left|\tanh\left(\frac{\Delta}{\delta_{\mathrm{wall}}}\right)\right| \ll \left|\frac{1}{\beta^2\gamma^2}\frac{\mathrm{d}}{\delta_{\mathrm{wall}}}\right| \quad , \quad \left|\coth\left(\frac{\Delta}{\delta_{\mathrm{wall}}}\right)\right| \ll \left|\frac{1}{\beta^2\gamma^2}\frac{\mathrm{d}}{\delta_{\mathrm{wall}}}\right| \tag{3.73}$$

which occurs for not too small values of $|\Delta/\delta_{wall}|$, one has: [11]

$$\tilde{G}_m(k,r,r_0) = \tilde{G}_m^{\infty}(k,r,r_0) + \frac{q_0}{2\pi\varepsilon_0}\left(\frac{rr_0}{b^2}\right)^m\left[\beta^2\gamma^2\frac{\delta_{\mathrm{wall}}}{\mathrm{b}}\coth\left(\frac{\Delta}{\delta_{\mathrm{wall}}}\right)\right] \tag{3.74}$$

In the extreme limiting case $|\Delta/\delta_{wall}| \ll 1$,where:

$$\left|\tanh\left(\frac{\Delta}{\delta_{\text{wall}}}\right)\right| \ll \left|\frac{1}{m\beta^2\gamma^2}\frac{\mathrm{d}}{\delta_{\text{wall}}}\right| \quad , \quad \left|\coth\left(\frac{\Delta}{\delta_{\text{wall}}}\right)\right| \gg \left|\frac{1}{m\beta^2\gamma^2}\frac{\mathrm{d}}{\delta_{\text{wall}}}\right| \tag{3.75}$$

one has: [11]

$$\tilde{G}_m(r,r_0) \approx \tilde{G}_m^{\,free\ space}(r,r_0) - \frac{q_0}{2\pi\varepsilon_0}\frac{1}{2m}\left(\frac{rr_0}{b^2}\right)^m\left[1-2\left(1+\frac{\mathrm{b}}{\mathrm{d}}\right)^{-1}\right] \tag{3.76}$$

which reduces to the free-space term, if $\Delta\to 0$, i.e. $d \to b$, as expected.

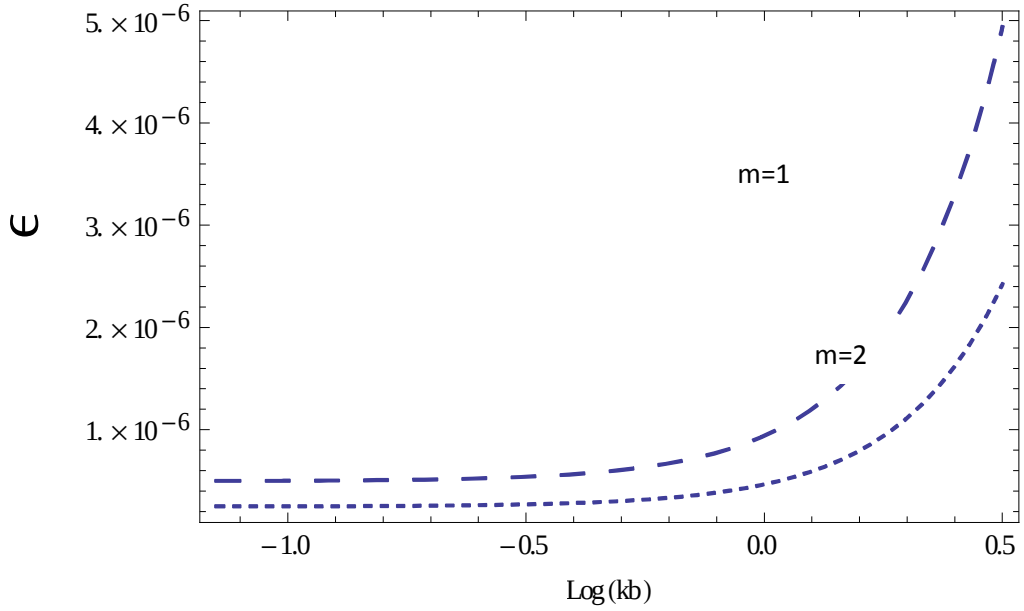

Fig. 3.4 Relative error $\epsilon = (2\pi\varepsilon_0/q)[\tilde{G}_m - \tilde{G}_m^{\infty}]$ produced by using equation (3.64) in place of equation (3.37) for dipole and quadrupole terms (m=1,2).

3.6 Back to Space-Time domain

In separable coordinate systems, $\tilde{G}_m(k, r, r_0)$ can be factored as follows:

$$\tilde{G}_m(k, r, r_0) = R_m(r, r_0)\zeta_m(k) \tag{3.77}$$

This is also true for $\Phi(r, \phi, s)$: [11]

$$\Phi(r, \phi, s) = \frac{1}{2\pi}\sum_{m=-\infty}^{+\infty} e^{jm\phi}\left(\int_0^b r_0 dr_0\, \rho_{t,m}(r_0)\right) R_m(r, r_0)\Lambda_m(s) \tag{3.78}$$

The function $\Lambda_m(s)$ describes the wake effects and contains both the wall thickness and the conductivity:

$$\Lambda_m(s) = \int_{-\infty}^{+\infty} \zeta_m(k)\, F(k) e^{jks} dk \tag{3.79}$$

3.6.1 Monopole term

Using equations (3.41-3.46) into (3.60), one has: [11]

$$\tilde{G}_0(n) - \tilde{G}_0^{\infty}(n) \equiv \tilde{G}_0^{\,wall}(n) = \frac{q_0}{2\pi\varepsilon_0}\frac{\beta^2\gamma^2}{2b}\cdot \Re\left[(1+j)\left(\frac{N_T}{n}\right)^{1/2}\sqrt{\frac{2\sigma_s}{Z_0\sigma\beta}}\cdot \coth\left[(1-j)\left(\frac{n}{N_T}\right)^{1/2}\Delta\sqrt{\frac{Z_0\sigma\beta}{2\sigma_s}}\right]\right] \tag{3.80}$$

where the integer n denotes the harmonics of the bunch fundamental wave number.

Then:

$$G_0{}^{wall}(s) = \frac{q_0\beta^2\gamma^2}{2\pi\varepsilon_0}\sum_{n\neq 0}^{-\infty,+\infty} e^{-\frac{1}{2}\left(\frac{n}{N_T}\right)^2}\left(\frac{N_T}{n}\right)^{1/2}\left(\frac{\Delta}{b}\right)\left(\frac{\delta_{min}}{\Delta}\right)\cdot\tanh\left[\left(\frac{n}{N_T}\right)^{1/2}\left(\frac{\Delta}{\delta_{min}}\right)\right]e^{j\frac{n}{N_T}\left(\frac{s}{\sigma_s}\right)} \qquad (3.81)$$

where:

$$\delta_{min} = \sqrt{2\sigma_s/Z_0\sigma\beta} \qquad (3.82)$$

is the minimum penetration of the field in the wall.

3.6.2 Multipole terms: LHC

Using equations (3.41-3.46) into (3.69), one has: [11]

$$\tilde{G}_m(n,r,r_0) - \tilde{G}_m^{\infty}(n,r,r_0) \equiv \tilde{G}_m^{wall}(n,r,r_0) = \frac{q_0}{2\pi\varepsilon_0}\frac{1}{m}\left(\frac{rr_0}{b^2}\right)^m$$

$$\cdot\,\Re\left[1 - \frac{1}{m\beta^2\gamma^2}(1-j)\left(\frac{n}{N_T}\right)^{1/2} b\sqrt{\frac{Z_0\sigma\beta}{2\sigma_s}}\cdot\coth\left[(1-j)\left(\frac{n}{N_T}\right)^{1/2}\Delta\sqrt{\frac{Z_0\sigma\beta}{2\sigma_s}}\right]\right] \qquad (3.83)$$

where the integer n denotes the harmonics of the bunch fundamental wave number. Then:

$$G_m{}^{wall}(s,r,r_0) = \frac{q_0}{2\pi\varepsilon_0}\frac{1}{m}\left(\frac{rr_0}{b^2}\right)^m \Re\left[1 - \frac{1}{m\beta^2\gamma^2}\sum_{n\neq 0}^{-\infty,+\infty} e^{-\frac{1}{2}\left(\frac{n}{N_T}\right)^2}(1-j)\left(\frac{n}{N_T}\right)^{1/2}\left(\frac{b}{\Delta}\right)\left(\frac{\Delta}{\delta_{min}}\right)\right.$$

$$\left.\cdot\coth\left[(1-j)\left(\frac{n}{N_T}\right)^{1/2}\left(\frac{\Delta}{\delta_{min}}\right)\right]e^{j\frac{n}{N_T}\left(\frac{s}{\sigma_s}\right)}\right] \qquad m \neq 0 \qquad (3.84)$$

3.6.3 Multipole terms: DAΦNE

Using equation (3.41-3-46) into (3.74), one has: [11]

$$\tilde{G}_m(n,r,r_0) - \tilde{G}_m^{\infty}(n,r,r_0) \equiv \tilde{G}_m^{wall}(n,r,r_0) = \frac{q_0}{2\pi\varepsilon_0}\left(\frac{rr_0}{b^2}\right)^m \frac{\beta^2\gamma^2}{2b} \cdot$$

$$\cdot \Re\left(\left[1+j \left(\frac{N_T}{n}\right)^{1/2} \sqrt{\frac{2\sigma_s}{Z_0\sigma\beta}} \cdot \coth\left[(1-j)\left(\frac{n}{N_T}\right)^{1/2} \Delta \sqrt{\frac{Z_0\sigma\beta}{2\sigma_s}} \right] \right] \right. \tag{3.85}$$

where the integer n denotes the harmonics of the bunch fundamental wave number. Then:

$$G_m{}^{wall}(s,r,r_0) = \frac{q_0}{2\pi\varepsilon_0}\left(\frac{rr_0}{b^2}\right)^m \frac{\beta^2\gamma^2}{2} \Re\left[\sum_{n\neq 0}^{-\infty,+\infty} e^{-\frac{1}{2}\left(\frac{n}{N_T}\right)^2} (1+j)\left(\frac{N_T}{n}\right)^{1/2} \left(\frac{\Delta}{b}\right)\left(\frac{\delta_{min}}{\Delta}\right) \right.$$

$$\left. \cdot \coth\left[(1-j)\left(\frac{n}{N_T}\right)^{1/2} \left(\frac{\Delta}{\delta_{min}}\right) \right] e^{j\frac{n}{N_T}\left(\frac{s}{\sigma_s}\right)} \right] \qquad m \neq 0 \tag{3.86}$$

Note that equations (3.81),(3.84),(3.86) contain a term depending on (r, r_0, m) and another term depending on a geometric factor b/Δ, and on the wall conductivity and frequency through $\frac{\Delta}{\delta_{min}}$.

Fig.s 3.5 a),b),c),d) show the behaviour of equations (3.81),(3.84),(3.86) as a function of s/σ_s for the monopole, dipole and quadrupole terms $(m = 0,1,2)$.

Different curves refer to different values of the ratio $\frac{\Delta}{\delta_{min}}$.

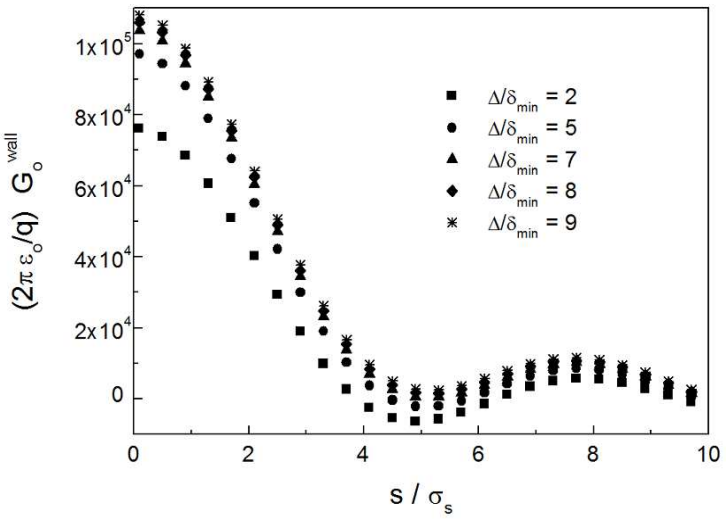

Fig. 3.5 a)

Fig. 3.5 a) Wake potential (monopole term) in a storage ring versus s/σ_s normalized distance from the leading particle. Different curves refer to different values of the ratio $\Delta/\delta_{\min}$.

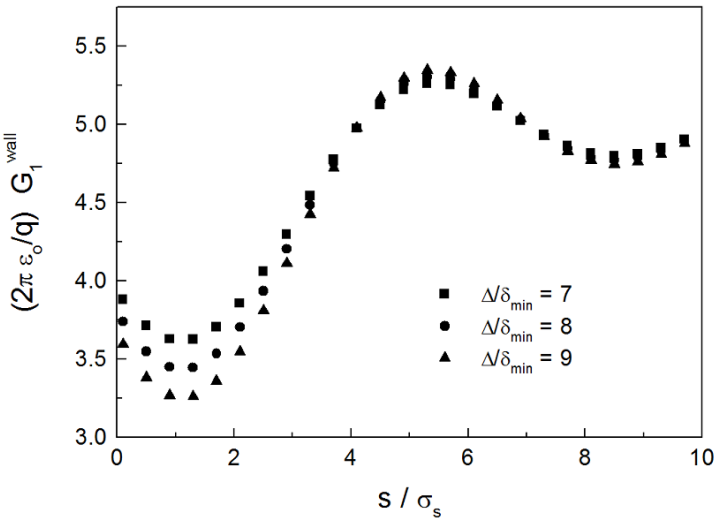

Fig. 3.5 b)

Fig. 3.5 b) Wake potential (dipole term) versus normalized distance from the leading particle in LHC. Different curves refer to different values of the ratio $\Delta/\delta_{\min}$.

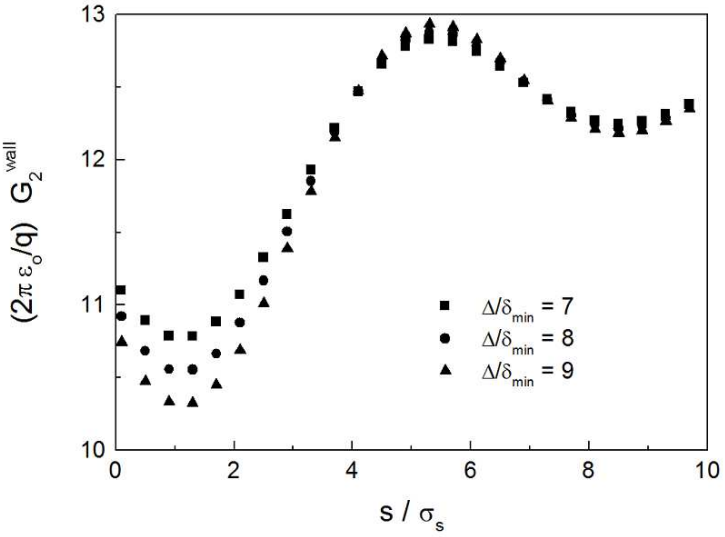

Fig. 3.5 c)

Fig. 3.5 c) Wake potential (quadrupole term) versus normalized distance from the leading particle in LHC. Different curves refer to different values of the ratio $\Delta/\delta_{\min}$.

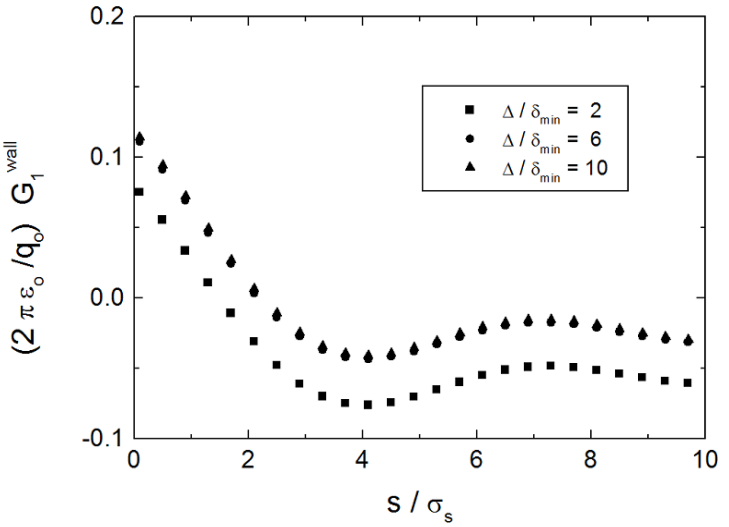

Fig. 3.5 d)

Fig. 3.5 d) Wake potential (dipole term) versus normalized distance from the leading particle in DAΦNE. Different curves refer to different values of the ratio $\Delta/\delta_{\min}$.

3.7 Tune Shifts

Space charge and image forces felt by charged particles travelling in a conducting vacuum pipe, affect the frequency of the transverse (vertical and radial) betatron oscillations. The betatron frequency changes are represented in terms of *Tune Shifts* and *Laslett coefficients*. The radial and vertical betatron oscillations are in general coupled, both in the coherent (whole beam) and incoherent (single particle) regime. The Tune Shift and image coefficients form non diagonal, 2nd rank tensors in which the off-diagonal terms play an important role. [13]

The transverse oscillations of a particle in a beam can be affected by space-charge and image forces.

The space-charge force $\boldsymbol{f}^{(sp.\ ch.)}$ is the same which would exist in free space due to all the other particles in the beam, and is accordingly computed by ignoring the presence of the conducting boundary.

The image force $\boldsymbol{f}^{(im.)}$ is due to the images of the beam, embodying the effect of the conducting boundary.

$$\boldsymbol{f}^{(sp.\ ch.)} = (\boldsymbol{r} - \boldsymbol{r}_b) \cdot (\nabla_{\boldsymbol{r}}\, \boldsymbol{f}^{(sp.\ ch.)})_{\boldsymbol{r}=\boldsymbol{r}_b} + (higher\ order\ terms) \tag{3.87}$$

$$f^{(im.)} = \left(\boldsymbol{r} - \boldsymbol{r}_{eq}\right) \cdot (\nabla_{\boldsymbol{r}}\, \boldsymbol{f}^{(im.)})_{\boldsymbol{r}=\boldsymbol{r}_b=\boldsymbol{r}_{eq}} + \left(\boldsymbol{r}_b - \boldsymbol{r}_{eq}\right) \cdot (\nabla_{\boldsymbol{r}_b}\, \boldsymbol{f}^{(im.)})_{\boldsymbol{r}=\boldsymbol{r}_b=\boldsymbol{r}_{eq}} + (higher\ order\ terms) \tag{3.88}$$

where: $\boldsymbol{r}_b$ is the beam center of charge

$\boldsymbol{r}_{eq}$ is the beam center of charge equilibrium position

$\nabla_{\boldsymbol{r}}, \nabla_{\boldsymbol{r}_b}$ are the nabla operators taken with respect to the subscript coordinate

It is convenient to distinguish two cases:

1) $\boldsymbol{r}_b = \boldsymbol{r}_{eq} \neq \boldsymbol{r}$: the beam center of charge is coincident with the equilibrium position, but the test particle is displaced therefrom (incoherent, single particle effect).
2) $\boldsymbol{r} = \boldsymbol{r}_b \neq \boldsymbol{r}_{eq}$: the test particle is coincident with the beam center of charge, but the latter is displaced off the equilibrium position (coherent, whole beam effect). [13]

For both cases, neglecting higher order terms, the transverse Lorentz force equation yields the betatron oscillation equation:

$$\frac{d^2\boldsymbol{\rho}}{d\tau^2} + \omega^2\nu^2\bar{\bar{U}} \cdot \boldsymbol{\rho} = 0 \tag{3.89}$$

where: $\boldsymbol{\rho} = \boldsymbol{r} - \boldsymbol{r}_{eq}$ is the displacement from the equilibrium position

$\tau = \frac{s}{c}$ is the orbital coordinate

ω is the angular revolution frequency

ν is the tune

$\bar{\bar{U}}$ is a 2nd rank tensor

$$\bar{\bar{U}} = \bar{\bar{I}} - \frac{q}{\omega^2\nu^2 m_0\gamma_0}\begin{Vmatrix}\delta_x u_x & \delta_y u_x \\ \delta_x u_y & \delta_y u_y\end{Vmatrix} \tag{3.90}$$

where:

$$\begin{cases}\delta_{x,y} = \partial_{x,y}|_{\boldsymbol{r}=\boldsymbol{r}_b=\boldsymbol{r}_{eq}} & u_{x,y} = \frac{{f_{x,y}}^{(im.)} + {f_{x,y}}^{(sp.ch.)}}{q} \quad incoherent\ case \\ \delta_{x,y} = (\partial_{x,y} + \partial_{x_b,y_b})|_{\boldsymbol{r}=\boldsymbol{r}_b=\boldsymbol{r}_{eq}} & u_{x,y} = \frac{{f_{x,y}}^{(im.)}}{q} \quad coherent\ case\end{cases} \tag{3.91}$$

In terms of Tune Shifts we can rewrite:

$$\bar{\bar{U}} = \bar{\bar{I}} + \frac{2}{\nu}\overline{\overline{\Delta\nu}} \tag{3.92}$$

where $\overline{\overline{\Delta\nu}}$ is a 2nd rank tensor with elements:

$$\Delta\nu_{i,j} = -\frac{q}{2\omega^2\nu m_0\gamma_0}\delta_j u_i \tag{3.93}$$

which can be written as:

$$\Delta\nu_{i,j} = \left(-\frac{NRr_0}{\pi\nu\beta_0^2\gamma_0 L^2}\right)\epsilon_{i,j} \tag{3.94}$$

where: N is the total number of particles in the beam

R is the ring radius

r_0 is the particle radius

L is the transverse dimension of the chamber

$\epsilon_{i,j} = \frac{L^2}{4\,\Lambda}\delta_j u_i$ are the Laslett coefficients with $\Lambda = \frac{Nq}{2\pi R}$ the linear charge density

Since the off-diagonal components are, in general, non-zero the radial and vertical betatron oscillations are coupled by the space charge and image forces. The possible relevance of the off-diagonal terms is clarified upon introducing the betatron normal modes through a coordinate transformation which makes the Tune Shift and Laslett tensors diagonal, both for the incoherent and coherent case. This betatron normal modes can be expressed in terms of Tune Shifts as:

$$\Omega_{1,2}^2 = \omega^2(\nu + \Delta\nu_{1,2})^2 \approx \omega^2\nu^2\left(1 + \frac{2\Delta\nu_{1,2}}{\nu}\right) \tag{3.95}$$

where $\Delta\nu_{1,2}$ can be written in terms of Laslett coefficients:

$$\Delta\nu_{1,2} = \left(-\frac{NRr_0}{\pi\nu\beta_0^2\gamma_0 L^2}\right)\epsilon_{1,2} \tag{3.96}$$

Hence:

$$\epsilon_{1,2} = \frac{L^2}{4\,\Lambda}\left\{\frac{\delta_x u_x + \delta_y u_y}{2} \pm \left[\left(\frac{\delta_y u_y - \delta_x u_x}{2}\right)^2 + \delta_x u_y\,\delta_y u_x\right]^{1/2}\right\} \tag{3.97}$$

The functions u_x, u_y are related to the pure image potential $\phi^{(im.)}$, and the coherent and incoherent normal mode Laslett coefficients can be written as:

$$\epsilon_{1,2}{}^{(inc.)} = \pm\frac{1}{2}\left|\frac{\partial^2\boldsymbol{\psi}^{(im.)}}{\partial\mathbf{z}^2}\right|_{\mathbf{z}=\mathbf{z}_b=\mathbf{z}_{eq}}$$

$$\epsilon_{1,2}{}^{(coh.)} = \frac{1}{2}\left\{-Re\left(\frac{\partial^2\boldsymbol{\psi}^{(im.)}}{\partial\mathbf{z}\,\partial\mathbf{z}_b^*}\right) \pm \left[\left|\frac{\partial^2\boldsymbol{\psi}^{(im.)}}{\partial\mathbf{z}\,\partial\mathbf{z}_b} + \frac{\partial^2\boldsymbol{\psi}^{(im.)}}{\partial\mathbf{z}^2}\right|^2 - Im^2\left(\frac{\partial^2\boldsymbol{\psi}^{(im.)}}{\partial\mathbf{z}\,\partial\mathbf{z}_b^*}\right)\right]^{1/2}\right\}_{\mathbf{z}=\mathbf{z}_b=\mathbf{z}_{eq}} \tag{3.98}$$

where $\boldsymbol{\psi}^{(im.)}$ is the complex image potential, and $\boldsymbol{z} = (x + jy)/L$. [14]

In our case, the potential for the calculation of Laslett coefficients, is the same as that of a perfectly conducting pipe except for an additional factor L depending only on the longitudinal coordinate, hence:

$$\epsilon^{inc.} = \pm\frac{1}{2}\frac{\boldsymbol{r}^2}{1-\boldsymbol{r}^2}L(s)$$

$$\epsilon^{coh.} = L(s)\begin{cases}\frac{1}{2}\frac{1}{1-\boldsymbol{r}^2} & 1st\ normal\ mode \\ \frac{1}{2}\frac{1+\boldsymbol{r}^2}{(1-\boldsymbol{r}^2)^2} & 2nd\ normal\ mode\end{cases} \tag{3.99}$$

where the s-independent factors are the incoherent and coherent Laslett coefficients for a perfect conductive circular pipe and $\boldsymbol{r}$ is the distance from the pipe axis scaled to the pipe radius, and:

$$L(s) = -\frac{1}{m^2\beta^2\gamma^2}\Re\left[\sum_{n=-\infty}^{\infty} e^{-\frac{1}{2}\left(\frac{n}{N_T}\right)^2}(1-j)\left(\frac{n}{N_T}\right)^{1/2}\left(\frac{b}{\Delta}\right)\left(\frac{\Delta}{\delta_{min}}\right)\right.$$
$$\left.\cdot\coth\left[(1-j)\left(\frac{n}{N_T}\right)^{1/2}\left(\frac{\Delta}{\delta_{min}}\right)\right]e^{j\frac{n}{N_T}\left(\frac{s}{\sigma_s}\right)}\right] \qquad m \neq 0 \tag{3.100}$$

Chapter 4

Existing Literature on the Wake Field in Particle Accelerators with Finite Thickness and Conductivity

The concept of coupling impedance in accelerators was first introduced for the studies of beam instabilities. In the design of accelerators it is desired to reduce the coupling impedance of the beam to its environment in order to prevent beam instabilities. Concerning the longitudinal dynamics of charged particle beams there are two important physical quantities, the longitudinal space charge and the resistive wall impedances. [16]

The coupling impedance of straight, uniform beams in a cylindrical vacuum chamber was treated by B. Zotter [2] who found an expression for the total impedance at the beam surface $r = a$, which did not give the impedance at any point r from the beam axis. Kurennoy and Wang [18],[19] reviewed the definition of the longitudinal space charge impedance and the corresponding geometry factors for smooth chambers of perfectly conducting walls. Recently, Zimmermann and Oide [20] obtained an expression for the resistive wall impedance using the wake field approach.

In Section 4.1 A. M. Al-Khateeb [15],[16] presents the derivation of the electromagnetic fields associated with a particle beam moving in a beam pipe of both finite and infinite wall conductivities. Accounting for finite surface currents within the wall by using the Leontovich boundary condition (See Appendix B) to find the fields outside the metallic wall, he presents a review on the calculation of the total longitudinal coupling impedance for a beam pipe with both thick and thin wall and then he gives a fitting formula with some values for the fitting parameters of the corresponding generalized geometry factor.

In Section 4.2 A. M. Al-Khateeb [17] presents the derivation of the dipole source term needed for the calculation of the transverse impedances for a wall of arbitrary thickness and also in the limit of thick and thin beam pipes.

In Section 4.3 Y. Shobuda and K. Yokoya [23] derive the resistive wall impedance for a chamber with a finite thickness and the relative Tune Shift, showing the effect of the thickness of the beam pipe to the resistive impedances.

In Section 4.4 M. Ivanyan [24] computes the exact solution for the longitudinal and transverse impedance multipoles in the case of a two-layer laminated vacuum chamber with circular cross section in the ultra-relativistic limit.

Finally, Section 4.5 contains a general approach for the analysis of the wake field of a point charge moving in a vacuum tunnel bored in dielectric material that is uniform in the direction parallel to the motion of the bunch and has arbitrary characteristics in the transverse directions.

4.1 Longitudinal impedance of a resistive beam pipe for arbitrary energy and frequency [15]

The longitudinal coupling impedance of a cylindrical beam pipe for arbitrary relativistic γ_0 and mode frequency is obtained analytically for finite wall conductivity and finite wall thickness. For perfectly conducting media such that $\sigma = \infty$, tangential and normal field components vanish on a given perfectly conducting surface.

On the other hand, when the conductivity is large but finite, surface currents will flow on the conducting surface leading to energy dissipation. The net energy flux is nonzero and can be characterized by a resistive wall impedance. The conductivity of most metals is very large but finite, and usually it is a function of temperature [21]. At very low temperatures, the conductivity may become infinite for direct currents if the metal becomes superconducting. It always remains finite for alternating currents.

In this Section A. M. Al-Khateeb [15],[16] investigates the problem of longitudinal space charge and resistive wall impedances in a smooth cylindrical beam pipe using the Leontovich boundary condition to relate the tangential field components at the metallic surface.

In Subsections 4.1.1, 4.1.2 he follows a first approach which consists in the volume integral over the transverse beam distribution for the calculation of the impedance of both thick and thin pipe wall.

In Subsection 4.1.3 he considers a second approach starting from the flux of the Poynting vector at the pipe wall for the calculation of the resistive wall impedance. Afterwards he compares the results with the expressions obtained from the volume integral over the beam distribution. [15]

4.1.1 Impedance of a thick pipe wall obtained as a volume integral over the transverse beam distribution

For an axially uniform transverse beam charge distribution in a beam pipe with a thick conducting wall, the beam pipe wall structure involves three regions where Maxwell's equations should be solved with appropriate boundary conditions on the various interfaces. It is important to find the unique solution for the electromagnetic field components to account for the correct boundary conditions on metallic surfaces and interfaces usually present in accelerators.

In the following analysis, A. M. Al-Khateeb [15] solves the Maxwell's equations in each region of the beam pipe wall structure for TM cylindrical waveguide modes and then match the fields at the beam-vacuum and vacuum-wall interfaces.

The z component of the electric field in the three regions involved satisfies the following differential equations:

$$\left[\frac{d^2}{dr^2}+\frac{1}{r}\frac{d}{dr}-\frac{k_z^2}{{\gamma_0}^2}\right]E_z^{(1)}(r,\omega)=j\frac{Q}{\pi a^2}\frac{k_z}{\varepsilon_0{\gamma_0}^2\beta c} \qquad 0\le r\le a \tag{4.1}$$

$$\left[\frac{d^2}{dr^2}+\frac{1}{r}\frac{d}{dr}-\frac{k_z^2}{{\gamma_0}^2}\right]E_z^{(2)}(r,\omega)=0 \qquad a\le r\le b \tag{4.2}$$

$$\left[\frac{d^2}{dr^2}+\frac{1}{r}\frac{d}{dr}-\frac{k_z^2}{\underline{\gamma}^2}\right]E_z^{(3)}(r,\omega)=0 \qquad b\le r<\infty \tag{4.3}$$

The general solution is:

$$E_z(r,\omega)=\begin{cases}A_1I_0(\sigma_0 r)-j\dfrac{Q}{\pi a^2\varepsilon_0 k_z\beta c} & 0\le r\le a\\ A_2I_0(\sigma_0 r)+A_3K_0(\sigma_0 r) & a\le r\le b\\ A_4K_0\left(\underline{\sigma}r\right) & b\le r\end{cases} \tag{4.4}$$

where $\underline{\sigma}=\frac{k_z}{\underline{\gamma}}$, I_0 and K_0 are modified Bessel functions of first and second kinds.

Upon matching the tangential field components E_z and H_ϑ at the beam surface $r=a$ and at the pipe wall at $r=b$, one obtains the coefficients A_1, A_2, A_3, A_4: [15]

$$A_1=j\frac{Q\sigma_0 a}{\pi a^2\varepsilon_0 k_z\beta c}[K_1(\sigma_0 a)+F^{-1}I_1(\sigma_0 a)] \tag{4.5}$$

$$A_2=j\frac{Q\sigma_0 a}{\pi a^2\varepsilon_0 k_z\beta c}I_1(\sigma_0 a)F^{-1} \tag{4.6}$$

$$A_3=-j\frac{Q\sigma_0 a}{\pi a^2\varepsilon_0 k_z\beta c}I_1(\sigma_0 a) \tag{4.7}$$

$$A_4=-j\frac{Q\sigma_0 a}{\pi a^2\varepsilon_0 k_z\beta c}\frac{\eta I_1(\sigma_0 a)}{FK_1\left(\underline{\sigma}b\right)}[I_1(\sigma_0 b)+FK_1(\sigma_0 b)] \tag{4.8}$$

where:

$$F=\frac{I_0(\sigma_0 b)+\eta\dfrac{K_0\left(\underline{\sigma}b\right)}{K_1\left(\underline{\sigma}b\right)}I_1(\sigma_0 b)}{K_0(\sigma_0 b)-\eta\dfrac{K_0\left(\underline{\sigma}b\right)}{K_1\left(\underline{\sigma}b\right)}K_1(\sigma_0 b)} \tag{4.9}$$

$$\eta = \frac{\omega \varepsilon_0 \gamma_0}{j\underline{\gamma}(S - j\omega\varepsilon_0)} \tag{4.10}$$

The corresponding total longitudinal coupling impedance is: [2]

$$Z_{\parallel}(r,\omega) = \frac{1}{Q^2}\int_{V_{beam}} d^3x' E_z(\boldsymbol{r}',\omega) J_z^*(\boldsymbol{r}',\omega) \tag{4.11}$$

Substituting for $J_z(r,z,\omega) = \frac{Q}{\pi a^2} e^{ik_z z}$ and making use of the harmonic number $n = k_z R$ into (4.11) one obtains:

$$Z_{\parallel}(\omega) = -j\frac{nZ_0}{2\beta\gamma_0^2} g^{tot} = -jn\chi_0 g^{tot} \tag{4.12}$$

where:

$$g^{tot} = \frac{4\gamma_0^2}{k_z^2 a^2}\left[\frac{r^2}{a^2} - 2\frac{r}{a} I_1(\sigma_0 a)[K_1(\sigma_0 a) + F^{-1} I_1(\sigma_0 a)]\right] \tag{4.13}$$

is the *total geometric factor* and $\chi_0 = \frac{Z_0}{2\beta\gamma_0^2}$.

For $r = a$ the total geometric factor becomes:

$$\begin{aligned} g^{tot} &= \frac{4\gamma_0^2}{k_z^2 a^2}\{1 - 2I_1(\sigma_0 a)[K_1(\sigma_0 a) + F^{-1} I_1(\sigma_0 a)]\} \\ &= \frac{4\gamma_0^2}{k_z^2 a^2}\left[1 - 2I_1(\sigma_0 a)\left(K_1(\sigma_0 a) + I_1(\sigma_0 a)\frac{K_0(\sigma_0 b)}{I_0(\sigma_0 b)}\right)\right] + \frac{8\gamma_0^2}{k_z^2 a^2} I_1^2(\sigma_0 a)\left[\frac{K_0(\sigma_0 b)}{I_0(\sigma_0 b)} - F^{-1}\right] \\ &= g^{sc} + g^{rw} \end{aligned} \tag{4.14}$$

where g^{sc} characterizes the longitudinal space-charge impedance for infinite conductivity and g^{rw} characterizes the longitudinal resistive-wall impedance for finite conductivity. [15]

Substituting the equation (4.9) into (4.14), the geometric factor g^{rw} becomes:

$$g^{rw} = \frac{8\gamma_0^2}{k_z^2 a^2} \frac{I_1^2(\sigma_0 a)}{\sigma_0 b I_0(\sigma_0 b)} \frac{K_0(\underline{\sigma} b)}{K_1(\underline{\sigma} b)} \frac{\eta}{I_0(\sigma_0 b) + \eta \frac{K_0(\underline{\sigma} b)}{K_1(\underline{\sigma} b)} I_1(\sigma_0 b)} \tag{4.15}$$

In the limit $k_z \delta_s \ll 1$, corresponding to good conducting wall, the parameter η takes the following limiting value:

$$\eta = \frac{\omega \varepsilon_0 \gamma_0}{j\underline{\gamma}(S - j\omega\varepsilon_0)} \approx \frac{1+j}{2} \frac{\beta^2 k_z^2 \delta_s}{\sigma_0} = (1+j) \frac{\beta^2 \gamma_0 k_z \delta_s}{2} \tag{4.16}$$

Accordingly, the geometric factor g^{rw} and the corresponding impedance $Z_{\parallel}^{rw}(\omega)$ are:

$$g^{rw} \approx \frac{8\gamma_0^2}{k_z^2 a^2} \frac{I_1^2(\sigma_0 a)}{\sigma_0 b I_0(\sigma_0 b)} \frac{1+j}{I_0(\sigma_0 b)} \frac{\beta^2 k_z^2 \delta_s}{2\sigma_0} \tag{4.17}$$

$$Z_{\parallel}^{rw}(\omega) = -j \frac{nZ_0}{2\beta\gamma_0^2} \, g^{rw} = (1-j) \frac{nZ_0 \beta \delta_s^*}{2\sqrt{n} b} \frac{4 I_1^2(\sigma_0 a)}{a^2 \sigma_0^2 I_0^2(\sigma_0 b)} \tag{4.18}$$

where δ_s^* is the skin depth at the revolution frequency $\omega_0 = \beta c / R$. [15]

4.1.2 Impedance of a thin pipe wall obtained as a volume integral over the transverse beam distribution

In this Subsection it is calculated the coupling impedance of a thin metallic cylindrical pipe of thickness d, extending from $r = b$ to $r = b + d = h$. The z component of the electric field in the four regions involved satisfies the following differential equations: [15]

$$\left[\frac{d^2}{dr^2} + \frac{1}{r}\frac{d}{dr} - \frac{k_z^2}{{\gamma_0}^2} \right] E_z^{(1)}(r, \omega) = j \frac{Q}{\pi a^2} \frac{k_z}{\varepsilon_0 {\gamma_0}^2 \beta c} \qquad 0 \le r \le a \tag{4.19}$$

$$\left[\frac{d^2}{dr^2}+\frac{1}{r}\frac{d}{dr}-\frac{k_z^2}{{\gamma_0}^2}\right]E_z^{(2)}(r,\omega)=0 \qquad a\le r\le b \tag{4.20}$$

$$\left[\frac{d^2}{dr^2}+\frac{1}{r}\frac{d}{dr}-\frac{k_z^2}{\underline{\gamma}^2}\right]E_z^{(3)}(r,\omega)=0 \qquad b\le r\le h \tag{4.21}$$

$$\left[\frac{d^2}{dr^2}+\frac{1}{r}\frac{d}{dr}-\frac{k_z^2}{{\gamma_0}^2}\right]E_z^{(4)}(r,\omega)=0 \qquad h\le r<\infty \tag{4.22}$$

The general solution is:

$$E_z(r,\omega)=\begin{cases} A_1I_0(\sigma_0 r)-j\dfrac{Q}{\pi a^2\varepsilon_0 k_z\beta c} & 0\le r\le a \\ A_2I_0(\sigma_0 r)+A_3K_0(\sigma_0 r) & a\le r\le b \\ A_4I_0(\underline{\sigma} r)+A_5K_0(\underline{\sigma} r) & b\le r\le h \\ A_6K_0(\sigma_0 r) & h\le r<\infty \end{cases} \tag{4.23}$$

Requiring the continuity of the tangential field components, E_z and H_ϑ at $r=a\,, r=b, r=h,$ one obtains the following coefficients: [15]

$$A_1=-j\frac{Q\sigma_0 a}{\pi a^2\varepsilon_0 k_z\beta cH}\left[I_1(\sigma_0 a)-HK_1(\sigma_0 a)\right] \tag{4.24}$$

$$A_2=\frac{I_1(\sigma_0 a)}{I_1(\sigma_0 a)-HK_1(\sigma_0 a)}A_1 \tag{4.25}$$

$$A_3=HA_2 \tag{4.26}$$

$$A_4=\frac{I_0(\sigma_0 b)+HK_0(\sigma_0 b)}{I_0(\underline{\sigma} b)+HK_0(\underline{\sigma} b)}A_2 \tag{4.27}$$

$$A_5=FA_4 \tag{4.28}$$

$$A_6=\frac{FK_1(\underline{\sigma} h)-I_1(\underline{\sigma} h)}{\eta K_1(\sigma_0 h)}A_4 \tag{4.29}$$

where:

$$F = \frac{I_1(\underline{\sigma}h)K_0(\sigma_0 h) + \eta K_1(\sigma_0 h)I_0(\underline{\sigma}h)}{K_1(\underline{\sigma}h)K_0(\sigma_0 h) - \eta K_1(\sigma_0 h)K_0(\underline{\sigma}h)} \tag{4.30}$$

$$G = \frac{1}{\eta}\frac{I_1(\underline{\sigma}b) - FK_1(\underline{\sigma}b)}{I_0(\underline{\sigma}b) + FK_0(\underline{\sigma}b)} \tag{4.31}$$

$$H = \frac{I_1(\sigma_0 b) - GI_0(\sigma_0 b)}{K_1(\sigma_0 b) + GK_0(\sigma_0 b)} \tag{4.32}$$

The corresponding longitudinal coupling impedance is:

$$Z_{\parallel}(r,\omega) = \frac{1}{Q^2}\int_{V_{beam}} d^3x' \boldsymbol{E}(r',z,\omega)\boldsymbol{J}^*(r',z,\omega) = -j\frac{nZ_0}{2\beta\gamma_0^2}g^{tot} = -jn\chi_0 g^{tot} \tag{4.33}$$

where the geometric factor is: [15]

$$g^{tot} = \frac{4\gamma_0^2}{k_z^2 a^2}\left[\frac{r^2}{a^2} - 2\frac{r}{a}I_1(\sigma_0 a)[K_1(\sigma_0 a) - H^{-1}I_1(\sigma_0 a)]\right] \tag{4.34}$$

For $r = a$ the total geometric factor is:

$$\begin{aligned} g^{tot} &= \frac{4\gamma_0^2}{k_z^2 a^2}\{1 - 2I_1(\sigma_0 a)[K_1(\sigma_0 a) - H^{-1}I_1(\sigma_0 a)]\} \\ &= \frac{4\gamma_0^2}{k_z^2 a^2}\left[1 - 2I_1(\sigma_0 a)\left(K_1(\sigma_0 a) + I_1(\sigma_0 a)\frac{K_0(\sigma_0 b)}{I_0(\sigma_0 b)}\right)\right] + \frac{8\gamma_0^2}{k_z^2 a^2}I_1^2(\sigma_0 a)\left[\frac{K_0(\sigma_0 b)}{I_0(\sigma_0 b)} + H^{-1}\right] \\ &= g_1 + g_2 \end{aligned} \tag{4.35}$$

where g_1 is associated with the space-charge only for the case of a perfectly conducting thick wall at $r = b$ and g_2 accounts for the finite width and electric conductivity of the cylindrical shield.

Substituting for H into (4.35) the geometric factor g_2 can be written in terms of F:

$$g_2 = \frac{8\gamma_0^2}{k_z^2 a^2} \frac{I_1^2(\sigma_0 a)}{\sigma_0 b I_0(\sigma_0 b)} \frac{1}{I_1(\sigma_0 b) - \frac{I_0(\sigma_0 b)}{\eta} \frac{I_1(\underline{\sigma} b) - F K_1(\underline{\sigma} b)}{I_0(\underline{\sigma} b) + F K_0(\underline{\sigma} b)}} \tag{4.36}$$

In the limit $k_z \delta_s \ll 1$, one has the following relations:

$$F \approx \frac{e^{2\underline{\sigma} h}}{\pi} \frac{K_0(\sigma_0 h) + \eta K_1(\sigma_0 h)}{K_0(\sigma_0 h) - \eta K_1(\sigma_0 h)} \tag{4.37}$$

$$G \approx -\frac{1}{\eta} \frac{K_0(\sigma_0 h) \tanh \underline{\sigma} d + \eta K_1(\sigma_0 h)}{K_0(\sigma_0 h) + \eta K_1(\sigma_0 h) \tanh \underline{\sigma} d} \tag{4.38}$$

Accordingly, the geometric factor g_2 and the corresponding impedance $Z_{2\parallel}(\omega)$ are: [15]

$$g_2 = \frac{1}{\sigma_0 b} \frac{4 I_1^2(\sigma_0 a)}{\sigma_0^2 a^2 I_0^2(\sigma_0 b)} \frac{(1+j) k_z \delta_s \beta^2 \gamma_0 \left[1 + \eta \frac{K_1(\sigma_0 h)}{K_0(\sigma_0 h)} \tanh \underline{\sigma} d\right]}{\tanh \underline{\sigma} d + \eta \left(\frac{K_1(\sigma_0 h)}{K_0(\sigma_0 h)} + \frac{I_1(\sigma_0 b)}{I_0(\sigma_0 b)}\right) + \eta^2 \frac{K_1(\sigma_0 h)}{K_0(\sigma_0 h)} \frac{I_1(\sigma_0 b)}{I_0(\sigma_0 b)} \tanh \underline{\sigma} d} \tag{4.39}$$

$$Z_{2\parallel}(\omega) = -j \frac{n Z_0}{2\beta\gamma_0^2} g_2$$

$$= (1-j) \frac{n Z_0 \beta \delta_s^*}{2\sqrt{n} b} \frac{4 I_1^2(\sigma_0 a)}{a^2 \sigma_0^2 I_0^2(\sigma_0 b)} \frac{1 + \eta \frac{K_1(\sigma_0 h)}{K_0(\sigma_0 h)} \tanh \underline{\sigma} d}{\tanh \underline{\sigma} d + \eta \left(\frac{K_1(\sigma_0 h)}{K_0(\sigma_0 h)} + \frac{I_1(\sigma_0 b)}{I_0(\sigma_0 b)}\right) + \eta^2 \frac{K_1(\sigma_0 h)}{K_0(\sigma_0 h)} \frac{I_1(\sigma_0 b)}{I_0(\sigma_0 b)} \tanh \underline{\sigma} d} \tag{4.40}$$

4.1.3 Impedance obtained using the flux of the Poynting vector at the pipe wall

Using another approach based on the flux of the Poynting vector at the pipe wall A. M. Al-Khateeb [16] computes the resistive wall impedance and then he compares it with the expression obtained from the volume integral over the beam distribution.

The axial component of the electric field at the pipe wall gives rise to a Poynting vector component directed into the pipe wall.

This accounts for a power loss in the pipe wall, which it is expressed in terms of the following coupling impedance:

$$Z_{||}^{rw}(\omega) = \frac{4\pi^2 bR}{Q^2} S(r=b,\omega) = \frac{4\pi^2 bR}{Q^2} [E_z(r=b,\omega) H_\vartheta^*(r=b,\omega)] \tag{4.41}$$

where the flux of the Poynting vector has the following expression:

$$S(r=b,\omega) = \frac{Q^2}{\pi^2 b^2 \sigma_w \delta_s \sigma^2 a^2} \frac{I_1^2(\sigma a)(1+j)}{I_0^2(\sigma b) - 2\alpha I_1(\sigma b) I_0(\sigma b) + 2\alpha^2 I_1^2(\sigma b)} \tag{4.42}$$

and the corresponding resistive wall impedance is:

$$Z_{||}^{rw}(\omega) = (1+j) \frac{R}{b\sigma_w \delta_s \sigma^2 a^2} \frac{4I_1^2(\sigma a)}{I_0^2(\sigma b) - 2\alpha I_1(\sigma b) I_0(\sigma b) + 2\alpha^2 I_1^2(\sigma b)} \tag{4.43}$$

Using $Z_0 = \mu_0 c$ and $n = k_z R$ the resistive wall impedance becomes:

$$Z_{||}^{rw}(\omega) = (1+j) \frac{nZ_0 \beta \delta_s}{2b\sigma^2 a^2} \frac{4I_1^2(\sigma a)}{I_0^2(\sigma b) - 2\alpha I_1(\sigma b) I_0(\sigma b) + 2\alpha^2 I_1^2(\sigma b)} \tag{4.44}$$

Introducing $\delta_s^* = \sqrt{2/\mu_0 \omega_0 \sigma_w}$ and $\alpha \ll 1$ the equation (4.44) becomes:

$$Z_{||}^{rw}(\omega) \approx (1+j) \frac{nZ_0 \beta \delta_s^*}{2\sqrt{n} b} \frac{4I_1^2(\sigma a)}{\sigma^2 a^2 I_0^2(\sigma b)} \tag{4.45}$$

In this expression, through the Poynting vector approach, the real and imaginary parts of the resistive wall impedance are equal, contrary to the approach based on the volume integral over the transverse beam distribution.

4.2 Transverse resistive wall impedances for beam pipes of arbitrary wall thickness [17]

Using *field matching techniques* (See Appendix D), A. M. Al-Khateeb [17] presents closed form analytic expressions for the transverse coupling impedance of a smooth cylindrical beam pipe of arbitrary thickness and also in the limit of thick and thin beam pipes. In this Section it is first presented the derivation of the dipole source term needed for the calculation of the transverse impedances for a wall of arbitrary thickness and then it is given a generalized expression for the longitudinal coupling impedance through which it is derived the transverse coupling impedance using the Panofsky-Wenzel theorem.[17]

The source terms used by Gluckstern [22] to calculate the transverse impedance for a displaced particle beam are:

$$\rho_1(r,\vartheta,z,t) = \frac{P}{\pi a^2}\delta(a-r)\cos\vartheta\frac{e^{jk_z z}}{\beta c} \tag{4.46}$$

$$J_z(r,\vartheta,z,t) = \frac{P}{\pi a^2}\delta(a-r)\cos\vartheta\, e^{jk_z z} \tag{4.47}$$

It is derived the transverse coupling impedance by introducing a generalized expression for the computation of the longitudinal coupling impedance of an arbitrary azimuthal mode l as a volume integral over the corresponding longitudinal electric field within the beam and the source electric current density: [17]

$$Z_{l,\parallel}(\omega) = -\frac{1}{M_l^2}\int_0^a\int_0^{2\pi}\int_0^L E_{l,z}^{(r\le a)}(r,\omega)\cos l\vartheta\, e^{jk_z z} J_z^*(r,\vartheta,z,\omega) r dr d\vartheta dz \tag{4.48}$$

where $M_l = Qd^l$ is the lth electric moment.

Imposing $l = 1$ into equation (4.48) and applying the Panofsky – Wenzel theorem (2.46) one obtains, finally, the transverse coupling impedance : [17]

$$Z_{1,\perp}(\omega) = -\frac{1}{k_z M_1^2}\int_0^a \int_0^{2\pi} \int_0^L E_{1,z}^{(r\le a)}(r,\omega)\cos\vartheta\, e^{jk_z z} J_z^*(r,\vartheta,z,\omega) r dr d\vartheta dz \tag{4.49}$$

4.2.1 Dipolar electromagnetic fields and transverse impedance for arbitrary wall thickness

In the case of arbitrary wall thickness electric and magnetic field components have to satisfy the following equations: [17]

$$\left[\frac{d^2}{dr^2} + \frac{1}{r}\frac{d}{dr} - \frac{l^2}{r^2} - \frac{k_z^2}{{\gamma_0}^2}\right] E_{1,z}(r,\omega) = j\frac{P}{\pi a^2}\frac{k_z \cos\vartheta}{\varepsilon_0 {\gamma_0}^2 \beta c}\delta(a-r) \tag{4.50}$$

$$\left[\frac{d^2}{dr^2} + \frac{1}{r}\frac{d}{dr} - \frac{l^2}{r^2} - \frac{k_z^2}{{\gamma_0}^2}\right] B_{1,z}(r,\omega) = 0 \tag{4.51}$$

General solutions for the longitudinal components are:

$$E_{1,z}(r,z,\omega) = e^{jk_z z}\begin{cases} A_1 I_1(\sigma_0 r) & 0 \le r \le a \\ A_2 I_1(\sigma_0 r) + A_3 K_1(\sigma_0 r) & a \le r \le b \\ A_4 I_1(\underline{\sigma} r) + A_5 K_1(\underline{\sigma} r) & b \le r \le h \\ A_6 K_1(\sigma_0 r) & h \le r < \infty \end{cases} \tag{4.52}$$

$$B_{1,z}(r,z,\omega) = e^{jk_z z}\begin{cases} C_1 I_1(\sigma_0 r) & 0 \le r \le b \\ C_2 I_1(\underline{\sigma} r) + C_3 K_1(\underline{\sigma} r) & b \le r \le h \\ C_4 K_1(\sigma_0 r) & h \le r < \infty \end{cases} \tag{4.53}$$

Solving for the transverse electromagnetic field components in terms of $E_{1,z}(r,\vartheta,z,\omega)$ and $B_{1,z}(r,\vartheta,z,\omega)$ one obtains:

$$E_{1,r}(r,\vartheta,z,\omega) = -\frac{j\gamma_0^2}{k_z^2}\left[k_z\frac{\partial E_{1,z}}{\partial r} + \frac{\omega}{r}\frac{\partial B_{1,z}}{\partial \vartheta}\right] \tag{4.54}$$

$$E_{1,\vartheta}(r,\vartheta,z,\omega) = -\frac{j\gamma_0^2}{k_z^2}\left[\frac{k_z}{r}\frac{\partial E_{1,z}}{\partial \vartheta} - \omega\frac{\partial B_{1,z}}{\partial r}\right] \tag{4.55}$$

$$B_{1,r}(r,\vartheta,z,\omega) = \frac{j\gamma_0^2}{k_z^2}\left[\frac{\omega\varepsilon_0\mu_0}{r}\frac{\partial E_{1,z}}{\partial \vartheta} - k_z\frac{\partial B_{1,z}}{\partial r}\right] \tag{4.56}$$

$$B_{1,\vartheta}(r,\vartheta,z,\omega) = -\frac{j\gamma_0^2}{k_z^2}\left[\omega\varepsilon_0\mu_0\frac{\partial E_{1,z}}{\partial r} + \frac{k_z}{r}\frac{\partial B_{1,z}}{\partial \vartheta}\right] \tag{4.57}$$

In order to find the integration constants one needs ten boundary conditions, one of which is obtained from the discontinuity of $\frac{\partial E_{1,z}}{\partial r}$ at $r = a$, while the other nine are obtained from the continuity of $E_{1,z}$ at $r = a, r = b, r = h$ and from the continuity of $B_{1,z}$, $E_{1,\vartheta}$, $B_{1,\vartheta}$ at $r = b, r = h$.

Applying these conditions on the interfaces at $r = a, r = b, r = h$ one obtains:

$$E_{1,z}^{(r\le a)} = -j\frac{P}{\pi a^2}\frac{\sigma_0 a I_1(\sigma_0 a)}{\varepsilon_0\gamma_0\beta c}\left(\frac{I_1(\underline{\sigma}b)}{I_1(\sigma_0 b)}\frac{\alpha_{22}\beta_{11}-\alpha_{12}\beta_{22}}{\alpha_{11}\alpha_{22}-\alpha_{12}\alpha_{21}} + \frac{K_1(\underline{\sigma}b)}{I_1(\sigma_0 b)}\frac{\alpha_{11}\beta_{22}-\alpha_{21}\beta_{11}}{\alpha_{11}\alpha_{22}-\alpha_{12}\alpha_{21}} + \frac{K_1(\sigma_0 a)}{I_1(\sigma_0 a)} - \frac{K_1(\sigma_0 b)}{I_1(\sigma_0 b)}\right) I_1(\sigma_0 r) \tag{4.58}$$

Knowing the longitudinal electric field component and the source current density, one can find the corresponding longitudinal coupling impedance for an arbitrary wall thickness:

$$Z_{1,\parallel}^{(arbit\ wall)}(\omega) = j\frac{LI_1(\sigma_0 a)}{Pa}\frac{P}{\pi a^2}\frac{\sigma_0 a I_1(\sigma_0 a)}{\varepsilon_0\gamma_0\beta c}F = j\frac{nZ_0}{2\beta\gamma_0^2}\frac{4I_1^2(\sigma_0 a)}{a^2}F \tag{4.59}$$

where:

$$F = \frac{I_1(\underline{\sigma}b)}{I_1(\sigma_0 b)}\frac{\alpha_{22}\beta_{11}-\alpha_{12}\beta_{22}}{\alpha_{11}\alpha_{22}-\alpha_{12}\alpha_{21}} + \frac{K_1(\underline{\sigma}b)}{I_1(\sigma_0 b)}\frac{\alpha_{11}\beta_{22}-\alpha_{21}\beta_{11}}{\alpha_{11}\alpha_{22}-\alpha_{12}\alpha_{21}} + \frac{K_1(\sigma_0 a)}{I_1(\sigma_0 a)} - \frac{K_1(\sigma_0 b)}{I_1(\sigma_0 b)} \tag{4.60}$$

Accordingly, the transverse coupling impedance is obtained from the application of Panofsky – Wenzel theorem (2.46): [17]

$$Z_{1,\perp}^{(arbit\ wall)}(\omega) = \frac{Z_{1,\parallel}^{(arbit\ wall)}(\omega)}{k_z}$$
$$= j\frac{nZ_0}{2\beta\gamma_0^2}\frac{4I_1^2(\sigma_0 a)}{a^2 k_z}\left(\frac{I_1(\underline{\sigma}b)}{I_1(\sigma_0 b)}\frac{\alpha_{22}\beta_{11}-\alpha_{12}\beta_{22}}{\alpha_{11}\alpha_{22}-\alpha_{12}\alpha_{21}}+\frac{K_1(\underline{\sigma}b)}{I_1(\sigma_0 b)}\frac{\alpha_{11}\beta_{22}-\alpha_{21}\beta_{11}}{\alpha_{11}\alpha_{22}-\alpha_{12}\alpha_{21}}+\frac{K_1(\sigma_0 a)}{I_1(\sigma_0 a)}\right.$$
$$\left.-\frac{K_1(\sigma_0 b)}{I_1(\sigma_0 b)}\right) \qquad (4.61)$$

4.2.2 Dipolar electromagnetic fields and transverse impedance for a thick conducting wall

In the limit of a thick beam pipe conducting wall, the general solutions of equations (4.50), (4.51) are: [17]

$$E_{1,z}(r,z,\omega) = e^{jk_z z}\begin{cases} A_1 I_1(\sigma_0 r) & 0 \le r \le a \\ A_2 I_1(\sigma_0 r) + A_3 K_1(\sigma_0 r) & a \le r \le b \\ A_4 K_1(\underline{\sigma} r) & b \le r < \infty \end{cases} \qquad (4.62)$$

$$B_{1,z}(r,z,\omega) = e^{jk_z z}\begin{cases} C_1 I_1(\sigma_0 r) & 0 \le r \le b \\ C_2 K_1(\underline{\sigma} r) & b \le r < \infty \end{cases} \qquad (4.63)$$

In order to find the integration constants one needs six boundary conditions, one of which is obtained from the discontinuity of $\frac{\partial E_{1,z}}{\partial r}$ at $r = a$, while the other five are obtained from the continuity of $E_{1,z}$ at $r = a$ and from the continuity of $E_{1,z}$, $B_{1,z}$, $E_{1,\vartheta}$, $B_{1,\vartheta}$ at $r = b$.

Applying these conditions on the interfaces at $r = a, r = b$ one obtains:

$$E_{1,z}^{(r\le a)}(r,\omega) = -j\omega\frac{P}{\pi a}\frac{I_1(\sigma_0 a)}{\varepsilon_0\gamma_0^2\beta^2 c^2}\left(\frac{K_1(\sigma_0 a)}{I_1(\sigma_0 a)}-\frac{K_1(\sigma_0 b)}{I_1(\sigma_0 b)}+\eta\frac{\gamma_{21}}{\gamma_{22}}\frac{K_1(\underline{\sigma}b)}{I_1(\sigma_0 b)}\right)I_1(\sigma_0 r) \qquad (4.64)$$

The corresponding transverse coupling impedance is: [17]

$$Z_{1,\perp}^{(thick\ wall)}(\omega) = j\frac{LZ_0 I_1^2(\sigma_0 a)}{\pi a^2 {\gamma_0}^2 \beta}\left(\frac{K_1(\sigma_0 a)}{I_1(\sigma_0 a)} - \frac{K_1(\sigma_0 b)}{I_1(\sigma_0 b)} + \eta\frac{\gamma_{21}}{\gamma_{22}}\frac{K_1(\underline{\sigma} b)}{I_1(\sigma_0 b)}\right) \tag{4.65}$$

The electric field caused by transverse dipole oscillations vanishes for a wall thickness comparable to the skin depth. Thinner walls can be regarded as transparent. This is in contrast to the electric field caused by longitudinal perturbations, where wave reflection is dominating and the radial electric field drops already for very small wall thicknesses.

4.3 Resistive wall impedance and tune shift for a chamber with a finite thickness [23]

In the following analysis the authors K. Yokoya and Y. Shobuda [23] derive the resistive wall impedance for a chamber with a finite thickness and the associated Tune Shift, showing that by reducing the thickness of the chamber it can be reduced the Tune Shift linearly. It is important to consider the effect of the thickness of the beam pipe. In fact, a beam pipe of non-round cross section causes an incoherent Tune Shift because the resistive wall impedance, due to the source particle, depends not only on the coordinates of the source particle, but also on those of the witness particle.

One considers a wall with thickness d (**Fig. 4.1**) that can be divided into three regions:

1) $x < d$ Region I
2) $0 < x < d$ Region II
3) $d < x < \infty$ Region III

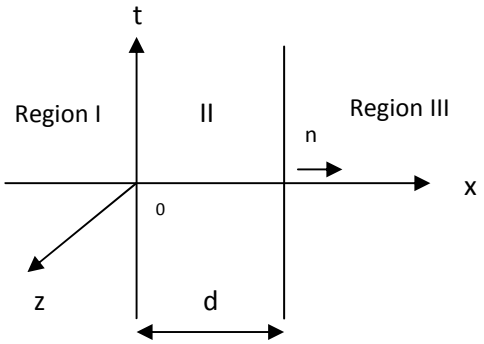

Fig. 4.1 The beam runs in Region I.

The beam creates fields on the inner surface of the wall at $x = 0$.

The Maxwell's equations in the Region II are written as:

$$jkH_t(x) = (\sigma + jkc\varepsilon_0)E_n(x)$$

$$\varepsilon_0 \frac{\partial E_n(x)}{\partial x} - jk\varepsilon_0 E_z(x) = 0$$

$$-\frac{\partial E_z(x)}{\partial x} - jkE_n(x) = -jkc\mu_0 H_t(x)$$

$$\frac{\partial H_t(x)}{\partial x} = (\sigma + jkc\varepsilon_0)E_z(x) \qquad (4.66)$$

whose solutions are:

$$E_z(x) = c_1 e^{\frac{\sqrt{2j}x}{\delta}} + c_2 e^{-\frac{\sqrt{2j}x}{\delta}} \qquad (4.67)$$

$$H_t(x) = \frac{\sqrt{2j}}{\delta}\frac{1 + jk\rho_0}{jkZ_0}(c_1 - c_2) \qquad (4.68)$$

By imposing the boundary conditions one obtains the following relation:

$$E_z(0) = -k\delta Z_0 \frac{1 + j}{2} \mathcal{G} H_t(0) \qquad (4.69)$$

where the $\mathcal{G}$ factor is given by:

$$\mathcal{G} = \frac{e^{\frac{\sqrt{2j}d}{\delta}} - e^{\frac{-\sqrt{2j}d}{\delta}}}{e^{\frac{\sqrt{2j}d}{\delta}} + e^{\frac{-\sqrt{2j}d}{\delta}}} \tag{4.70}$$

In this way E_z for a chamber with a finite thickness is that with an infinite thickness multiplied by the $\mathcal{G}$ factor.

Knowing the following function:

$$F_{\perp}(x,y) = \frac{\delta(1+j)}{j} \frac{e^{\frac{\sqrt{2j}d}{\delta}} - e^{\frac{-\sqrt{2j}d}{\delta}}}{e^{\frac{\sqrt{2j}d}{\delta}} + e^{\frac{-\sqrt{2j}d}{\delta}}} \frac{Z_0}{2\pi b^3} D_{\perp} \tag{4.71}$$

where $D_{\perp} = \left\{ \begin{pmatrix} D_{1x}x_1 \\ D_{1y}y_1 \end{pmatrix} + D_{2xy} \begin{pmatrix} x \\ -y \end{pmatrix} + \cdots \right\}$ and its inverse Fourier transformation, one obtains the transverse wake function:

$$W_{\perp}(s) = \int_{-\infty}^{\infty} dk\, e^{jks} \frac{c}{2\pi} \frac{Z_0}{2\pi b^3}\, D_{\perp} \frac{\delta(1+j)}{j} \frac{e^{\frac{\sqrt{2j}d}{\delta}} - e^{\frac{-\sqrt{2j}d}{\delta}}}{e^{\frac{\sqrt{2j}d}{\delta}} + e^{\frac{-\sqrt{2j}d}{\delta}}} \tag{4.72}$$

This function can be divided into the part proportional to the coordinate of the source particle and the part proportional to the coordinate of the witness particle:

$$W_{\perp}(s) = \begin{pmatrix} W_{1x}(s)x_1 + W_2(s)x \\ W_{1y}(s)y_1 - W_2(s)x \end{pmatrix} \tag{4.73}$$

$W_{1x,y}(s)$ causes a coherent tune shift $\delta\nu_{coh,x,y}^{(\mu)}$:

$$\delta\nu_{coh,x,y}^{(\mu)} = -\frac{L\langle\beta_{x,y}\rangle}{4\pi} \frac{Z_0 I_0}{E} \frac{L\sqrt{\rho_0}}{\pi\sqrt{\pi}b^3\sqrt{2L}} D_{1x,y} \sum_{k=1}^{\infty} \sqrt{\frac{2}{k}} \left\{ \cos\left[2\pi\Delta\nu_{x,y}^{(\mu)}\left(k+\frac{1}{2}\right)\right] + j sin\left[2\pi\Delta\nu_{x,y}^{(\mu)}\left(k+\frac{1}{2}\right)\right] \right\} \tag{4.74}$$

$W_2(s)$ causes an incoherent tune shift $\delta\nu_{inc,x,y}^{(\mu)}$:

$$\delta\nu_{coh,x,y}^{(\mu)} = \mp D_{2xy}\frac{L\langle\beta_{x,y}\rangle}{4\pi}\frac{Z_0 I_0}{E}\frac{1}{\pi b^3}d \qquad (4.75)$$

The coherent tune shift is automatically finite even if $d \to \infty$ while the incoherent tune shift is infinite for $d \to \infty$.

4.4 Analytical presentation of resistive impedance for the laminated vacuum chamber [24]

In this Section M. Ivanyan [24] evaluates numerically the impedance of a vacuum chamber with laminated walls of finite thickness following the field matching technique. Although this method is valid only for the relativistic charge, the transformation to ultra-relativistic limit is performed after derivation of the analytical solution for the impedance.

The geometry of the considered problem is represented in (**Fig. 4.2**).

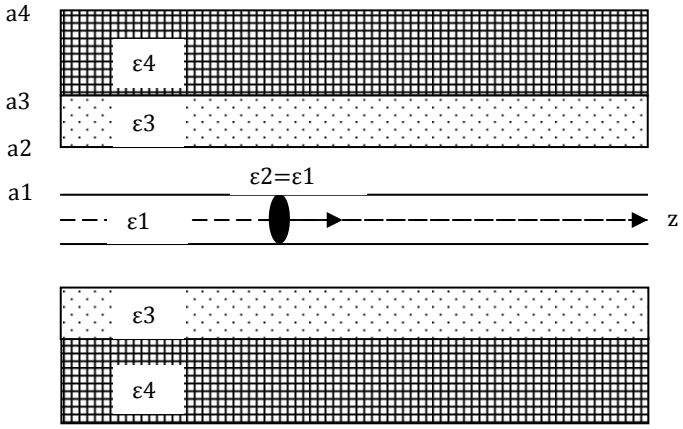

Fig. 4.2 A relativistic plane disk of radius a_1, total charge Q and charge transverse distribution $\rho(r,\vartheta)$ moving with velocity $v\sim c$ along the z-axis of uniform, circular cylindrical two-layer tube of inner radius $a_2 = b$. The disk center coincides with the tube axis. The boundary between two layers is located at $r = a_3$ and the outer radius of the tube is a_4. Outside the tube is vacuum and the layer can be either dielectrics or metals.

The cross section of the tube is divided into five concentric regions:

1) $0 \leq r \leq a_1$ vacuum
2) $a_1 \leq r \leq a_2 = b$ vacuum
3) $a_2 \leq r \leq a_3$ first layer
4) $a_3 \leq r \leq a_4$ second layer
5) $r \geq a_4$ vacuum

In general, multipole components of the electromagnetic fields in the frequency domain are:

$$\{E_r, E_z, B_\vartheta\}_m\,(\omega, r, \vartheta, s) = \{E_r, E_z, B_\vartheta\}_m(\omega, r) cosm\vartheta\; e^{-jkz} \tag{4.76}$$

$$\{B_r, B_z, E_\vartheta\}_m\,(\omega, r, \vartheta, s) = \{B_r, B_z, E_\vartheta\}_m(\omega, r) sinm\vartheta\; e^{-jkz} \tag{4.77}$$

The radial dependence of the frequency domain m-pole longitudinal electric and magnetic components in each region is given by:

$$E_{zm}^{(i)}\left[\frac{1}{r}\frac{\partial}{\partial r}\left(r\frac{\partial}{\partial r}\right) - \frac{m^2}{r^2} - \chi_i^2\right] = \frac{jQ\chi_i^2}{\omega\varepsilon_i T_m} q_m^{(i)} r^m$$

$$H_{zm}^{(i)}\left[\frac{1}{r}\frac{\partial}{\partial r}\left(r\frac{\partial}{\partial r}\right) - \frac{m^2}{r^2} - \chi_i^2\right] = 0 \tag{4.78}$$

where:

$$q_m = \int_0^{2\pi}\int_0^{a_1} \rho(r, \vartheta) r^{m+1} cosm\vartheta dr\, d\vartheta \tag{4.79}$$

$$T_m = \frac{\pi a_1^{2(m+1)}}{2(m+1)} \tag{4.80}$$

$$\chi_i = \sqrt{k^2 - \mu_0\varepsilon_i\omega^2} \tag{4.81}$$

The radial dependence of the transverse components of electric and magnetic fields is given by:

$$E_{rm} = jk\chi_i^{-2}\left(\frac{\partial E_{zm}}{\partial r} + v\mu_0\frac{m}{r}H_{zm}\right)$$

$$E_{\vartheta m} = -jk\chi_i^{-2}\left(v\mu_0\frac{\partial H_{zm}}{\partial r} + \frac{m}{r}E_{zm}\right)$$

$$H_{rm} = jk\chi_i^{-2}\left(\frac{\partial H_{zm}}{\partial r} + v\varepsilon_i\frac{m}{r}E_{zm}\right)$$

$$H_{rm} = jk\chi_i^{-2}\left(v\varepsilon_i\frac{\partial E_{zm}}{\partial r} + \frac{m}{r}H_{zm}\right) \qquad (4.82)$$

In the beam region (1) the longitudinal electric and magnetic fields are:

$$E_{zm}^{(1)}(r) = F_1 I_m(\lambda r) + G_1(r)$$

$$H_{zm}^{(1)}(r) = P_1 I_m(\lambda r) \qquad (4.83)$$

where I_m is the modified Bessel function of first kind.

In the subsequent regions (2,3,4) the longitudinal fields components are:

$$E_{zm}^{(i)} = F_i R_i(r) + G_i S_i(r)$$

$$H_{zm}^{(i)} = P_i R_i(r) + Q_i S_i(r) \qquad (4.84)$$

where:

$$R_i(r) = K_m(\chi_i a_i) I_m(\chi_i r) - I_m(\chi_i a_i) K_m(\chi_i r) \qquad (4.85)$$

$$S_i(r) = K'_m(\chi_i a_i) I_m(\chi_i r) - I'_m(\chi_i a_i) K_m(\chi_i r) \qquad (4.86)$$

where K'_m and I'_m are the modified Bessel functions of second kind.

For the transverse field components one has:

$$R_i'(r) = K_m(\chi_i a_i)I_m'(\chi_i r) - I_m(\chi_i a_i)K_m'(\chi_i r) \tag{4.87}$$

$$S_i'(r) = K_m'(\chi_i a_i)I_m'(\chi_i r) - I_m'(\chi_i a_i)K_m'(\chi_i r) \tag{4.88}$$

In the outer region (5) the longitudinal field components are:

$$E_{zm}^{(5)}(r) = F_5 K_m(\lambda r)$$

$$H_{zm}^{(5)}(r) = P_5 K_m(\lambda r) \tag{4.89}$$

In the ultra-relativistic limit the longitudinal electric field in the beam region (1) is:

$$E_{zm}^{(1)}(r,k) = -j\frac{Q}{\pi\varepsilon_0 ckU_m(k)}\frac{q_m}{a_1^m}(\frac{r}{a_2})^m(\frac{a_1}{a_2})^m \tag{4.90}$$

After accounting the field one can determine the m-pole component of longitudinal impedance:

$$\tilde{Z}_{zm}(r,k) = \frac{1}{Q}E_{zm}^{(1)}(r,k) = \frac{q_m}{a_1^m}\left(\frac{r}{a_2}\right)^m\left(\frac{a_1}{a_2}\right)^m Z_{zm}(k) \tag{4.91}$$

where:

$$Z_{zm}(k) = -j\frac{Z_0}{\pi k U_m(k)} \tag{4.92}$$

Using the Panofsky – Wenzel theorem one obtains the m-pole components of transverse impedance:

$$\tilde{Z}_{\perp m}(r,k,\vartheta) = \frac{q_m}{a_1^m}\left(\frac{r}{a_2}\right)^{m-1}\left(\frac{a_1}{a_2}\right)^m Z_{\perp m}(k)[cosm\vartheta\vec{\imath}_r - sinm\vartheta\vec{\imath}_\vartheta] \tag{4.93}$$

where:

$$Z_{\perp m}(k) = \frac{m}{ka_2}Z_{zm}(k) \tag{4.94}$$

4.5 Wake field in dielectric acceleration structures [25]

In this study L. Schachter , R. L. Byer and R. H. Siemann [25] present a general approach for the analysis of the wake field of a point charge moving in a vacuum tunnel surrounded by a dielectric medium (**Fig. 4.3**). The reflecting structure is represented by a reflecting wall and it may be either an asymmetric structure consisting of an array of vacuum cylinders surrounding the central one, known as a photonic band gap structure, or an azimuthally symmetric Bragg structure consisting of a series of concentric dielectric layers.

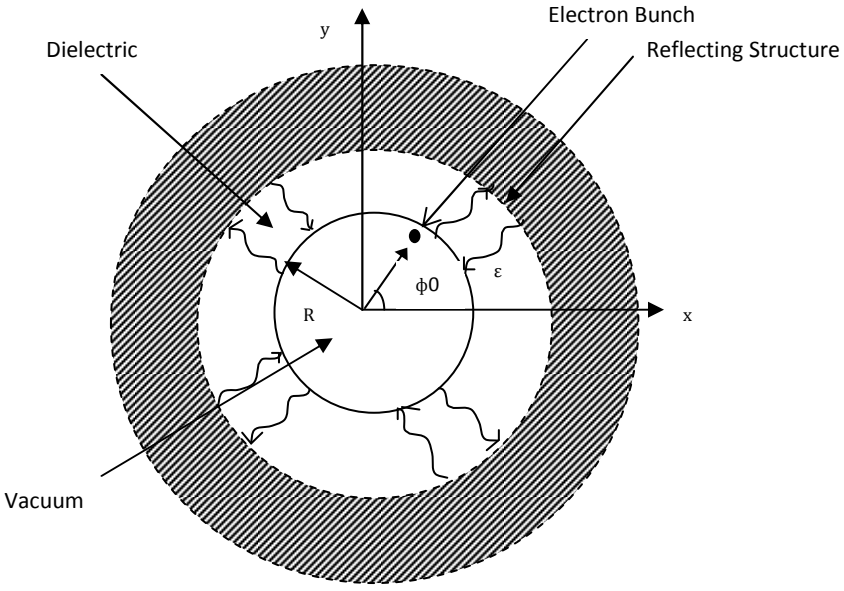

Fig. 4.3 A point charge q located at $r = r_0$ and $\phi = \phi_0$ moves parallel to the z-axis at a velocity v in a vacuum tunnel of radius R. The latter is surrounded by a dielectric structure that confines the electromagnetic mode.

When a bunch is injected into a dielectric acceleration structure, the wake field is responsible for a decelerating field that ought to be as small as possible.

In this Section it has been developed a quasi-analytical expression that relates this decelerating force to the first dielectric layer of the structure, the radius of the vacuum tunnel where the bunch moves and the reflection characteristics of the structure.

After introducing a cylindrical coordinate system whose z-axis coincides with the axis of the central vacuum tunnel it is possible to attribute to a point charge a current density:

$$J_z(r,z,\phi,t) = -\frac{qv}{r}\delta(r-r_0)\delta(\phi-\phi_0)\delta(z-vt) \tag{4.95}$$

that generates a primary field which satisfies the following non-homogeneous wave equation:

$$\nabla^2 - \frac{1}{c^2}\frac{\partial^2}{\partial t^2}A_z(r,z,\phi,t) = -\mu_0 J_z(r,z,\phi,t) \tag{4.96}$$

After imposing the continuity of the tangential field components at $r = R > r_0$ one obtains the corresponding primary components of the electromagnetic field:

$$\begin{pmatrix} E_z \\ E_\phi \\ H_z \\ H_\phi \end{pmatrix} = -\frac{q\mu_0}{(2\pi)^2}\int_{-\infty}^{\infty} d\omega\, e^{j\omega(t-z/v)} \sum_{n=-\infty}^{\infty} e^{jn(\phi-\phi_0)} \mathrm{I_n}(\Gamma r_0) \begin{pmatrix} \frac{\mathrm{j}\omega}{(\gamma\beta)^2}\mathrm{K_n}(\Gamma r) \\ \frac{\mathrm{j}\omega}{\left(\frac{\omega}{\mathrm{c}}\mathrm{r}\right)\beta}\mathrm{K_n}(\Gamma r) \\ -\frac{\Gamma}{\mu_0}\dot{\mathrm{K}}_\mathrm{n}(\Gamma r) \end{pmatrix} \tag{4.97}$$

where $\Gamma = \frac{\omega}{c}\frac{1}{\gamma\beta}$.

This primary field is valid in the central vacuum tunnel of the structure and in the absence of the dielectric structure.

In the case $r < R$ it is generated a secondary field that is determined by two longitudinal components of the electromagnetic field:

$$\begin{pmatrix} E_z \\ H_z \end{pmatrix} = -\frac{q\mu_0}{(2\pi)^2}\int_{-\infty}^{\infty} d\omega\, e^{j\omega(t-z/v)} \sum_{n=-\infty}^{\infty} e^{jn(\phi-\phi_0)} \mathrm{I_n}(\Gamma r) \begin{pmatrix} \frac{\mathrm{j}\omega}{(\gamma\beta)^2}\mathrm{A_n} \\ -\frac{\Gamma}{\mu_0(\gamma\beta)^2}\mathrm{B_n} \end{pmatrix} \tag{4.98}$$

In the dielectric region, $r > R$, the secondary components of the electromagnetic field are:

$$\begin{pmatrix} E_z \\ H_z \end{pmatrix} = -\frac{q\mu_0}{(2\pi)^2}\int_{-\infty}^{\infty} d\omega\, e^{j\omega(t-z/v)} \sum_{n=-\infty}^{\infty} e^{jn(\phi-\phi_0)} \mathrm{I_n}(\Gamma r) \begin{pmatrix} \frac{\mathrm{j}\omega}{(\gamma\beta)^2}[\mathrm{C_n H_n^{(2)}}(\Lambda r) + \mathrm{D_n H_n^{(1)}}(\Lambda r)] \\ \frac{\Lambda}{\mu_0(\gamma\beta)^2}[\mathrm{E_n H_n^{(2)}}(\Lambda r) + \mathrm{F_n H_n^{(1)}}(\Lambda r)] \end{pmatrix} \tag{4.99}$$

where $\Lambda = \frac{\omega}{c}\sqrt{\varepsilon_r - \beta^{-2}}$.

With the longitudinal components one can find the other two tangential components in each of the regions, based on:

$$\bar{E}_\phi = \frac{n}{\beta\bar{\varepsilon}\left(\frac{\omega}{c}\right)r}\bar{E}_z - \frac{1}{j\omega\varepsilon_0\bar{\varepsilon}}\frac{\partial\bar{H}_z}{\partial r}$$

$$\bar{H}_\phi = \frac{n}{\beta\bar{\varepsilon}\left(\frac{\omega}{c}\right)r}\bar{H}_z + \frac{1}{j\omega\mu_0}\frac{\varepsilon_r}{\bar{\varepsilon}}\frac{\partial\bar{E}_z}{\partial r} \qquad (4.100)$$

after assuming that the field components have the spatial dependence $E \sim \bar{E}(r)e^{j\omega(t-z/v)}e^{jn\phi}$ and $\bar{\varepsilon} = \varepsilon_r - \beta^{-2}$.

In order to determine the coefficients $\mathrm{A_n}, \mathrm{B_n}, \mathrm{C_n}, \mathrm{D_n}, \mathrm{E_n}, \mathrm{F_n}$ it is necessary to impose four boundary conditions for the tangential components of the field. To determine the decelerating field on the point charge it is sufficient to calculate the coefficient $\mathrm{A_n}$. In fact, the decelerating power is given by:

$$P = -qv\int_{-\infty}^{\infty} d\omega\ \frac{j\omega}{(\gamma\beta)^2}\sum_{n=-\infty}^{\infty} A_n I_n(\Gamma r_0) = -qv\varepsilon_{\|} \qquad (4.101)$$

where $\varepsilon_{\|}$ denotes the decelerating field on the point charge.

Whatever structure surrounds the vacuum tunnel where the electron bunch propagates, causes a reflection process and it can be represented mathematically by a matrix that relates the outgoing waves with the incoming ones. In this case one has:

$$\begin{pmatrix} D_n H_n^{(1)}(\Lambda R) \\ F_n H_n^{(1)}(\Lambda R) \end{pmatrix} = \sum_n \begin{pmatrix} R_{nm}^{(11)} & R_{nm}^{(12)} \\ R_{nm}^{(21)} & R_{nm}^{(22)} \end{pmatrix} \begin{pmatrix} C_m H_m^{(1)}(\Lambda R) \\ E_m H_m^{(1)}(\Lambda R) \end{pmatrix} \qquad (4.102)$$

where $R_{nm}^{(11)}$and $R_{nm}^{(22)}$ couple between the amplitudes of the incoming and outgoing TM waves and TE waves, respectively; while, $R_{nm}^{(12)}$ couples between the amplitudes of the incoming TE mode and the outgoing ones of the TM wave and $R_{nm}^{(21)}$ couples between the amplitudes of the incoming TM mode and the outgoing ones of the TE wave.

The simulation results, obtained either numerically or analytically, indicate that if the effective location where the reflection occurs in the dielectric is sufficiently apart from the edge of the vacuum tunnel, it has no effect on the point charge. In fact, the decelerating field converges exponentially as this distance increases, to its asymptotic value set by the first layer of the dielectric material. [25]

Appendix A - Maxwell's Equations

To compute electromagnetic field components, generated by a bunched particle beam, one has to find the solution of a system of differential, partial, linear and inhomogeneous Maxwell's equations by including the source terms and the appropriate boundary conditions:

$$\nabla \times \boldsymbol{H} = \frac{\partial \boldsymbol{D}}{\partial t} + \boldsymbol{J}$$

$$\nabla \times \boldsymbol{E} = -\frac{\partial \boldsymbol{B}}{\partial t} \qquad (A1)$$

$$\nabla \cdot \boldsymbol{D} = \rho$$

$$\nabla \cdot \boldsymbol{B} = 0$$

that one has to add the following relations:

$$\boldsymbol{D} = \varepsilon\, \boldsymbol{E}$$
$$\boldsymbol{B} = \mu\, \boldsymbol{H} \qquad (A2)$$

$$\boldsymbol{J} = \boldsymbol{J}_{cond} \cdot \boldsymbol{J}_{conv} = \sigma_c\, \boldsymbol{E} + \rho\, \boldsymbol{v}$$

Substituting these relations in the system (1) one obtains:

$$\nabla \times \boldsymbol{H} = \varepsilon \frac{\partial \boldsymbol{E}}{\partial t} + \sigma_c\, \boldsymbol{E} + \rho\, \boldsymbol{v}$$

$$\nabla \times \boldsymbol{E} = -\mu \frac{\partial \boldsymbol{H}}{\partial t} \qquad (A3)$$

$$\nabla \cdot \boldsymbol{E} = \frac{\rho}{\varepsilon}$$

$$\nabla \cdot \boldsymbol{H} = 0$$

This calculation can be performed analytically in the case of idealized geometries or numerically in more realistic cases. Limitations in numerical calculations justify the development of analytical or semi-analytical methods which can provide explicit solutions.

With the vector Laplacian operator, defined by $\Delta E = \nabla(\nabla \cdot \mathrm{E}) - \nabla \times \nabla \times \mathrm{E}$, one obtains the wave equations for the electric and magnetic fields:

$$\left[\Delta - \mu\varepsilon\frac{\partial^2}{\partial \mathrm{t}^2}\right]\mathbf{E} = \mu\frac{\partial \boldsymbol{J}}{\partial t} + \frac{1}{\varepsilon}\nabla\rho$$

$$\left[\Delta - \mu\varepsilon\frac{\partial^2}{\partial \mathrm{t}^2}\right]\mathbf{H} = -\nabla \times \boldsymbol{J} \qquad (A4)$$

In the frequency domain the partial derivatives are replaced by the factor $j\omega$ and the wave equations are then called *Helmholtz's equations*.

Electromagnetic fields can be described in terms of vector potential $\boldsymbol{A}$ and of scalar potential Φ:

$$\boldsymbol{E} = -\nabla\Phi - \frac{\partial \boldsymbol{A}}{\partial t} \qquad (A5)$$

$$\boldsymbol{B} = \nabla \times \boldsymbol{A}$$

Whence the wave equations:

$$\left[\Delta - \mu\varepsilon\frac{\partial^2}{\partial \mathrm{t}^2}\right]\mathbf{A} = -\mu\,\boldsymbol{J} + \nabla\left[\nabla \cdot \boldsymbol{A} + \mu\,\varepsilon\frac{\partial\Phi}{\partial t}\right]$$

$$\left[\Delta - \mu\varepsilon\frac{\partial^2}{\partial \mathrm{t}^2}\right]\Phi = -\frac{\rho}{\varepsilon} - \frac{\partial}{\partial t}\left[\nabla \cdot \boldsymbol{A} + \mu\,\varepsilon\frac{\partial\Phi}{\partial t}\right] \qquad (A6)$$

When the electromagnetic field is excited by a relativistic beam, it is convenient to separate its longitudinal and transverse parts:

$$\boldsymbol{E}(\boldsymbol{r}) = \boldsymbol{E}_{\perp}(\boldsymbol{r}) + \hat{\boldsymbol{z}}E_z(\boldsymbol{r}) \qquad (A7)$$

$$\boldsymbol{H}(\boldsymbol{r}) = \boldsymbol{H}_{\perp}(\boldsymbol{r}) + \hat{\boldsymbol{z}}H_z(\boldsymbol{r})$$

where $\hat{\boldsymbol{z}}$ is the unit vector in the longitudinal direction and the subscripts $\perp$ and z indicate the transverse and longitudinal components.

The problem of finding the electromagnetic field is restricted to solving the Maxwell's equations with the source terms:

$$\rho(\boldsymbol{r}) = \rho_{\perp}(\boldsymbol{r}_{\perp})\,\lambda(s) \qquad (A8)$$

$$\boldsymbol{J}(\boldsymbol{r}) = \hat{\boldsymbol{z}}\,v\,\rho(\boldsymbol{r})$$

Performing a Fourier transformation in the variable s one obtains equations for the electric and magnetic fields:

$$\widetilde{\boldsymbol{E}}(\boldsymbol{r}_{\perp}, k) = \int_{-\infty}^{\infty} ds\, \boldsymbol{E}(\boldsymbol{r}_{\perp}, s) e^{-jks}$$

$$\widetilde{\boldsymbol{H}}(\boldsymbol{r}_{\perp}, k) = \int_{-\infty}^{\infty} ds\, \boldsymbol{H}(\boldsymbol{r}_{\perp}, s) e^{-jks} \qquad (A9)$$

The Fourier transformations lead to the following rules for differentiation:

$$\partial_t \widetilde{\boldsymbol{E}} = j\omega \widetilde{\boldsymbol{E}} \quad , \quad \partial_z \widetilde{\boldsymbol{E}} = -jk\widetilde{\boldsymbol{E}} \qquad (A10)$$

The Maxwell's equations for the Fourier transforms can be written:

$$\nabla_{\perp} \times \widetilde{\boldsymbol{H}}_{\perp} = \left(j\omega\varepsilon\, \tilde{E}_z + \tilde{\rho}\, v\right)\hat{\boldsymbol{z}}$$

$$\nabla_{\perp} \times \widetilde{\boldsymbol{E}}_{\perp} = -j\omega\mu \widetilde{H}_z \hat{\boldsymbol{z}}$$

$$\hat{\boldsymbol{z}} \times \left(-\mathrm{jk}\widetilde{\boldsymbol{E}}_{\perp} - \nabla_{\perp}\tilde{E}_z\right) = -j\omega\mu\widetilde{\boldsymbol{H}}_{\perp}$$

$$\hat{\boldsymbol{z}} \times \left(-\mathrm{jk}\widetilde{\boldsymbol{H}}_{\perp} - \nabla_{\perp}\widetilde{H}_z\right) = j\omega\varepsilon\widetilde{\boldsymbol{E}}_{\perp} \qquad (A11)$$

$$\nabla_{\perp} \cdot \widetilde{\boldsymbol{E}}_{\perp} = jk\tilde{E}_z + \frac{\tilde{\rho}}{\varepsilon}$$

$$\nabla_{\perp} \cdot \widetilde{\boldsymbol{H}}_{\perp} = jk\widetilde{H}_z$$

The last two equations allow the elimination of the longitudinal components of the fields from the first four equations:

$$\nabla_\perp \times \widetilde{\boldsymbol{E}}_\perp = -v\mu\hat{\boldsymbol{z}}\nabla_\perp \cdot \widetilde{\boldsymbol{H}}_\perp$$

$$\nabla_\perp \times \widetilde{\boldsymbol{H}}_\perp = v\varepsilon\hat{\boldsymbol{z}}\ \nabla_\perp \cdot \widetilde{\boldsymbol{E}}_\perp$$

$$\hat{\boldsymbol{z}} \times \left[-\mathrm{k}\widetilde{\boldsymbol{E}}_\perp + \frac{1}{k}\nabla_\perp\left(\nabla_\perp \cdot \widetilde{\boldsymbol{E}}_\perp - \frac{\tilde{\rho}}{\varepsilon}\right)\right] = -\omega\mu\widetilde{\boldsymbol{H}}_\perp \qquad (A12)$$

$$\hat{\boldsymbol{z}} \times \left[-\mathrm{k}\widetilde{\boldsymbol{H}}_\perp + \frac{1}{k}\nabla_\perp\left(\nabla_\perp \cdot \widetilde{\boldsymbol{H}}_\perp\right)\right] = \omega\varepsilon\widetilde{\boldsymbol{E}}_\perp$$

The transverse components of the electric field can be divided, in turn, into two parts:

$$\widetilde{\boldsymbol{E}}_\perp = \widetilde{\boldsymbol{E}}^{irr} + \widetilde{\boldsymbol{E}}^{sol} \qquad (A13)$$

where $\widetilde{\boldsymbol{E}}^{irr}$ is the irrotational field, for which $\nabla_\perp \times \widetilde{\boldsymbol{E}}^{irr} = 0$, and $\widetilde{\boldsymbol{E}}^{sol}$ is the solenoidal field, for which $\nabla_\perp \cdot \widetilde{\boldsymbol{E}}^{sol} = 0$.

Using these properties, equations (A6) become:

$$\nabla_\perp \times \widetilde{\boldsymbol{E}}^{sol} = -v\mu\hat{\boldsymbol{z}}\nabla_\perp \cdot \widetilde{\boldsymbol{H}}^{irr}$$

$$\nabla_\perp \times \widetilde{\boldsymbol{H}}^{sol} = v\varepsilon\hat{\boldsymbol{z}}\,\nabla_\perp \cdot\ \widetilde{\boldsymbol{E}}^{irr}$$

$$\hat{\boldsymbol{z}} \times \left[-\mathrm{k}^2\widetilde{\boldsymbol{E}}^{irr} - \mathrm{k}^2\widetilde{\boldsymbol{E}}^{sol} + \nabla_\perp\left(\nabla_\perp \cdot \widetilde{\boldsymbol{E}}^{irr} - \frac{\tilde{\rho}}{\varepsilon}\right)\right] = -k\omega\mu\left(\widetilde{\boldsymbol{H}}^{irr} + \widetilde{\boldsymbol{H}}^{sol}\right) \qquad (A14)$$

$$\hat{\boldsymbol{z}} \times \left[-\mathrm{k}^2\widetilde{\boldsymbol{H}}^{irr} - \mathrm{k}^2\widetilde{\boldsymbol{H}}^{sol} + \nabla_\perp\left(\nabla_\perp \cdot \widetilde{\boldsymbol{H}}^{irr}\right)\right] = k\omega\varepsilon\left(\widetilde{\boldsymbol{E}}^{irr} + \widetilde{\boldsymbol{E}}^{sol}\right)$$

Applying the vector identity $\boldsymbol{a} \times \boldsymbol{b} \times \boldsymbol{c} = \boldsymbol{b}(\boldsymbol{a} \cdot \boldsymbol{c}) - \boldsymbol{c}(\boldsymbol{a} \cdot \boldsymbol{b})$ one obtains:

$$\hat{\boldsymbol{z}} \times \widetilde{\boldsymbol{E}}^{sol} = v\mu\widetilde{\boldsymbol{H}}^{irr}$$

$$\hat{\boldsymbol{z}}\ \times \widetilde{\boldsymbol{H}}^{sol} = -v\varepsilon\,\widetilde{\boldsymbol{E}}^{irr}$$

$$\hat{\boldsymbol{z}} \times \left[\mathrm{k}^2 \tilde{\boldsymbol{E}}^{irr} - \nabla_\perp \left(\nabla_\perp \cdot \tilde{\boldsymbol{E}}^{irr} - \frac{\tilde{\rho}}{\varepsilon} \right) \right] = v\mu \, \tilde{\boldsymbol{H}}^{sol} \qquad (A15)$$

$$\hat{\boldsymbol{z}} \times \left[\mathrm{k}^2 \tilde{\boldsymbol{H}}^{irr} - \nabla_\perp \left(\nabla_\perp \cdot \tilde{\boldsymbol{H}}^{irr} \right) \right] = -v\varepsilon \tilde{\boldsymbol{E}}^{sol}$$

The first two equations can also written in the following form:

$$\tilde{\boldsymbol{E}}^{sol} = -v\mu \hat{\boldsymbol{z}} \times \tilde{\boldsymbol{H}}^{irr}$$

$$\tilde{\boldsymbol{H}}^{sol} = v\varepsilon \hat{\boldsymbol{z}} \times \tilde{\boldsymbol{E}}^{irr} \qquad (A16)$$

One can eliminate $\tilde{\boldsymbol{H}}^{sol}$ and $\tilde{\boldsymbol{E}}^{sol}$ from the second two equations and, by substituting the transverse Laplacian operator, obtain:

$$\Delta_\perp \tilde{\boldsymbol{E}}^{irr} - \mathrm{k}^2 (1 - \varepsilon\mu \mathrm{v}^2) \tilde{\boldsymbol{E}}^{irr} = \nabla_\perp \frac{\tilde{\rho}}{\varepsilon}$$

$$\Delta_\perp \tilde{\boldsymbol{H}}^{irr} - \mathrm{k}^2 (1 - \varepsilon\mu \mathrm{v}^2) \tilde{\boldsymbol{H}}^{irr} = 0 \qquad (A17)$$

The Fourier transforms of the fields can be written in terms of the Debye's potentials, $\tilde{\Phi}$ *e* $\tilde{\Psi}$, which have been used to calculate the impedance due to small perturbations of simple structures:

$$\tilde{\boldsymbol{E}}^{irr} = -\nabla_\perp \tilde{\Phi} \quad , \quad \tilde{\boldsymbol{H}}^{irr} = -\nabla_\perp \tilde{\Psi} \qquad (A18)$$

One thus obtains the following wave equations:

$$\Delta_\perp \tilde{\Phi} - \mathrm{k}^2 (1 - \varepsilon\mu \mathrm{v}^2) \tilde{\Phi} = -\frac{\tilde{\rho}}{\varepsilon} + C_1$$

$$\Delta_\perp \tilde{\Psi} - \mathrm{k}^2 (1 - \varepsilon\mu \mathrm{v}^2) \tilde{\Psi} = C_2 \qquad (A19)$$

In this way the irrotational parts and the longitudinal components can be determined :

$$E_z = jk(1 - \varepsilon\mu \mathrm{v}^2) \tilde{\Phi} + j \frac{C_1}{k}$$

$$H_z = jk(1 - \varepsilon\mu \mathrm{v}^2) \tilde{\Psi} + j \frac{C_2}{k} \qquad (A20)$$

and also the solenoidal parts:

$$\widetilde{\boldsymbol{E}}^{sol} = v\mu\hat{\boldsymbol{z}} \times \nabla_{\perp}\widetilde{\Psi}$$

$$\widetilde{\boldsymbol{H}}^{sol} = -v\varepsilon\hat{\boldsymbol{z}} \times \nabla_{\perp}\widetilde{\Phi} \qquad (A21)$$

Appendix B - Boundary conditions

The arbitrariness in the solutions of Maxwell's equations is removed by imposing boundary conditions on the electromagnetic fields. In the case of infinite thickness the electric and magnetic fields have to satisfy the following conditions:

$$\boldsymbol{n} \times \boldsymbol{E} = 0 \qquad on\ S$$

$$\boldsymbol{n} \cdot \boldsymbol{B} = 0 \qquad on\ S \qquad (B1)$$

where $\boldsymbol{n}$ is the unit vector orthogonal to the perfectly conducting surface S. This implies that the tangential component of the electric field and the normal one of the magnetic field are zero. In the case of finite conductivity the normal component of the electric field is zero. However, its tangential, two component vector does not vanish and is related to the magnetic field by the relation, known as *Leontovich condition*:

$$\boldsymbol{E}_t = Z_m \boldsymbol{J}_s = Z_m \hat{\boldsymbol{n}} \times \boldsymbol{H} \qquad (B2)$$

where Z_m is the complex surface impedance:

$$\mathrm{Z_m} = \sqrt{\frac{\mathrm{j}\mu_0\omega}{\sigma}} = (1+\mathrm{j})\sqrt{\frac{\mu_0\omega}{2\sigma}} = \frac{1+\mathrm{j}}{\sigma\delta_\mathrm{s}} \qquad (B3)$$

Appendix C - Green's functions

A Green's function is the solution of a linear differential equation with delta functions whose arguments are the difference between the *field coordinate* r and the *source coordinate* r'.
For the wave equations the Green's functions also depend on times t and t'. With the vector Laplacian operator, defined by $\Delta G = \nabla(\nabla \cdot \mathrm{G}) - \nabla \times \nabla \times \mathrm{G}$, these functions have to satisfy the following equations:

$$\Delta G - \mu_c \varepsilon_c \frac{\partial^2 G}{\partial t^2} = \delta(\boldsymbol{r} - \boldsymbol{r}')\delta(t - t')$$

$$\Delta \tilde{G} + k_c^2 \tilde{G} = \delta(\boldsymbol{r} - \boldsymbol{r}') \qquad (C1)$$

The Green's functions can be written as a product of a spatial and a time dependent part:

$$G(\boldsymbol{r}, \boldsymbol{r}', t, t') = G(\boldsymbol{r}, \boldsymbol{r}')\delta(t - t') \qquad (C2)$$

Solutions of the wave equations can be written as integrals over the volume V, whose integrands are products of the spatial part of the Green's function $G(\boldsymbol{r}, \boldsymbol{r}')$ and the charge density $\rho(\boldsymbol{r}', t')$ or the current density $J(\boldsymbol{r}', t')$:

$$\Phi(\boldsymbol{r}, t) = \int_V d\boldsymbol{r}' \frac{\rho(\boldsymbol{r}', t')}{\varepsilon_c} G(\boldsymbol{r}, \boldsymbol{r}')$$

$$\boldsymbol{A}(\boldsymbol{r}, t) = \int_V d\boldsymbol{r}' \mu_c J(\boldsymbol{r}', t') G(\boldsymbol{r}, \boldsymbol{r}') \qquad (C3)$$

In general, it is quite difficult to find exact expressions for the Green's function. For example, in free space the spatial Green's function can be written as:

$$G(\boldsymbol{r}, \boldsymbol{r}') = \frac{1}{|\boldsymbol{r} - \boldsymbol{r}'|} \qquad (C4)$$

whose Fourier transform is:

$$\widetilde{\mathrm{G}}(\boldsymbol{r},\boldsymbol{r}') = \frac{1}{4\pi|\boldsymbol{r}-\boldsymbol{r}'|}\, e^{-jk|\boldsymbol{r}-\boldsymbol{r}'|} \qquad (C5)$$

The Green's function can also be represented in the following form:

$$\widetilde{\mathrm{G}}(\boldsymbol{r},\boldsymbol{r}') = -\frac{j}{8\pi}\int_{-\infty}^{\infty} dp\; \tilde{G}_p(r,r')e^{[-jp(z-z')]} \qquad (C6)$$

where:

$$\tilde{G}_p(r,r') = \begin{cases} \sum_{m=0}^{\infty} \varepsilon_{m0} J_m(\nu r) H_m^{(1)}(\nu r') \cos m\vartheta & r' > r \\ \sum_{m=0}^{\infty} \varepsilon_{m0} J_m(\nu r') H_m^{(1)}(\nu r) \cos m\vartheta & r' < r \end{cases} \qquad (C7)$$

where $\varepsilon_{m0} = \begin{cases} 1 & \text{for m} = 0 \\ 2 & \text{for m} \neq 0 \end{cases}$, $J_m, H_m^{(1)}$ are Bessel and Hankel functions of order m.

Solutions of the wave equations in the frequency domain, $\widetilde{\boldsymbol{H}}_n(\boldsymbol{r})$, constitute a full set of orthogonal functions which can be normalized by division with the coefficients $N_n^{1/2}$, to obtain the following normalized functions:

$$\tilde{h}_n = \frac{\widetilde{\boldsymbol{H}}_n}{N_n^{1/2}} \qquad (C8)$$

where:

$$N_n = \int_V dr\; \widetilde{\boldsymbol{H}}_n(\boldsymbol{r}) \cdot \widetilde{\boldsymbol{H}}_n^*(\boldsymbol{r}) \qquad (C9)$$

These functions satisfy the *orthogonality relations*:

$$\int_V d\boldsymbol{r}\widetilde{\boldsymbol{h}}_n(\boldsymbol{r}) \cdot \widetilde{\boldsymbol{h}}_n^*(\boldsymbol{r}) = \delta_{mn} = \begin{cases} 1 & for\ n = m \\ 0 & for\ n \neq m \end{cases} \qquad (C10)$$

and the *completeness condition*:

$$\sum_{\mathrm{n}} \widetilde{\boldsymbol{h}}_n(\boldsymbol{r}) \cdot \widetilde{\boldsymbol{h}}_n^*(\boldsymbol{r}) = \delta(\mathbf{r} - \mathbf{r}') \tag{C11}$$

Through these conditions one can find the following representation of the Green's function:

$$\tilde{G}(\boldsymbol{r} - \mathbf{r}') = \sum_{\mathrm{n}} \frac{\widetilde{\boldsymbol{h}}_n(\boldsymbol{r}) \cdot \widetilde{\boldsymbol{h}}_n^*(\boldsymbol{r}')}{\mathrm{k}^2 - \mathrm{k}_{\mathrm{n}}^2} \tag{C12}$$

Appendix D - Field matching techniques

The wave equation is a partial differential equation and thus cannot be solved directly. However, in a limited number of coordinate system it is possible to reduce it to a system of ordinary differential equations by the method called *separation of variables*. With this method one can obtain analytical solutions. Moreover, one can also find analytical solutions for the electromagnetic fields excited by a particle beam passing a structure which can be divided into a number of regions, which are bounded by piecewise constant coordinate surfaces. They are generally given in terms of infinite series over transcendental functions, which are difficult to evaluate numerically. However the integrals of their products are always orthogonal over the region considered. The electromagnetic fields have to fulfill boundary conditions at the walls of the structure, and also have to be continuous across the interfaces between neighbouring regions. The equations expressing these matching conditions contain infinite series with unknown expansion coefficients for each region. Using the orthogonality of the expansion functions these coefficients in any one region can be obtained explicitly in terms of infinite sums over coefficients in adjacent regions. In this way, one can reduce the problem to a single system of linear, algebraic equations for one set of coefficients, from which one can determine all the others. This approach is generally known as the *field matching technique*.

Bibliography

[1] P.J.Bryant, K.Johnsen, The Principles of Circular Accelerators and Storage Rings, Cambridge University Press.

[2] B.Zotter, S.Kheifets, Impedances and Wakes in High-Energy Particle Accelerators, World Scientific.

[3] D.A. Edwards, M.J. Syphers, An Introduction to the Physics of High Energy Accelerators, J.Wiley , 1993.

[4] A.W.Chao, Physics of Collective Beam Instabilities in High-Energy Accelerators, Wiley, Ney York, 1993.

[5] F.Ruggiero, Single-Beam Collective Effects in the LHC, CERN SL/95-09 (AP) and LHC Note 313, 1995.

[6] N. Piwinski, DESY 1972/72.

[7] L. Palumbo, V.G. Vaccaro, Wake fields, Impedances and Green's functions, CERN-CAS, 1987.

[8] Y. Shobuda and K. Yokoya, Phys. Rev. E56, 056501, 2002.

[9] L. Cappetta, Th. Demma, S. Petracca, University of Sannio and INFN, Wakefields of Bunched Beams in Rings with Resistive Walls of Finite Thickness, Proceedings of RuPAC XIX, Dubna 2004.

[10] L. Cappetta, Th. Demma, S. Petracca, University of Sannio and INFN, Electromagnetic Fields of an off-axis Bunched Beam in a Circular Pipe with Finite Conductivity and Thickness-I , Proceedings of EPAC 2004, Lucerne, Switzerland.

[11] L. Cappetta, I. M. Pinto, Dipartimento di Ingegneria dell'Informazione ed Ingegneria Elettrica, University of Salerno, Wakefields of Bunched Beams in Rings with Resistive Walls of Finite Thickness.

[12] M. Abramowitz, A. Stegun, Handbook of Mathematical Functions, Dover, 1965.

[13] S. Petracca, The Tensor Nature of Laslett Coefficients: Square vs Circular Cross Section Liners, Particle Accelerators, Vol. 48, pp. 181-192, 1994.

[14] B. Zotter, Transverse Oscillations of a Relativistic Particle Beam in a Laminated Vacuum Chamber, CERN Rept. 69-15 Rev., 1969.

[15] Ahmed M. Al-Khateeb, Longitudinal Impedance and Shielding Effectiveness of a Resistive Beam Pipe for arbitrary energy and frequency, Physical Review E 71, 026501, 2005.

[16] Ahmed M. Al-Khateeb, Analytical Calculation of the Longitudinal Space Charge and Resistive Wall Impedances in a Smooth Cylindrical Pipe, Physical Review E, Volume 63, 026503, 2001.

[17] Ahmed M. Al-Khateeb, Transverse Resistive Wall Impedances and Shielding Effectiveness for Beam Pipes of arbitrary Wall Thickness, Physical Review Special Topics – Accelerators and beams 10, 064401, 2007.

[18] S.S. Kurennoy, Workshop on Instabilities of High Intensity Hadron Beams in Rings, edited by T. Roser and S.Y. Zhang, AIP Conf. Proc. No. 496 (AIP, New York, 1999), p.361.

[19] J.G. Wang, Workshop on Instabilities of High Intensity Hadron Beams in Rings, edited by T. Roser and S.Y. Zhang, AIP Conf. Proc. No. 496 (AIP, New York, 1999), p.277.

[20] F. Zimmermann and K. Oide, Phys. Rev. ST Accel. Beams 7, 044201, 2004.

[21] L. D. Landau, E. M. Lifshitz, and L. P. Pitaevskii, Electrodynamics of Continuous Media, 2nd ed., Pergamon , Oxford, 1984.

[22] R. L. Gluckstern, CERN Report No. 2000-011, p. 9, 2000.

[23] Y. Shobuda and K. Yokoya, Resistive wall impedance and tune shift for a chamber with a finite thickness, Physical Review E66, 056501, 2002.

[24] Mikayel Ivanyan, Analytical presentation of resistive impedance for the laminated vacuum chamber, Physical Review Special Topics – Accelerators and Beams 9, 034404, 2006.

[25] L. Schächter, R. L. Byer, R. H. Siemann, Wake Field in Dielectric Acceleration Structure, Physical Review E 68, 036502, 2003.